

ANALYSIS OF PROPELLANT FEEDLINE DYNAMICS

W. J. Astleford
J. L. Holster
C. R. Gerlach

INTERIM TECHNICAL REPORT NO. 1

Contract No. NAS8-25919
Control No. DCN 1-1-75-10051 (1F)
SwRI Project No. 02-2889

Prepared for
National Aeronautics and Space Administration
George C. Marshall Space Flight Center
Marshall Space Flight Center, Alabama 35812

CR-123913

August 1972

(NASA-CR-123913) ANALYSIS OF PROPELLANT
FEEDLINE DYNAMICS Interim Technical Report
W.J. Astleford, et al (Southwest Research
Inst.) Aug. 1972 131 p CSDL 211 G3/27

N73-11785

Unclas
16515



SOUTHWEST RESEARCH INSTITUTE
SAN ANTONIO HOUSTON

Reproduced by
NATIONAL TECHNICAL
INFORMATION SERVICE
U.S. Department of Commerce
Springfield, VA. 22151

153

2
MK

SOUTHWEST RESEARCH INSTITUTE
Post Office Drawer 28510, 8500 Culebra Road
San Antonio, Texas 78284

ANALYSIS OF PROPELLANT FEEDLINE DYNAMICS

W. J. Astleford
J. L. Holster
C. R. Gerlach

INTERIM TECHNICAL REPORT NO. 1

Contract No. NAS8-25919
Control No. DCN 1-1-75-10051 (1F)
SwRI Project No. 02-2889

Prepared for
National Aeronautics and Space Administration
George C. Marshall Space Flight Center
Marshall Space Flight Center, Alabama 35812

August 1972

Approved:

C. Richard Gerlach

C. Richard Gerlach, Manager
Hydro-Mechanical Systems
Department of Mechanical Sciences

U

PRECEDING PAGE BLANK NOT FILMED

FOREWORD

This report summarizes all work performed by Southwest Research Institute during the past yearly period, under Contract No. NAS8-25919, "Analysis of Propellant Feedline Dynamics." This study is being performed for the George C. Marshall Space Flight Center of the National Aeronautics and Space Administration, and is administered technically by Messrs. Larry Kiefling and Gary Muller of the Aero-Astrodynamic Laboratory.

PRECEDING PAGE BLANK

ACKNOWLEDGMENTS

The authors of this report wish to express their sincere gratitude to Mrs. Adeline Raeke who cheerfully typed the entire text, and to Mr. V. J. Hernandez for his skillful work on the figures.

TABLE OF CONTENTS

	<u>Page</u>
LIST OF FIGURES	vii
LIST OF SYMBOLS	ix
I. INTRODUCTION	1
I. 1 Background and Objectives	1
I. 2 General Feedline Problem	2
II. GENERAL LINE MODEL WITH MEAN FLOW	4
II. 1 Physical Picture and Requirements	4
II. 2 Possible Convective Influences	7
II. 3 Effect of Turbulence on Damping and Phase Velocity	9
III. DISTRIBUTED COMPLIANCES	13
III. 1 Distributed Bubbles	13
III. 2 Distributed Wall Compliance	16
III. 3 Axial Wall Stiffness	21
IV. LOCAL COMPLIANCES - LARGE BUBBLES AND CAVITATION ZONES	26
V. COUPLED RESPONSES	29
V. 1 Accelerated Line	29
V. 2 Relative Motion of Bellows and PVC Joints	32
V. 3 Forced Changes in Line Length	37
V. 4 Mounting Stiffness	41
VI. GENERALIZED FEEDLINE COMPUTER CODE	45
VII. CONCLUSIONS AND RECOMMENDATIONS	50
VII. 1 Conclusions	50
VII. 2 Recommendations	51
REFERENCES	52
APPENDICES:	
A. Rational Approximate Model for Distributed Parameter Systems	A-1
B. Speed of Sound in a Liquid Containing a Homogeneous Distribution of Bubbles	B-1

TABLE OF CONTENTS (Cont'd.)

	<u>Page</u>
APPENDICES (Cont'd.)	
C. Compliance of Large Bubbles and the Polytropic Exponent	C-1
D. Forced Changes in Line Length	D-1
E. Mounting Stiffness	E-1
F. Parallel Lines	F-1
G. Complex Side Branch	G-1
H. User's Manual for Generalized Feedline Program	H-1

LIST OF FIGURES

<u>Figure No.</u>		<u>Page</u>
1	Hypothetical Feed System and Engine	3
2	General Physical Picture of Flow Behavior in Feed Line	5
3	Predictions of Attenuation Factor for Turbulent Flow (Reference 7)	10
4	Predicted Phase Velocity with Turbulent Flow (Reference 7)	11
5	Variation of Speed of Sound with Mass Ratio	15
6	Effect of Frequency and Bubble Size on Phase Velocity of Air and Water Mixture	17
7	Zeroth Mode Spatial Attenuation Versus Fre- quency Number for a Rigid and an Elastic Flexible Wall	19
8	Zeroth Mode Dimensionless Phase Velocity, c/c_0 , Versus Frequency Number for a Rigid and an Elastic Flexible Wall	20
9	Axial Velocity Profile Function, $F_{zn}(r)$, for Four Modes ($\omega r_0/c_0 = 1.0$, $\nu/r_0 c_0 = 0.01$)	22
10	Axial Velocity Profile Function, $F_{zn}(r)$, for Four Modes ($\omega r_0/c_0 = 0.2$, $\nu/r_0 c_0 = 0.001$)	23
11	Plot of the Spatial Attenuation Factor Versus Radial Frequency Number for Three Modes	25
12	Polytropic Exponent for O ₂ Bubble in LOX vs. Dimensionless Frequency and Bubble Size	28
13	Fluid Conduit with Axial Vibration	30
14	Nomenclature for Relative Motion of Bellows	34
15	Illustration of Typical PVC Joint	36
16	Geometry for Forced Changes in Line Length	38
17	Illustration of Approximate Modeling Procedure for Forced Changes in Line Length	39
18	Model for a Line with Mounting Stiffness	42
19	Matrix Representation of a Feedline in the Laplace Domain	48

LIST OF FIGURES (Cont'd.)

<u>Figure No.</u>		<u>Page</u>
A-1	Variation of the Approximate Model Parameter F_{cn} With Axial Damping Number	A-3
A-2	Variation of the Approximate Model Parameter ζ_{cn} With Axial Damping Number	A-4
A-3	Variation of the Approximate Model Parameter F_{sn} With Axial Damping Number	A-5
A-4	Variation of the Approximate Model Parameter ζ_{sn} With Axial Damping Number	A-6
D-1	Geometry for Forced Changes in Line Length	D-2
E-1	Model for a Line With Mounting Stiffness	E-3
F-1	Parallel Line Model	F-3
G-1	Example Treatment of More General "Local Compliance" in Feed Line	G-3
H-1	Line Model for Example Problem No. 1	H-32
H-2	Frequency Response for the Feedline in Example Problem No. 1	H-35
H-3	Line Model for Example Problem No. 2	H-37
H-4	Frequency Response of the Feedline in Example Problem No. 2	H-40
H-5	Line Model for Example Problem No. 3	H-43
H-6	Frequency Response of the Feedline in Example Problem No. 3	H-44
H-7	Line Model for Example Problem No. 4	H-46
H-8	Frequency Response of the Feedline in Example Problem No. 4	H-49
H-9	Line Model for Example Problem No. 5	H-52
H-10	Frequency Response of the Feedline in Example Problem No. 5	H-53

LIST OF SYMBOLS

A	= cross-sectional area
A_b	= cross-sectional area of the side branch
A_z	= Laplace transform of the axial acceleration
$a_1(s)$	= Laplace transform of the applied structural acceleration
$a_\ell(s)$	= Laplace transform of the resultant line acceleration
\underline{B}_j	= column matrix of one of the \underline{C}_i matrices pre-multiplied by one or more \underline{D} matrices
b	= coefficient of damping
b_{1j}	= elements of matrix \underline{B}_j
C	= compliance of a fluid element; also a constant
\underline{C}_i	= column matrix, present only if the particular line component is externally excited
C_p	= specific heat at constant pressure
c	= phase velocity corrected for wall elasticity effects
c_g	= speed of sound in a pure gas
c_ℓ	= speed of sound in a pure liquid
c_o	= speed of sound in the fluid medium
c_w	= speed of sound in the feedline wall
\underline{D}	= 2×2 square matrix characteristic of each line element
D_1	= thermal diffusivity of the entrained gas
D_n	= damping number
d_b	= side branch diameter
d_{1j}	= elements of the matrix \underline{D}
$F; F_z$	= externally applied forces; body force
$F(\rho V_2^2, G)$	= loss factor due to bellows or PVC joint
f_o	= resonant frequency of a gas bubble, (Hertz)
G	= bellows geometry factor
$G(s)$	= lag caused by PVC joint; also transfer function relating structural velocities at each end of a line

g_0	=	acceleration due to gravity
h	=	feedline wall thickness
I	=	line inertance, $\rho_0 L/A$
J_0, J_1	=	zero and first order Bessel functions of the first kind
K	=	Laplace transform of an external forcing function
K_b	=	volume change constant for a bellows
K_c	=	PVC volume compensation constant
k	=	spring constant; also bubble stiffness term, $\gamma P_0/V_0$
L	=	length of a line element
L_{1j}	=	elements of the matrix for an accelerated line
M	=	mass
MW	=	gas molecular weight
M_g	=	mass of the gas
M_l	=	mass of the liquid
m_2	=	equivalent mass term, $\rho_l/4\pi R_0$
N_R	=	Reynolds number
$P(s)$	=	Laplace transform of $p(t)$, often written as P
P_0, p_0	=	mean pressures
$p(t)$	=	perturbation pressure, often written as p
Q_d	=	side branch pulser flow perturbation amplitude
$Q(s)$	=	Laplace transform of the volume flow, $q(t)$
$q(t)$	=	volume flow perturbation, often written as q
R	=	resistance; also gas constant
R_0	=	mean radius of a gas bubble
r	=	radial coordinate, measured from centerline
r_0	=	line internal radius
s	=	Laplace variable, $\sqrt{-1} \omega$; also entropy
T	=	temperature
TDT	=	turbulent dissipation terms
t	=	time

U	= Laplace transform of $u(t)$
$u(t)$	= axial perturbation velocity
V_g	= volume of the gas
V_l	= volume of the liquid
V_o	= steady state or mean bubble volume, also written as V_{BUB}
$Vol(s)$	= apparent volume production (in Laplace domain)
V_z	= Laplace transform of v_z
v	= amplitude of bubble volume pulsations; also specific volume
\bar{v}	= dynamic velocity perturbation
v_f	= specific volume of the liquid
v_g	= specific volume of the gas
v_o	= mean velocity component
v_r	= radial velocity component
v_t	= turbulent velocity component
v_z	= perturbation velocity component in the axial direction
X	= Laplace transform of the axial displacement
x	= mixture quality; also axial coordinate
y	= axial displacement of a point in the wall
Z_c	= characteristic impedance
Z_{c2}	= characteristic impedance of the horizontal line segment 1 to 2 of Figure E-1.
Z_i	= impedance at the tank outlet
Z_s	= structural impedance
Z_t	= terminal impedance of the line
z	= coordinate in the axial direction
β	= separation constant
Γ_o	= turbulent attenuation contribution to the propagation operator for a line of length L .
Γ_L	= laminar propagation operator for a line of length L
Γ_t	= turbulent propagation operator for a line of length L

γ	=	propagation operator; also ratio of specific heats for a gas
γ_{lam}	=	laminar propagation operator
γ_r	=	spatial attenuation factor
δ	=	damping constant
ζ_{cn}	=	constants in rational approximate model, $n=0, 1, 2, \dots$
ζ_{sn}	=	constants in rational approximate model, $n=0, 1, 2, \dots$
η	=	polytropic exponent
κ	=	liquid bulk modulus
λ	=	separation constant
μ	=	dynamic viscosity
ν	=	kinematic viscosity
ρ	=	density of the fluid medium
ρ_g	=	density of the gas
ρ_l	=	density of the liquid
ρ_o	=	mean density (steady state value)
ρ_t	=	density of feedline wall material
τ	=	time constant
ϕ	=	mass ratio, mass of gas/mass of liquid
ω	=	angular frequency, radian/sec
ω_{cn}	=	constant in rational approximate model, $n=0, 1, 2, \dots$
ω_o	=	natural frequency, radian/sec
ω_{sn}	=	constant in rational approximate model, $n=0, 1, 2, \dots$

I. INTRODUCTION

I. 1. Background and Objectives

At least three classes of feed system instabilities have been identified for liquid propellant rockets^{1, 2, 3, 4*}. In each case, the dynamic behavior of the feed line plays a major role in the instability. Probably the best known problem^{1, 2} involves a closed-loop coupling of the vehicle longitudinal structural modes, the feed system and the engine. A second problem³ showed up on Saturn flight AS-504 when the S-II center engine displayed severe pressure and thrust oscillations rather late in the stage burn. In this case, the problem was localized, involving a closed-loop instability of the engine support structure, the feed system, and the engine. A third type of problem which can exist⁴ involves only the feed system, the inducer-pump combination and the engine. This instability is traceable directly to the inducer dynamics, with the feed system and engine providing an impedance loading which governs the resultant oscillation frequency.

All of the above instabilities pose a threat to the success of a mission. For simulation purposes, it is readily recognized that adequate modeling procedures are needed for each portion of the vehicle involved in a given instability. The objective of this study was to develop an analytical method, and its corresponding computer program, to allow the study of disturbances of liquid propellants in typical engine feedline systems. This method was to include (1) the effect of steady flow, (2) the influence of distributed compliances and axial wall stiffness, (3) the effects of local compliances, such as vapor bubbles, and (4) various factors causing coupled responses between the line and structure, i. e., bends, mounting stiffness, forced changes in line length, and bellows and PVC couplings.

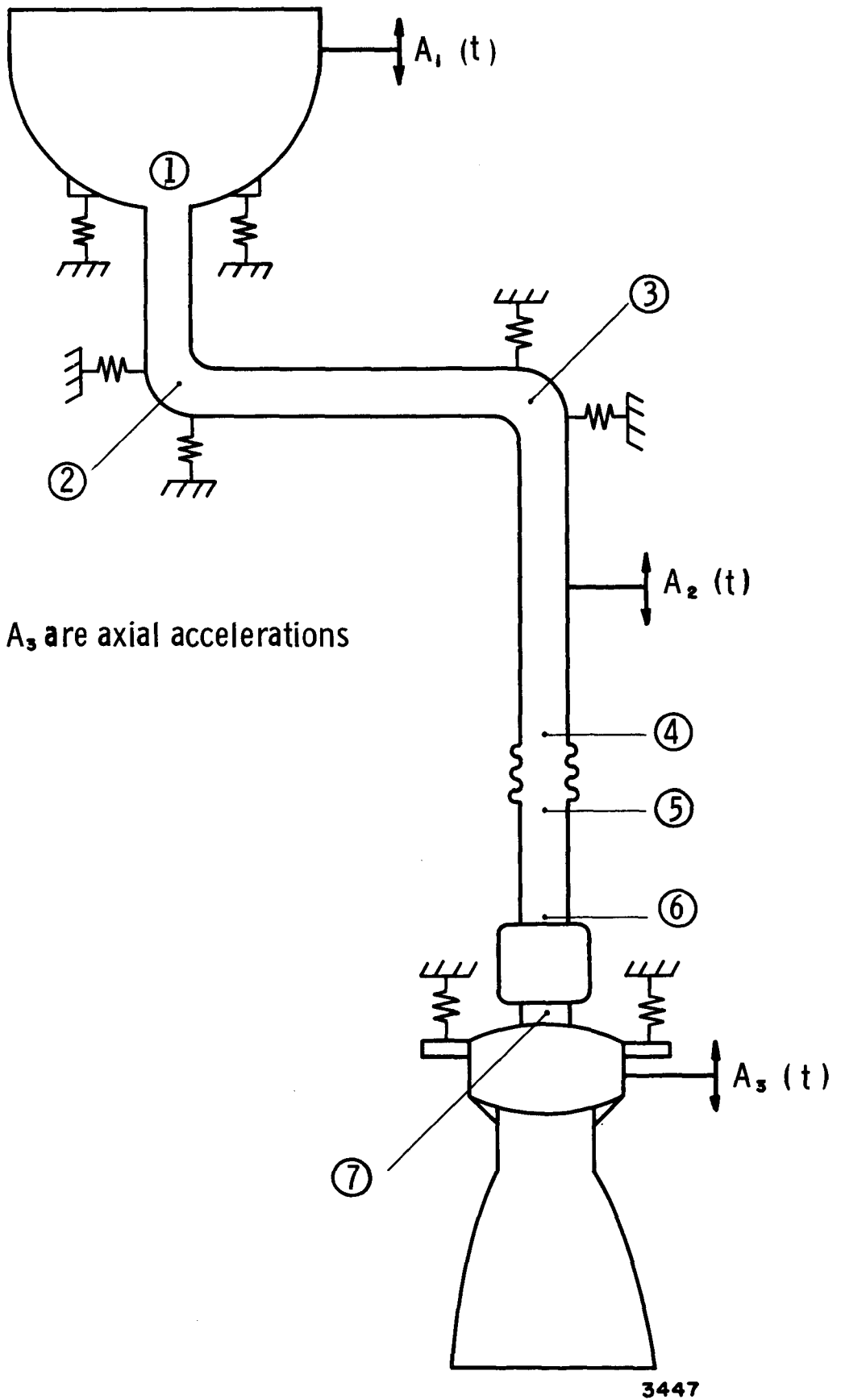
In all respects, this objective has been satisfied. This report summarizes the modeling results for each item defined above, and presents a generalized computer program which allows the user to easily determine dynamic performance of a line containing any number of elemental components. Use of this computer program is illustrated by way of a detailed set of instructions contained in Appendix H, plus a presentation of several example problems.

* Superscript numbers in the text refer to References presented on page 52 of this report.

I. 2. General Feedline Problem

The problem of modeling a given feedline can best be illustrated by an example. Figure 1 shows a hypothetical case involving a propellant tank, a feedline, a pump and an engine. In general, each element of the model is elastically supported and can experience some motion relative to a frame of reference on the vehicle. These accelerations, plus pressure oscillations in the engine combustion chamber and cavitating inducer instabilities, represent disturbance inputs to the feed system which can cause flow and pressure oscillations. These flow disturbances may, in turn, couple back with the engine and/or structure to produce a large amplitude, closed-loop instability. The modeling problem, with respect to the feed system, is to describe analytically the dynamic pressure and flow at an arbitrary point in the system, with proper treatment of the end conditions, the acceleration inputs and the flexible supports.

Generally, a feedline may be regarded as a series of elements, such as lengths of line, bends, bellows PVC coupling, etc. Therefore, it is necessary to describe each element individually, and then define means for mathematically combining these elements so as to produce the proper overall system mode. In this report, each element is basically defined by a four-terminal representation in the Laplace domain. Overall system model formulation is also achieved in the Laplace or operator domain. Where problem solution is required only in the frequency domain, this Laplace formulation is the one to use, and the present computer program is set up on this basis. For problem solution in the time domain, the Laplace operator formulation must be converted to an equivalent time domain formulation (rational approximate model). The procedure for accomplishing this conversion is described herein.



- A_1, A_2, A_3 are axial accelerations

Figure 1. Hypothetical Feed System And Engine

II. GENERAL LINE MODEL WITH MEAN FLOW

II. 1. Physical Picture and Requirements

An illustration of the physical picture of the flow behavior in a feedline is given in Figure 2. For the present, only the fluid dynamic effects in a line, assumed cylindrical, straight, and with infinitely stiff walls, will be considered.

The line shown in Figure 2 is assumed to contain a turbulently flowing viscous liquid. The mean vector velocity is represented by \bar{v}_o , which contains only the axial component, $v_o(r)$. Superimposed on this mean flow are two dynamic velocity perturbation quantities, \bar{v} and \bar{v}_t . The velocity component \bar{v} represents the dynamic velocity perturbation of interest, and \bar{v}_t represents the turbulent velocity fluctuations. Similarly, the total pressure is the sum of a mean quantity, p_o , a dynamic perturbation part, p , and a turbulent part, p_t .

By substitution of the assumed summation forms for velocity into the Navier-Stokes equations⁵, and short-time averaging of the turbulence quantities, the following form results:

$$\frac{\partial \bar{v}}{\partial t} + v_o \frac{\partial \bar{v}}{\partial z} = -\frac{\nabla p}{\rho_o} + \nu \left\{ \frac{4}{3} \nabla(\nabla \cdot \bar{v}) - \nabla \times (\nabla \times \bar{v}) \right\} + \text{TDT} \quad (1)$$

In addition, we may complete our description of the dynamic fluid behavior with a continuity equation:

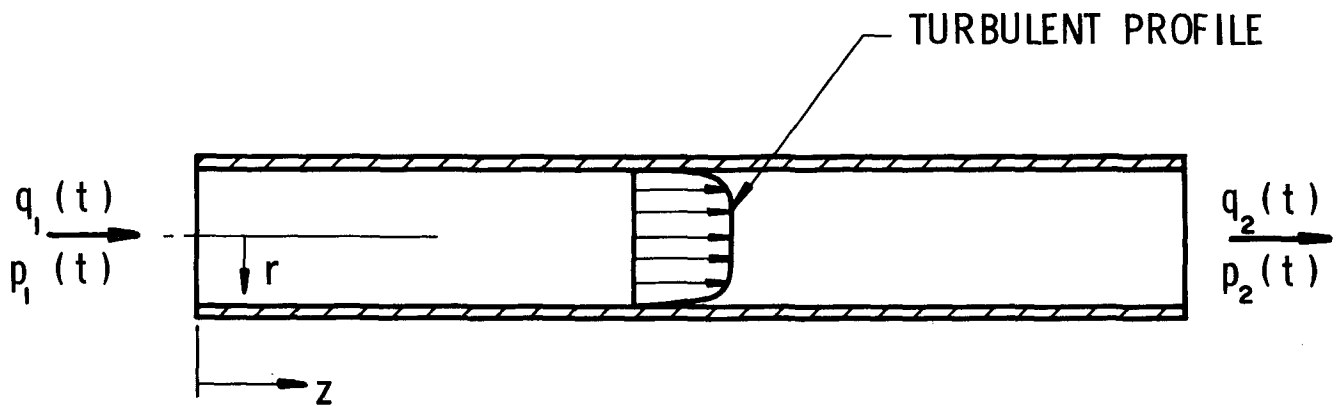
$$\frac{\partial \rho}{\partial t} + \rho_o \nabla \cdot \bar{v} + v_o \frac{\partial \rho}{\partial z} = 0 \quad (2)$$

and a liquid equation of state:

$$dp = \kappa \frac{d\rho}{\rho_o} \quad (3)$$

Equation (1) is a first-order form of the Navier-Stokes equations, including turbulent dissipation terms (TDT). Similarly, Equation (2) is a first-order continuity expression relating the dynamic velocity perturbation to density perturbations (ρ_o is the mean density).

Examination of Equations (1) and (2) shows that the presence of a mean turbulent flow has two possible effects. First, the



$\bar{v}_T(r, z, t) \equiv$ vector total velocity

$$\bar{v}_T = \bar{v}_0 + \bar{v} + \bar{v}_t$$

$\bar{v}_0 =$ time invariant mean flow

$\bar{v} =$ dynamic perturbation of interest

$\bar{v}_t =$ turbulent fluctuations

$$p_T = p_0 + p + p_t$$

2747

Figure 2. General Physical Picture Of Flow Behavior In Feed Line

turbulent dissipation terms introduce damping in addition to the conventional "laminar" damping accounted for by the terms in brackets on the right side of Equation (1). Second, the mean flow introduces a "convective" effect represented by the terms $v_o \partial v / \partial z$ and $v_o \partial \rho / \partial z$ in Equations (1) and (2) respectively.

The requirements for a dynamic feedline model with a mean flow are that (1) the attenuation effects of the turbulent flow be properly treated and (2) the possible convective influences be examined and included if necessary. The following sections treat these two topics. In general, the feedline model presented will be an extension of an existing distributed parameter model which exactly accounts for laminar viscous effects, but negligible mean flow. This existing model, which is discussed in References 5 and 6, may be given in the following form:

$$\begin{aligned} P_2(s) &= P_1(s) \cosh \gamma L - Z_o A^{-1} Q_1(s) \sinh \gamma L \\ Q_2(s) &= Q_1(s) \cosh \gamma L - Z_o^{-1} A P_1(s) \sinh \gamma L \end{aligned} \quad (4)$$

The laminar propagation operator takes the familiar form

$$\gamma_{\text{lam}} = \frac{s}{c} \left[1 - \frac{2J_1(\xi r_o)}{\xi r_o J_0(\xi r_o)} \right]^{\frac{1}{2}} \quad (5)$$

where c is the phase velocity in the fluid, J_0 and J_1 are zero and first-order Bessel functions of the first kind and

$$\xi^2 = -s/\nu \quad (6)$$

The characteristic impedance is related to the propagation operator by

$$Z_o = \rho_o c_o^2 \gamma / s \quad (7)$$

The magnitude of the additional attenuation due to turbulence is a function of the Reynold's number and the frequency range of interest; this aspect is discussed in Section II.3. The relationship between mean flow velocity and the adiabatic speed of sound dictates the phase velocity to be used in Equation (5). Section II.2 discusses the effect of mean flow convection.

II.2 Possible Convective Influences

As indicated previously, the terms $v_o \partial \bar{v} / \partial z$ and $v_o \partial \rho / \partial z$ in Equations (1) and (2), respectively, represent the convective effect of the mean flow v_o . The question to be answered at this point is: Are these terms of enough significance to be retained in the final model? Ideally we would like to retain the convective terms at all times, but, from a practical standpoint, they increase considerably the complexity of the final solution.

To judge the importance of the convective terms, it is convenient to consider a nondissipative, one-dimensional form of Equations (1) and (2) or

$$\frac{\partial v_z}{\partial t} + v_o \frac{\partial v_z}{\partial z} = -\frac{1}{\rho_o} \frac{\partial p}{\partial z} \quad (8)$$

and

$$\frac{\partial \rho}{\partial t} + \rho_o \frac{\partial v_z}{\partial z} + v_o \frac{\partial \rho}{\partial z} = 0 \quad (9)$$

Transformation of Equations (3), (8), and (9) into the Laplace domain, and the subsequent elimination of ρ and P , yields one equation in V_z (V_z is the transform of v_z), or

$$(c_o^2 - v_o^2) \frac{d^2 V_z}{dz^2} - 2s v_o \frac{dV_z}{dz} - s^2 V_z = 0 \quad (10)$$

where

$$\begin{aligned} s &= \text{Laplace variable} \\ c_o &= (\kappa / \rho_o)^{\frac{1}{2}} = \text{isentropic speed of sound} \\ v_o &= \text{axial mean flow velocity} \end{aligned}$$

Assuming a solution for Equation (10) of the form

$$V_z = C e^{\gamma z} \quad (11)$$

we find the characteristic equation to be

$$(c_o^2 - v_o^2) \gamma^2 - 2s v_o \gamma - s^2 = 0 \quad (12)$$

whose roots or values for γ are

$$\gamma = \left(\frac{sv_0}{c^{*2}} \right) \pm \left\{ \frac{s^2 v_0^2}{c^{*4}} + \frac{s^2}{c^{*2}} \right\}^{\frac{1}{2}}$$

$$\gamma = \left(\frac{sv_0}{c^{*2}} \right) \left\{ 1 \pm \left[1 + \frac{c^{*2}}{v_0^2} \right]^{\frac{1}{2}} \right\} \quad (13)$$

where $c^{*2} = c_0^2 - v_0^2$. The plus sign applies to waves traveling in the retrograde direction, and the negative sign to waves traveling in the mean flow direction.

From these results, it is found that for propagation in the +z direction, with the mean flow, the phase velocity is greater than c_0 . To demonstrate this result, recall that the propagation operator is functionally equivalent to the Laplace variable divided by a velocity quantity. Substituting the equivalent expression for c^* into Equation (13), the following result is obtained:

$$\gamma = \frac{s(v_0 \pm c_0)}{(v_0 + c_0)(v_0 - c_0)} \quad (14)$$

For propagation in the mean flow direction,

$$\gamma_{+z} = \frac{s}{c_0 + v_0} \quad (15)$$

Therefore, the phase velocity for downstream propagation is greater than the adiabatic speed of sound. Similar reasoning verifies that the phase velocity for retrograde propagation is less than the adiabatic speed of sound.

It is important to point out that for normal conditions of liquid propellants flowing in a feedline at velocities up to, say, 50 fps, the phase velocity with mean flow is so minutely changed that this convective effect may be neglected. The reason for this is that the mean velocity is much smaller than the liquid sonic velocity, c_0 . The only condition under which this might change would be where sufficient entrained gas is present in the fluid to cause the new effective c_0 value to be, say, an order of magnitude lower than for the pure liquid. Then the convective effect should be included. For example (see Section III.1), if the level of entrained gas were to approach 0.1 percent by weight of the total liquid mass, then the equivalent speed of sound of the mixture would be approximately 100 fps. In this case, the speed of sound is only twice as large as the maximum mean flow velocity, and the phase velocity would be

100 ± 50 fps, depending on the propagation direction. This example, however, is unrealistic because the gas concentration rarely approaches a level where the mean flow velocity is but a small fraction of the mixture speed of sound. Therefore, for all practical purposes, the phase velocity can be taken to be the adiabatic speed of sound.

II.3 Effect of Turbulence on Damping and Phase Velocity

It is known that the four terminal Laplace domain representation for pressure and flow in a line is extremely accurate when the flow is laminar and the propagation operator is of the following form:

$$\Gamma_L = \left(\frac{sL}{c_0} \right) \left[1 - \frac{2 J_1(\xi r_0)}{\xi r_0 J_0(\xi r_0)} \right]^{\frac{1}{2}} = \gamma_{\text{lam}} L \quad (16)$$

In reality, a turbulent flow condition exists for many propellant feedline operating points, as indicated by Reynold's numbers of the order of 10^5 to 5×10^7 . Therefore, the effect of turbulence must be reflected in the propagation operator. As shown in Figures 3 and 4 (from Reference 7), the predominant effect of turbulence is to increase the spatial attenuation at low frequencies. At high frequencies, the laminar and turbulent attenuations coincide. There is some tendency for turbulence to reduce the phase velocity at very low frequencies and high Reynold's numbers. However, after a thorough investigation into existing feedline geometries, propellant properties, mean flow velocities and frequency range for structural-hydraulic coupling, it was concluded that the effect of turbulence on the phase velocity could be neglected.

For the exact distributed parameter line model, the effect of turbulent attenuation was modeled by adding to the existing laminar propagation operator, Γ_L , an additional attenuation contribution, Γ_c , due to turbulence.

$$\Gamma_t = \Gamma_L + \Gamma_c = (\Gamma_{Lr} + \Gamma_c) + i\Gamma_{Li} \quad (17)$$

The form of turbulence induced increment in attenuation was derived from the form of the attenuation factor of a constant I-R-C, lumped parameter, representation of a line. That is,

$$\Gamma_c = \sqrt{Cs} \sqrt{IR/s + 1} L \quad (18)$$

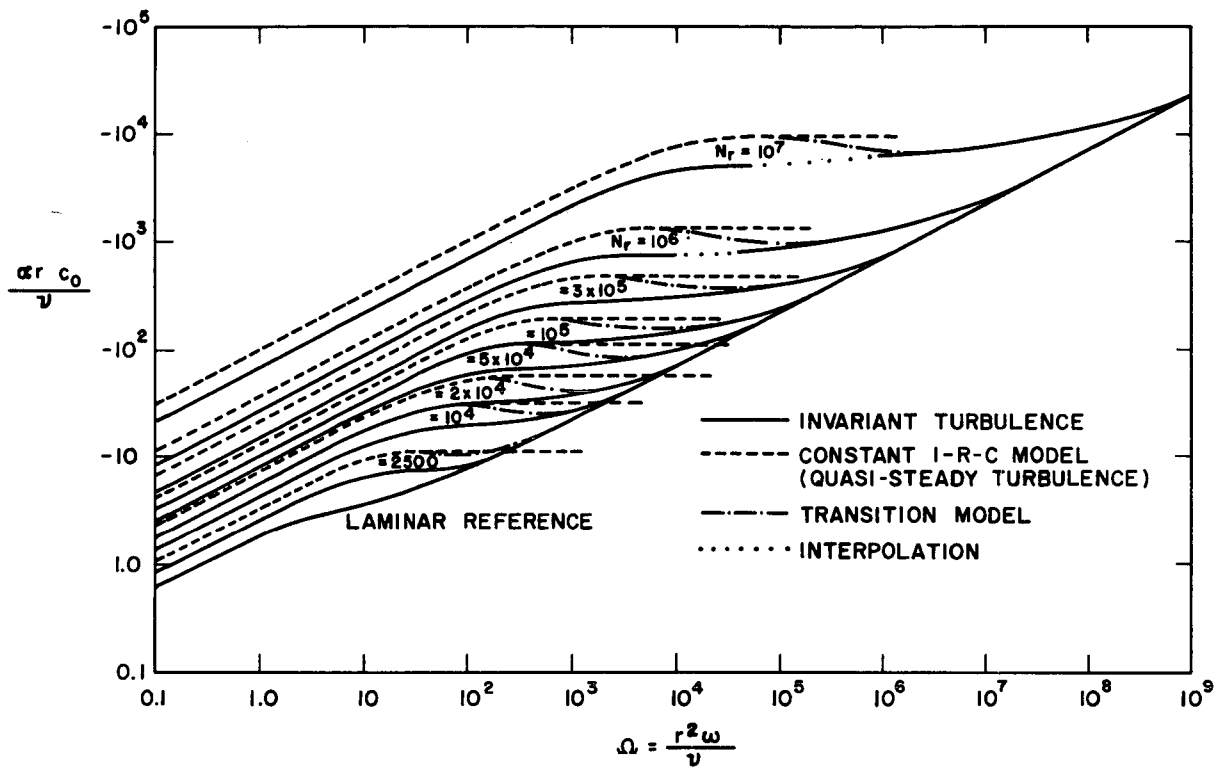


Figure 3. Predictions of Attenuation Factor for Turbulent Flow (Reference 7)

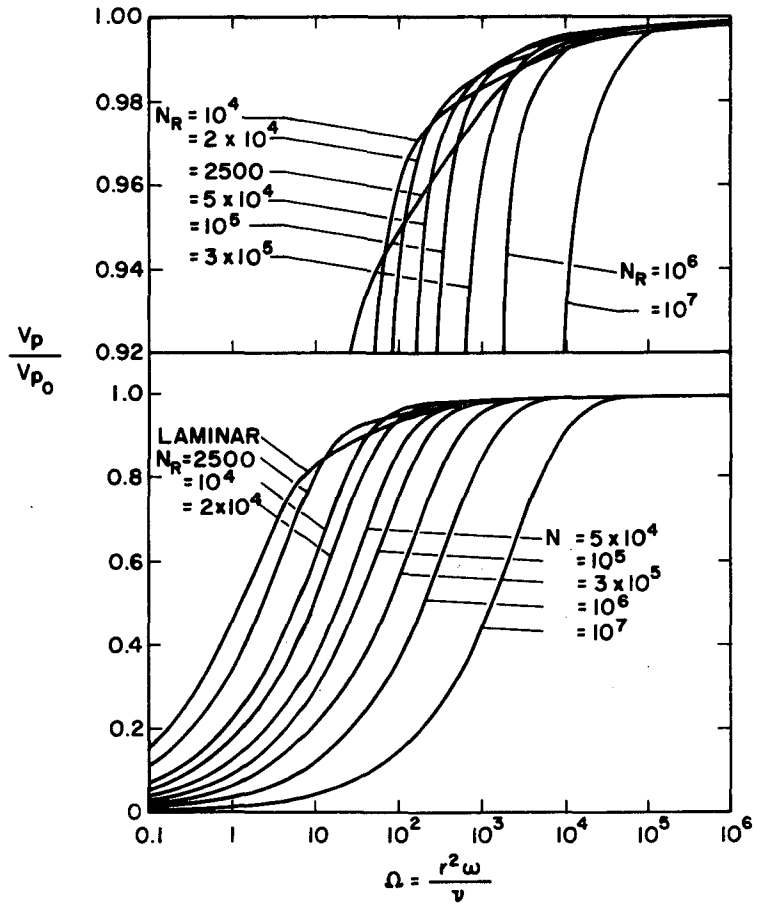


Figure 4. Predicted Phase Velocity with Turbulent Flow (Reference 7)

By analogy,

$$\Gamma_c = \text{Re} \left[\frac{sL}{c_o} \left(\frac{R_t}{s} + 1 \right)^{\frac{1}{2}} \right] \quad (19)$$

where

$$R_t = \frac{2\nu K N_R^n}{r_o^2} \quad (20)$$

The constants, K and n , were determined by surface fitting the turbulent attenuation increment in Figure 3 as a function of Reynold's number and frequency. The derived values of these constants are:

$$K = 0.0055$$

$$n = 0.85$$

III. DISTRIBUTED COMPLIANCES

III. 1 Distributed Bubbles

In most practical applications, the liquid rocket propellant in the feedline will contain quantities of either dissolved ullage gas or propellant vapor, or possibly both. It is assumed that the gases or vapor are in the form of small bubbles, homogeneously distributed throughout the liquid. The net effect of distributed bubbles in the liquid is to modify (reduce) the effective fluid sonic velocity and possibly to introduce added damping because of irreversible compression and expansion of the bubbles caused by a periodic disturbance.

Two types of entrained gases have been considered in the model for the acoustic velocity in a two-phase flow:

- (1) The flow of a single-component, two-phase mixture, such as LOX and oxygen vapor, and
- (2) The flow of a two-component, two-phase mixture, such as LOX with entrained helium ullage gas.

For a single-component, two-phase mixture, the actual flow process is theoretically bounded by the equilibrium process and the constant quality process. In the case of an equilibrium process, the vaporization and condensation rates are large enough to ensure that the vapor temperature and liquid temperature are always equal; both phases are saturated, and the quality (vapor fraction by weight) varies only with pressure. Based on the assumption of thermodynamic equilibrium, Gouse and Brown⁸ have shown that the speed of sound in a single-component, two-phase flow can be expressed as

$$c_o = \left(\frac{v_f}{v_g - v_f} + x \right) (S_g - S_f) \left[g_o \left(\frac{\Delta T}{\Delta S} \right)_v \right]^{\frac{1}{2}} \quad (21)$$

where x is the mixture quality and $(S_g - S_f)$ is the change in entropy between the saturated vapor and the saturated liquid state. Evaluation of Equation (21) requires the extensive use of a temperature-entropy chart or a tabular representation of the thermodynamic properties of the fluid being considered.

On the other hand, the condensation and vaporization rates in a constant quality process are assumed to be so low that no significant

phase change occurs. In a two-component mixture, a constant quality exists at all times if there is no liquid vapor present. Rearranging the derivation by Hsieh and Plesset⁹, the speed of sound in a two-component mixture is

$$\frac{1}{c_0^2} = \rho \left\{ \left(\frac{\rho_g}{\rho_g + \phi \rho_l} \right) \frac{1}{\rho_l} \frac{1}{c_l^2} + \left(\frac{\phi \rho_l}{\rho_g + \phi \rho_l} \right) \frac{1}{\rho_g} \frac{1}{c_g^2} \right\} \quad (22)$$

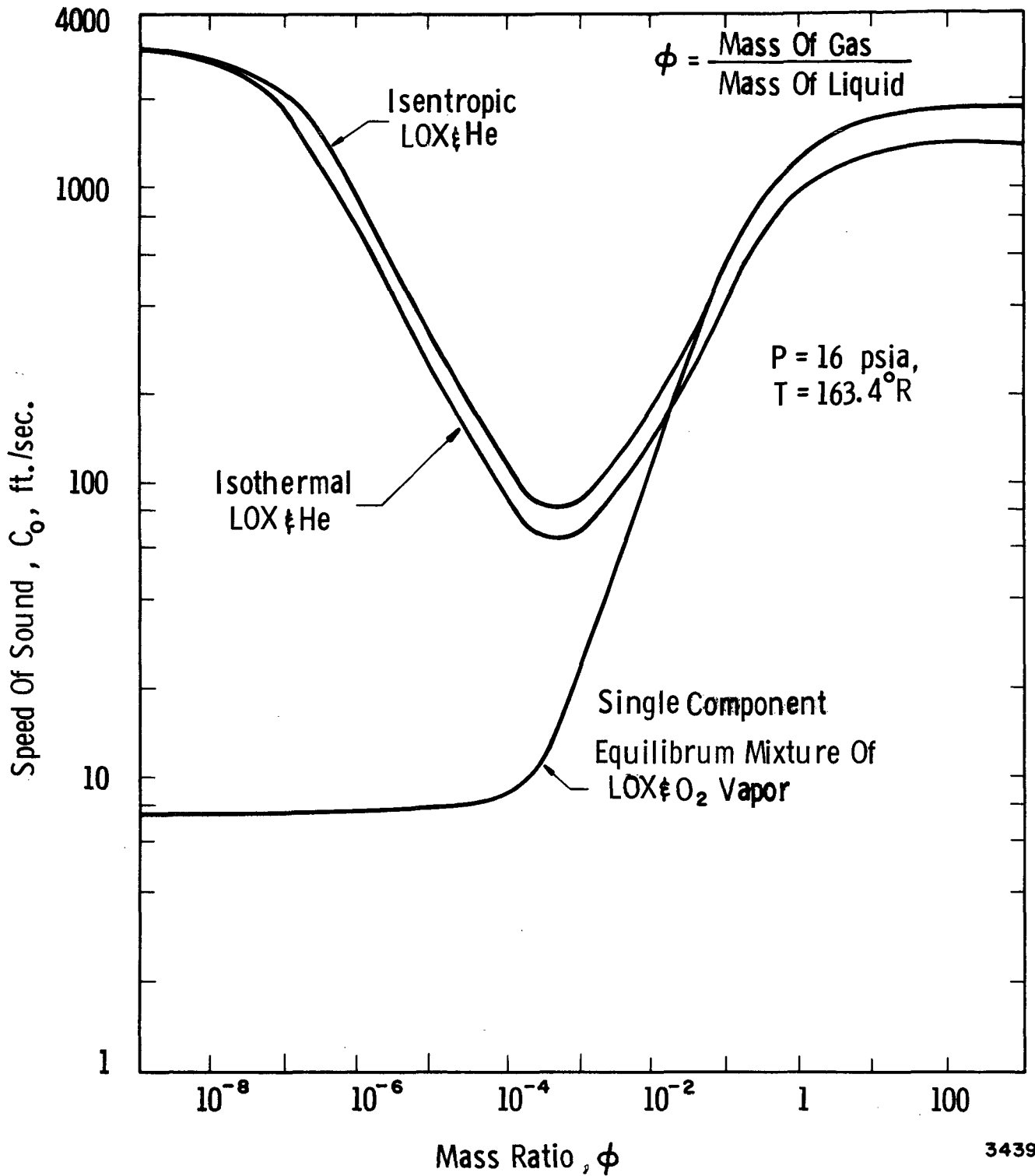
where

- ρ = mixture density
- ρ_g = gas density
- ρ_l = liquid density
- c_l = speed of sound in the liquid
- c_g = speed of sound in the gas

and ϕ = mass gas/mass liquid.

As the mass ratio, ϕ , approaches zero, the speed of sound approaches that for the pure liquid. Plesset and Hsieh¹⁰ have also shown that, for very small gas bubbles dissolved in a liquid, the adiabatic speed of sound in the gas should be replaced by the isothermal speed of sound. The reason is that the gas bubbles have a non-uniform temperature distribution in their interior due to the finite value of the heat conduction rate. Figure 5 presents the isothermal versus the adiabatic model for dissolved helium ullage gas in LOX. For comparison, the equilibrium model for LOX with O₂ vapor is also shown. Reliable experimental data are not available to determine which flow process actually occurs for the flow of a single-component, two-phase mixture. As can be seen by Figure 5, there is a great difference in the acoustic velocity between the equilibrium and the constant quality flow processes. These differences could lead to a large error in the predicted feedline system response, and more work should be devoted to a study of the actual flow process. In the present study, the constant quality model is applied to both single-component and two-component flows. A more detailed discussion of the acoustic velocity in two-phase flow is presented in Appendix B.

The wave propagation characteristics of the mixture depend not only on the gas-to-liquid mass ratio but also on the bubble size and disturbance frequency. Bubbles of a given size resonate when excited at their natural frequency; this natural or resonant frequency



3439

Figure 5. Variation Of Speed Of Sound With Mass Ratio

increases in inverse proportion to the bubble radius¹¹. An investigation has been made to determine the variation in effective sonic velocity in a liquid with uniformly distributed gas bubbles as the excitation frequency approaches the bubble resonant frequency.

At frequencies approaching resonance, Equation (22) is no longer useful, even as an approximation. Spitzer¹² derived an expression for the phase velocity at all frequencies by assuming that the gas concentration is small. If surface tension is neglected and if the bubble diameter is assumed to be larger than 0.001 ft, the bubble resonant frequency can be approximated by^{13, 14}

$$f_0 = \frac{1}{2\pi R_0} \left(\frac{3\eta P_0}{\rho_l} - \frac{4\mu_l^2}{\rho_l^2 R_0^2} \right)^{\frac{1}{2}} \quad (23)$$

where η , the polytropic exponent, is dependent primarily on the bubble size and gas thermal conductivity. For very small bubbles, such as those assumed to be distributed in the propellant feedline, the polytropic exponent is equal to unity.

The theoretical effect of frequency and bubble size on the phase velocity in a mixture of air bubbles in water has been programmed and is presented in Figure 6. The mass ratio, ϕ , was assumed to be 3.0×10^{-5} . Note that the speed of sound is only affected at or near the bubble resonant frequency, which increases with decreasing bubble size. For the homogeneous distribution of very small bubbles entrained in the liquid propellant, the net effect over the frequency range of interest is only to lower the phase velocity of the pure liquid, to the value predicted by Equation (22). The effect of larger bubbles, which are assumed to exist only locally (cavitation zones), is discussed in Section IV.

III.2 Distributed Wall Compliance

In general, the flexibility of the feedline wall will produce two possible effects which may be of concern. First, the wall compliance will reduce the phase velocity and increase the spatial attenuation for the longitudinal fluid wave propagation mode (called the zeroth mode in Reference 5), and second, the axial wall stiffness effect, will permit real wave propagation of the higher order modes at low frequency by virtue of a coupling between the fluid and axial wall modes. For typical feedline problems, we have concluded that the amount of energy which is fed into the higher order modes at the line terminations is so small that it can be neglected. Therefore, for all practical purposes, the effect of the axial wall stiffness on

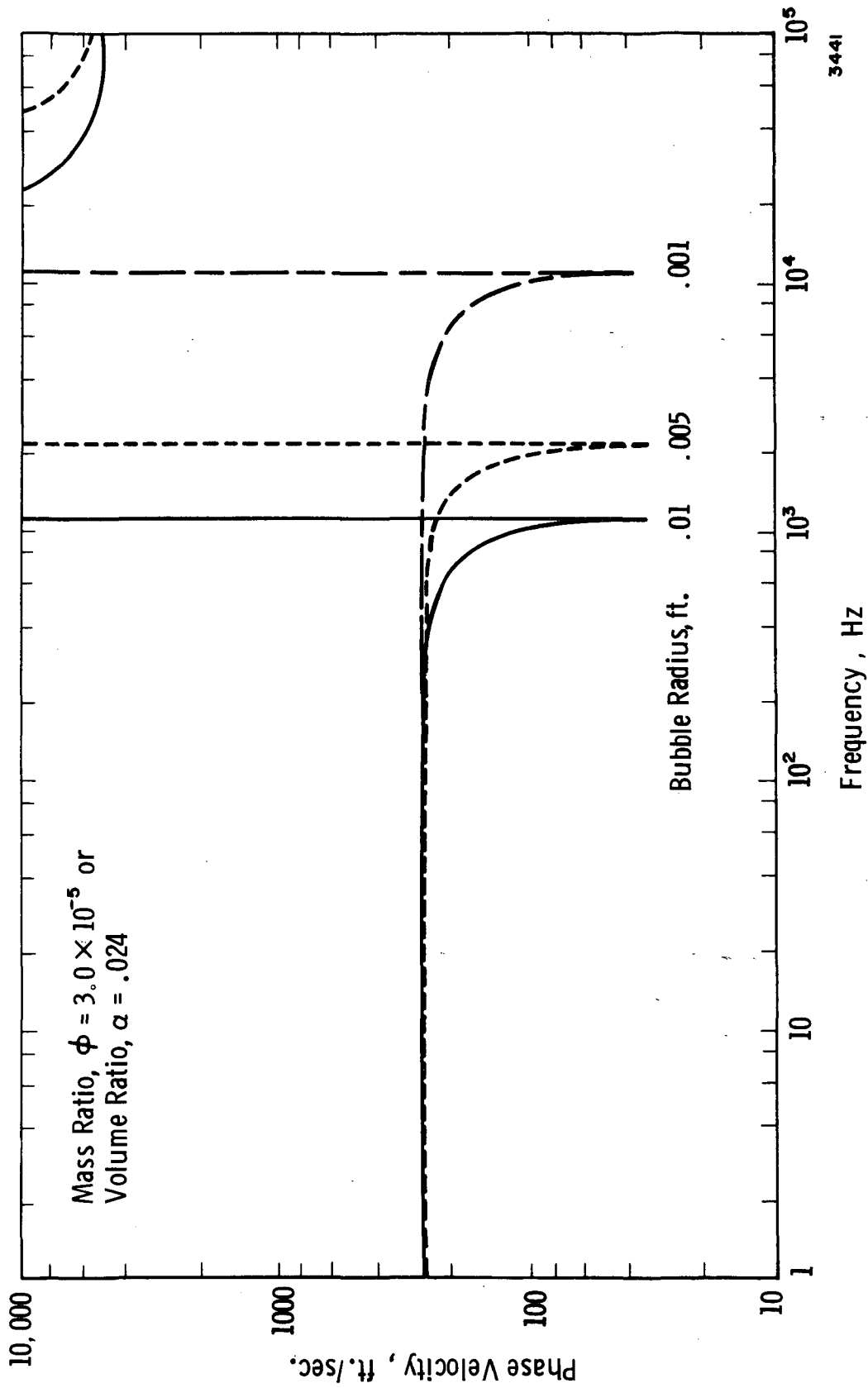


Figure 6. Effect Of Frequency And Bubble Size On Phase Velocity Of Air And Water Mixture

the wave propagation can be neglected. This topic is thoroughly discussed in Section III. 3.

The influence of the wall compliance (and mass) on the propagation of the zeroth mode cannot be neglected. Gerlach⁵ investigated the case of a viscous fluid flowing through a line having elastic flexible walls, i. e., a line whose walls have finite radial compliance and impedance but do not propagate disturbances axially. By equating the radial impedance of the wall to the radial impedance of the fluid, the latter being subject to the no-slip condition on axial fluid velocity at the wall, the following characteristic equation for the eigenvalue problem was obtained:

$$\left[\beta \frac{J_1(\beta r_o)}{J_0(\beta r_o)} - \frac{\gamma^2}{k} \frac{J_1(kr_o)}{J_0(kr_o)} \right] = \rho_t h s^2 + h E_t / r_o^2 \quad (24)$$

The parameters, β and k , are separation constants of the solution of the Navier-Stokes equations and are related by

$$\gamma^2 = k^2 + s/\nu = \beta^2 + s^2/c_o \quad (25)$$

where

- h = tube wall thickness
- r_o = tube radius
- E_t = Young's modulus for tube material
- ρ_t = density of tube wall
- s = Laplace variable
- c_o = isentropic speed of sound in the fluid
- ν = fluid kinematic viscosity
- ρ_o = fluid density
- J_o, J_1 = zero and first-order Bessel functions of the first kind.

Equations (24) and (25) were solved numerically on the computer. Figures 7 and 8 illustrate the effect of an "elastic, flexible wall" (a wall with radial compliance and mass) on the spatial attenuation and phase velocity for the zeroth mode. The area of interest in these figures corresponds to dimensionless frequency numbers, $\omega r_o / c_o$, less than 1.0, since it is known that coupled structural-

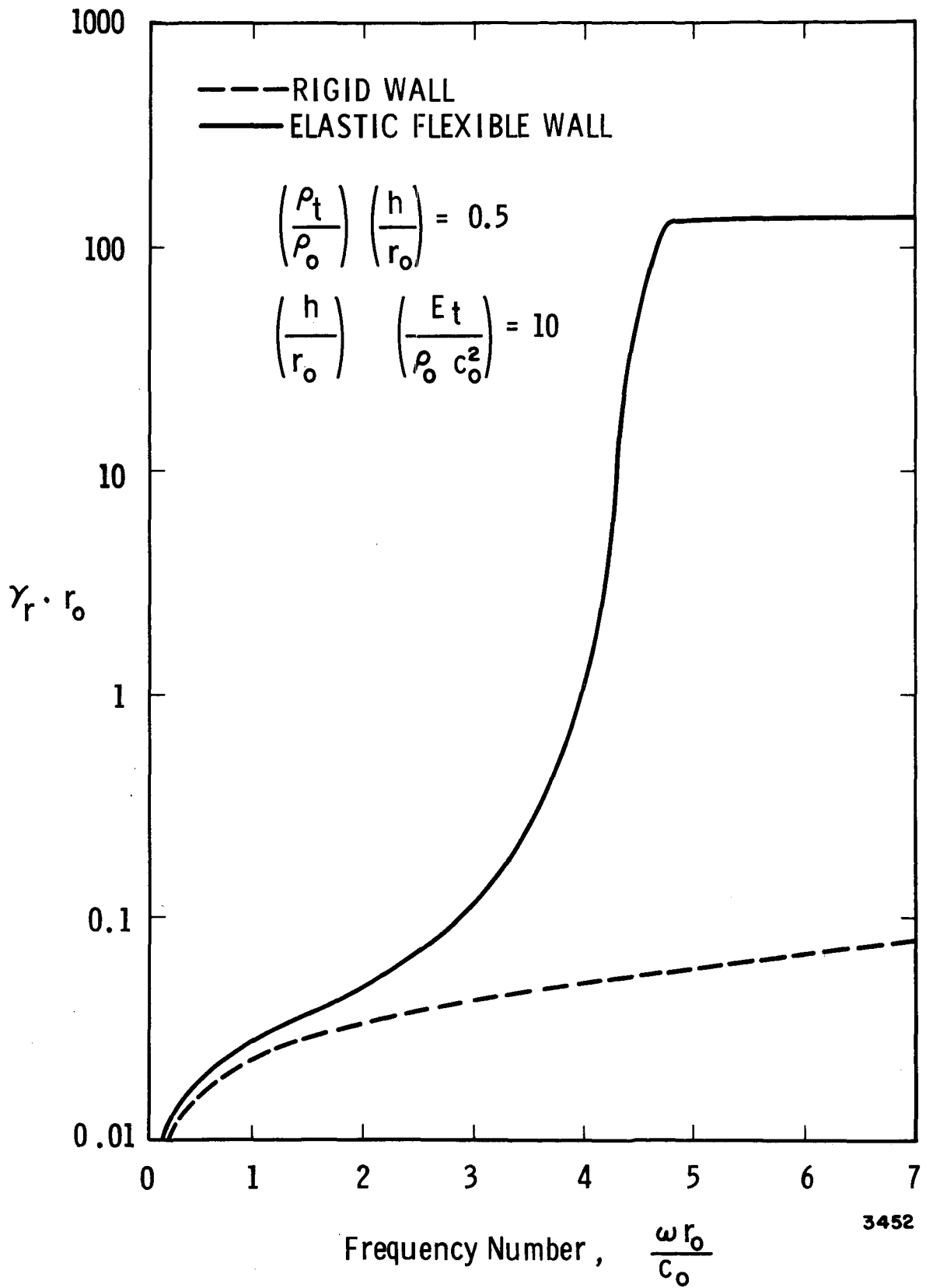


Figure 7. Zeroth Mode Spatial Attenuation Versus Frequency Number For A Rigid And An Elastic Flexible Wall

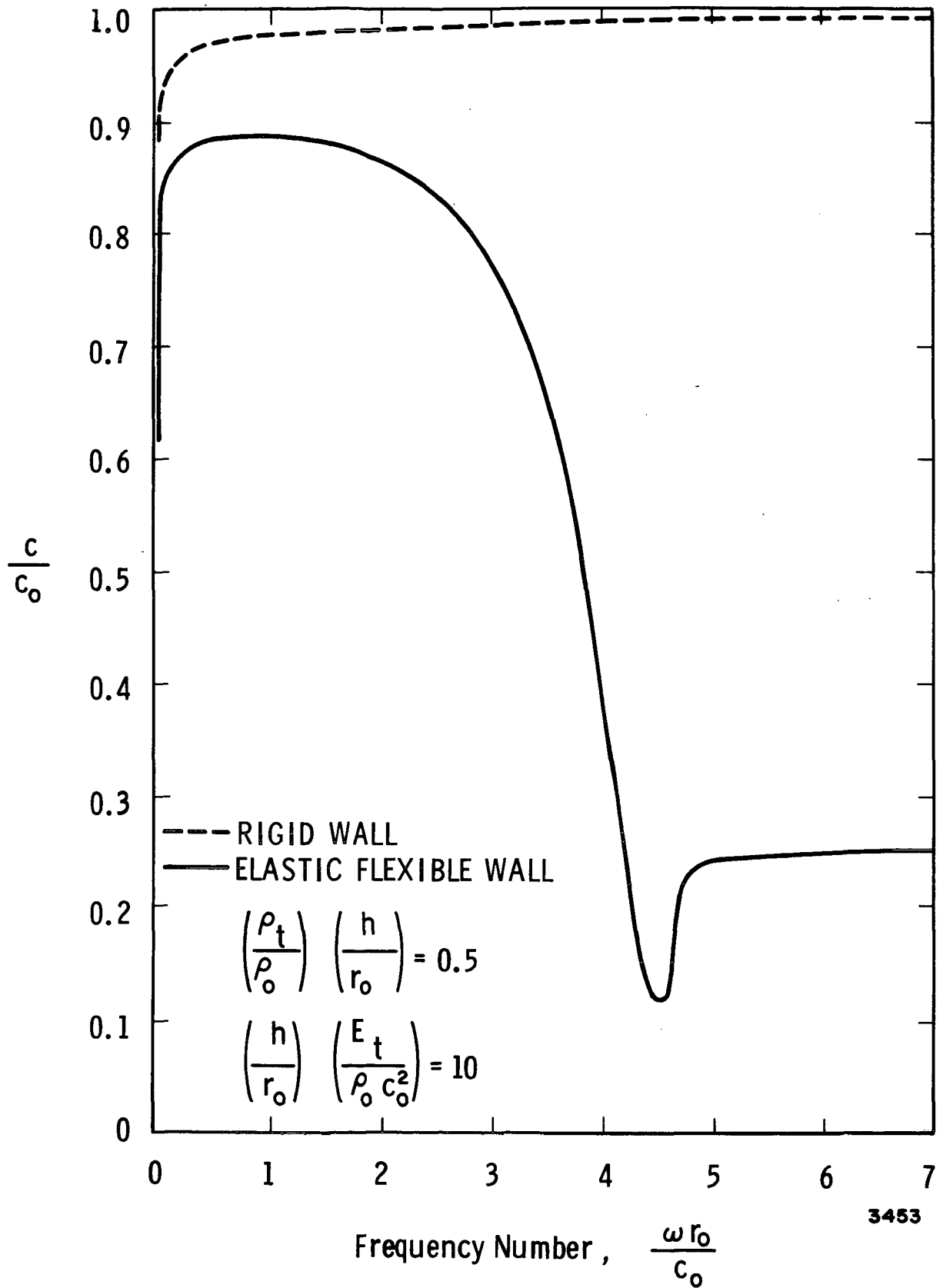


Figure 8. Zeroth Mode Dimensionless Phase Velocity, c/c_o , Versus Frequency Number For A Rigid And An Elastic Flexible Wall

feedsystem instabilities occur in this frequency range. In this range, the wall behaves in a spring-like manner and inertia effects are negligible; radial attenuation for the elastic wall is virtually indistinguishable from the attenuation of the rigid wall. It has been established that for any practical feedline problem, this is the case; hence, only the wall radial compliance need be considered. Wall mass effects are negligible. Therefore, the classic Korteweg correction to the phase velocity is valid. That is,

$$c = \frac{c_0}{\left(1 + \frac{2\rho_0 c_0^2 r_0}{E_t h}\right)^{\frac{1}{2}}} \quad (26)$$

It must be remembered, however, that this correction is the result of applying a boundary condition to the fluid dynamic formulation.

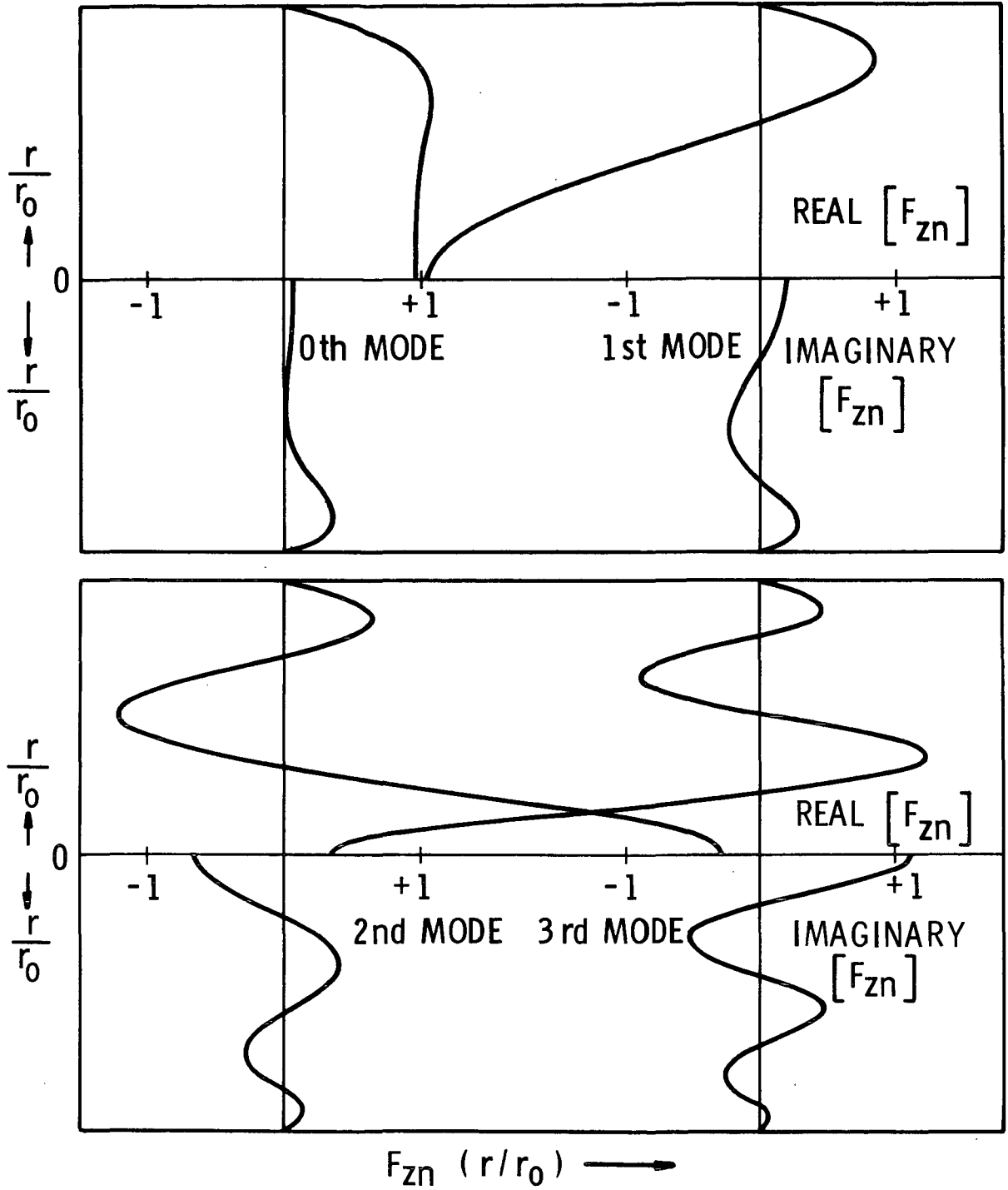
III. 3 Axial Wall Stiffness

In the preceding section, it was stated that the effect of axial wall stiffness on higher mode wave propagation could be neglected. That statement can be justified by proving the following points:

- (1) Due to observable flow processes in feedlines, there is a minimal amount of energy available in the higher modes of the fluid for coupling with the wall.
- (2) The energy that is available in each higher fluid mode has an attenuation rate, below the cut-off frequency, of approximately two orders of magnitude larger than that for the zeroth mode. Therefore, the energy level and attenuation rate do not permit sustained coupling of the fluid and the wall in the higher modes.

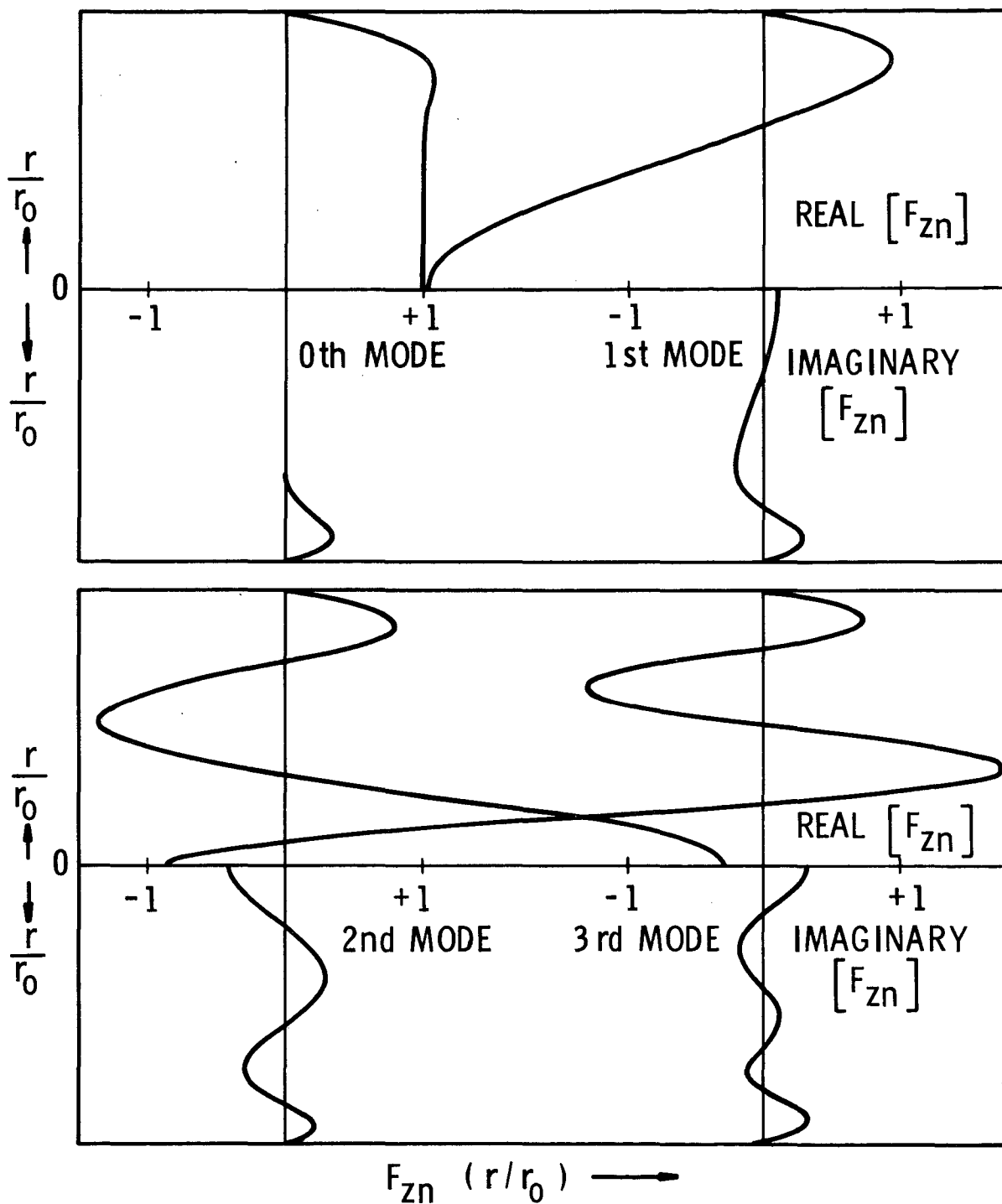
The physical effect of higher modes must be considered, because the proposed distributed parameter line model is based on only the zeroth mode of propagation, and the existence of substantially higher modes would invalidate its functional form.

Recall that the magnitude of Reynold's numbers in a typical feedline indicates a turbulent flow condition. Hence, the velocity profile should be relatively flat. Gerlach⁵ has calculated the perturbation velocity profiles of the first four modes for the laminar, viscous pipe-flow problem. Characteristic results are shown in Figures 9 and 10 where $F_{zn}(r)$ is the velocity distribution function. Observe closely that, for the wide range of frequencies and damping



3657

Figure 9. Axial Velocity Profile Function, $F_{zn}(r)$, for Four Modes ($\omega r_0/c_0 = 1.0$, $\nu/r_0 c_0 = 0.01$)



3658

Figure 10. Axial Velocity Profile Function, $F_{zn}(r)$, for Four Modes ($\omega r_0 / c_0 = 0.2$, $\nu / r_0 c_0 = 0.001$)

numbers considered, the zeroth mode velocity distribution is nearly constant across the cross-section. The obvious conclusion is that the zeroth mode perturbation profile approximates a turbulent profile, and, hence, a minimal contribution from the higher modes is required to fill out the turbulent profile. Therefore, it follows that the energy level in the higher modes is negligible.

Based on the foregoing discussion, there is admittedly a small contribution of the higher modes to the velocity profile. However, Gerlach⁵ has also shown that the spatial attenuation (the real part of the propagation operator) for these higher modes is substantially larger than for the zeroth mode. The net effect is that the higher modes are rapidly damped out over a broad frequency range, and therefore have neither the time nor the energy levels required to excite (couple) corresponding modes of transmission in the conduit wall. Figure 11 illustrates the elevated damping level of higher modes, while the zeroth mode attenuation is roughly insensitive to the frequency range.

The above discussion substantiates the validity of the zeroth mode transfer equations for the line. In addition, the foregoing conclusions which were derived on a qualitative basis, have also been verified quantitatively by Lin and Morgan¹⁵.

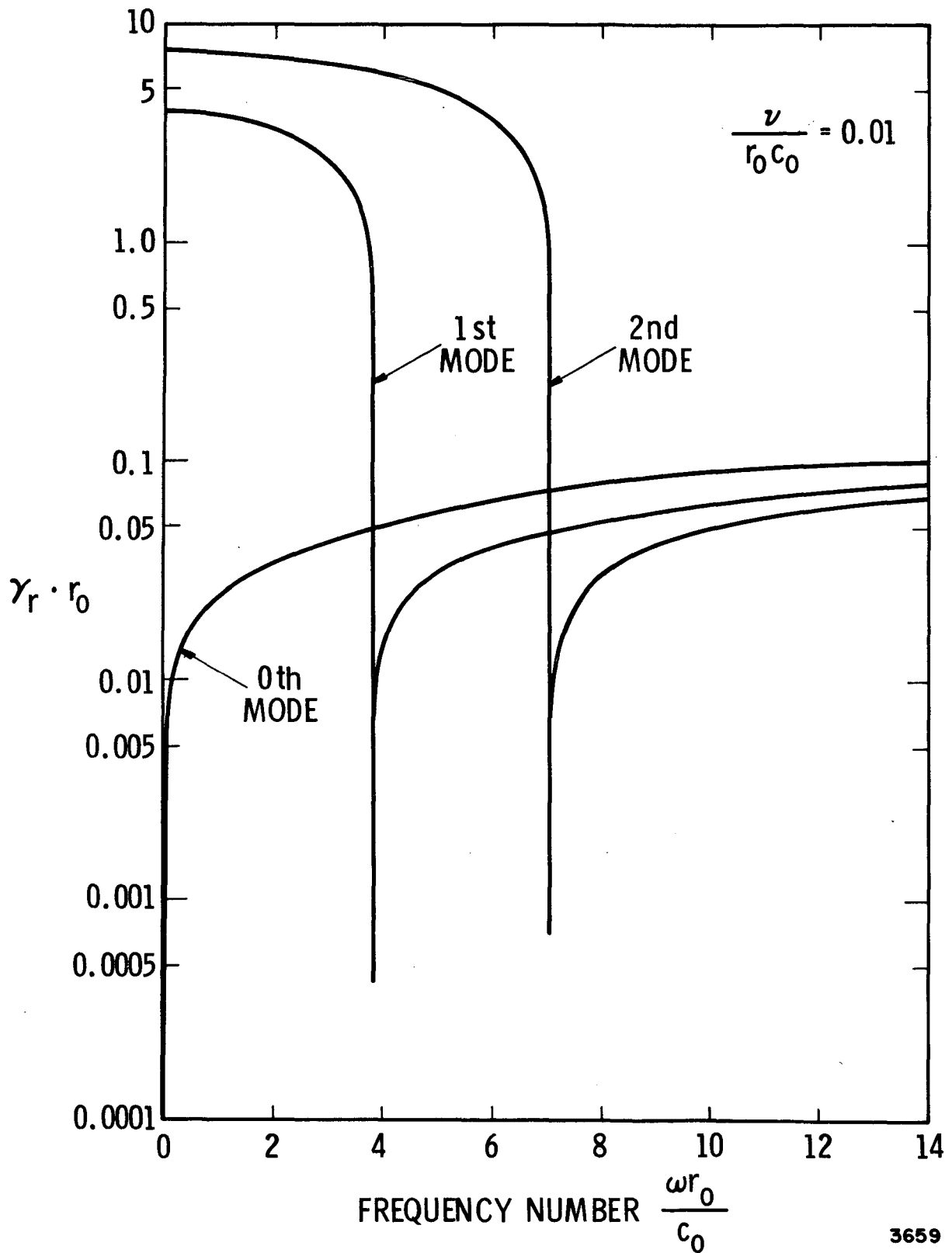


Figure 11. Plot of the Spatial Attenuation Factor Versus Radial Frequency Number for Three Modes

IV. LOCAL COMPLIANCES - LARGE BUBBLES AND CAVITATION ZONES

At elbows or bends in the feedline, or at the pump inlet, local pressure drops are likely to create regions of cavitation. In most cases, these regions are composed of localized bubbles of vapor. These larger cavitation bubbles in the line are modeled by considering the bubbles to be local compliances. As the excitation frequency approaches the bubble resonant frequency, which can be quite low for large bubbles, the volume pulsations may be described by the following linear, second-order differential equation:

$$\frac{\rho_l}{4\pi R_o} \ddot{v} + b\dot{v} + \frac{\eta P_o}{V_o} v = -p(t) \quad (27)$$

or

$$m_2 \ddot{v} + b\dot{v} + kv = -p(t) \quad (28)$$

where

- ρ_l = liquid density
- P_o = steady state line pressure
- V_o = steady state bubble volume
- R_o = steady state bubble radius
- b = coefficient accounting for viscous, thermal and radiation damping.

The continuity equation relating the flow upstream and downstream of the bubble is

$$q_2 - q_1 = dv/dt \quad (29)$$

where q_1 and q_2 represent the upstream and downstream volumetric flow rate, and dv/dt is the change in bubble volume with time. Equations (28) and (29) can be combined conveniently in the Laplace transform domain to yield an expression for the change in flow rate due to the presence of the bubble.

$$Q_2(s) - Q_1(s) = \frac{-sP(s)}{(m_2 s^2 + bs + k)} \quad (30)$$

where the term $1/(m_2 s^2 + bs + k)$ can be visualized as a "complex" compliance. The damping term, b , has been estimated by Devin¹⁶, and is represented by a combination of thermal damping, sound radiation damping, and viscous damping.

For zero damping of the oscillations,

$$Q_1(s) - Q_2(s) = \frac{s P(s)}{k \left(1 + \frac{m_2}{k} s^2 \right)} \quad (31)$$

At frequencies considerably below the bubble natural frequency, ω_0 ,

$$Q_1(s) - Q_2(s) = \frac{s P(s)}{k} \quad (32)$$

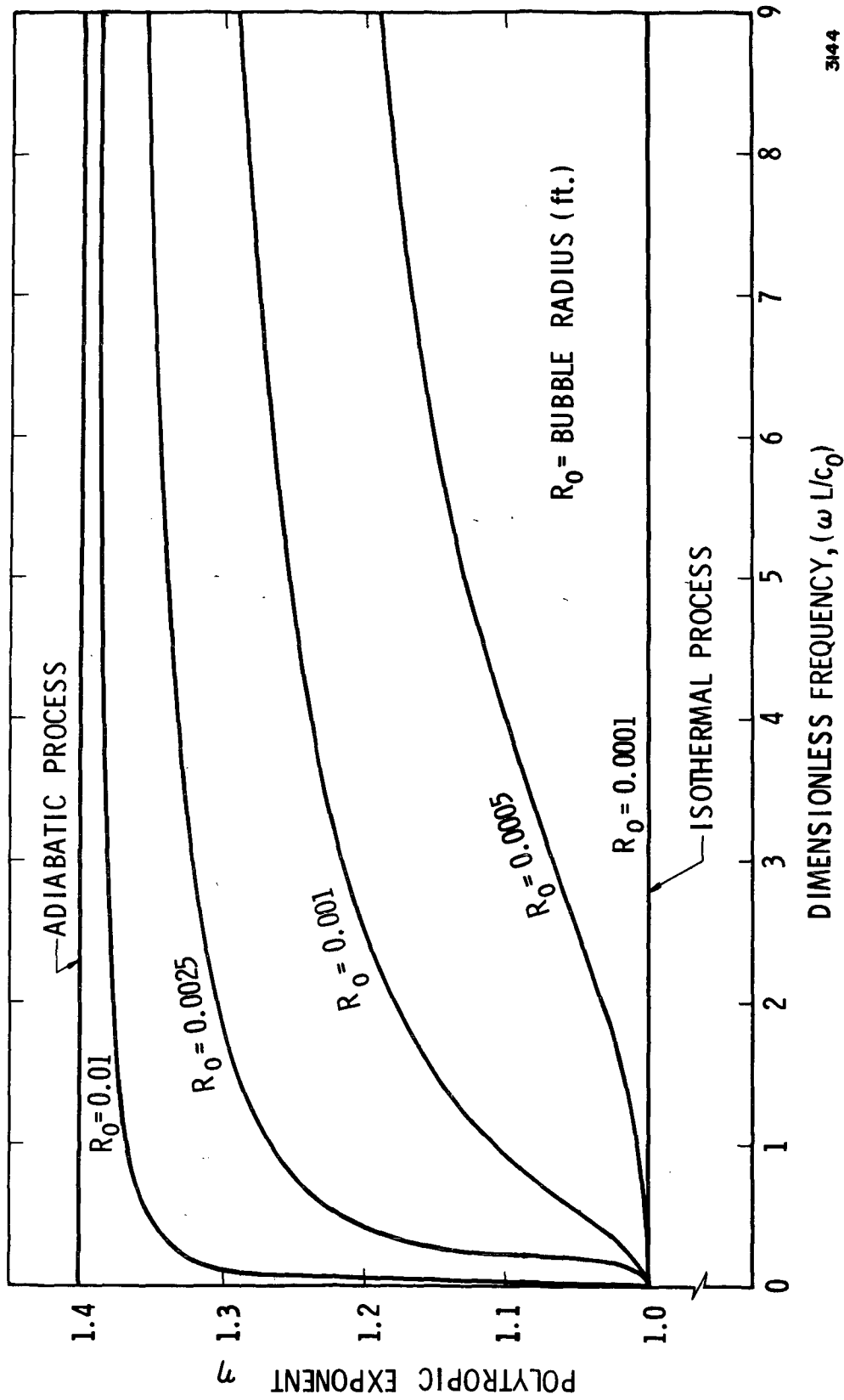
where ω_0 is defined as

$$\omega_0 = \sqrt{k/m_2} \quad (33)$$

For these low frequency cases, the compliance becomes simply

$$C = \frac{V_0}{\eta P_0} \quad (34)$$

The correct value of the polytropic exponent η in the stiffness term $k = \eta P_0/V_0$ depends on the bubble size and frequency, as well as the thermal properties of the gas and liquid. This variation with bubble size and frequency of excitation is shown in Figure 12. For a given bubble undergoing successive compressions, the gas near the center behaves adiabatically, while the gas near the liquid-gas interface undergoes no change in temperature since the liquid behaves as a large heat sink. The polytropic exponent, η , is calculated by the method described in Appendix C.



3144

Figure 12. Polyropic Exponent for O_2 Bubble in LOX vs Dimensionless Frequency and Bubble Size

V. COUPLED RESPONSES

V. 1. Accelerated Line

One possible mode of structural-hydraulic coupling is shown in Figure 13. An externally imposed, rigid-body acceleration acts on a length of feedline that is transporting liquid propellant. Because of viscous shearing forces at the propellant-conduit interface, the imposed line motion will couple with the fluid motion to produce modifications to the pressure-flow equations for the stationary line (Section II. 1). The functional form of these modifications can be easily derived.

The fluid may be characterized by the familiar axisymmetric, linearized, perturbation equations of motion, continuity and state.

$$\frac{\partial u}{\partial t} = -\frac{1}{\rho_0} \frac{\partial p}{\partial z} + \nu \left[\frac{\partial^2 u}{\partial r^2} + \frac{1}{r} \frac{\partial u}{\partial r} \right] + \frac{F_z}{\rho_0} \quad (35)$$

$$\frac{\partial \rho}{\partial t} + \rho_0 \frac{\partial u}{\partial z} = 0 \quad (36)$$

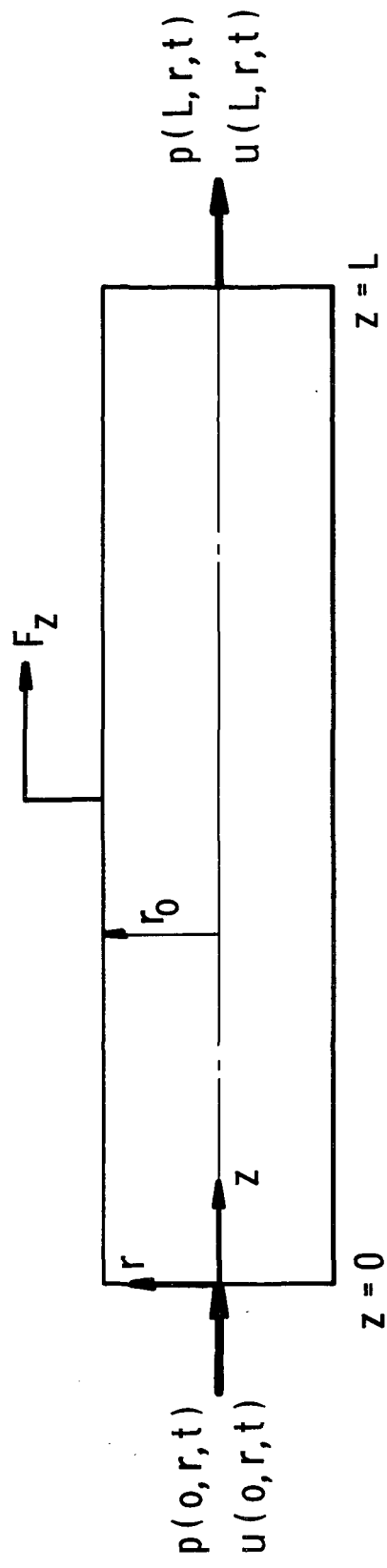
$$\frac{\partial \rho}{\rho_0} = \frac{\partial p}{\kappa}, \quad \kappa = \rho_0 c_0^2 \quad (37)$$

Implicit in this formulation is the assumption that the radial perturbation velocity is negligible compared to the axial perturbation velocity, u . Note that the pressure has not been assumed to be independent of the radial coordinate. The body force F_z , can be replaced by the equivalent D'Alembert force, $-\rho_0 a_z$, due to the imposed acceleration. Utilizing this substitution, combining the continuity and state equations and applying the Laplace transformation with zero initial conditions, yields the following pair of coupled differential equations:

$$sU = -\frac{1}{\rho_0} \frac{\partial P}{\partial z} + \nu \left[\frac{\partial^2 U}{\partial r^2} + \frac{1}{r} \frac{\partial U}{\partial r} \right] - A_z \quad (38)$$

$$P = -\frac{\rho_0 c_0^2}{s} \frac{\partial U}{\partial z} \quad (39)$$

where P and U represent the transformed fluid pressure and velocity. These equations can be combined into a single equation in the dependent variable U .



3656

Figure 13. Fluid Conduit with Axial Vibration

$$sU = \frac{c_o^2}{s} \frac{\partial^2 U}{\partial z^2} + \nu \left[\frac{\partial^2 U}{\partial r^2} + \frac{1}{r} \frac{\partial U}{\partial r} \right] - A_z \quad (40)$$

Making use of the fact that A_z is a function only of the Laplace variable, s , and redefining the dependent variable to be

$$V(r, z, s) = U + A_z/s \quad (41)$$

results in the following easily solved, ordinary differential equation:

$$\frac{\nu}{s} \left[\frac{\partial^2 V}{\partial r^2} + \frac{1}{r} \frac{\partial V}{\partial r} - \frac{s}{\nu} V \right] + \frac{c_o^2}{s^2} \frac{\partial^2 V}{\partial z^2} \quad (42)$$

This equation is amenable to solution by the standard separation of variables technique which yields

$$V = (A \cosh \lambda z + B \sinh \lambda z) J_o(\alpha r) \quad (43)$$

where

$$\alpha^2 = \frac{s}{\nu} \left(\lambda^2 \frac{c_o^2}{s^2} - 1 \right)$$

$\lambda^2 =$ separation constant

$A, B =$ integration constants.

By definition, λ is the propagation operator, γ , which governs the spatial attenuation of axially propagated waves in the fluid. This operator may be stated a priori:

$$\gamma = \frac{s}{c_o} \frac{1}{\left(1 - \frac{2 J_1(\xi r_o)}{\xi r_o J_o(\xi r_o)} \right)^{\frac{1}{2}}} \quad (44)$$

where

$$\xi^2 = -s/\nu, \quad r_o = \text{conduit radius}$$

In addition, the characteristic impedance of the line, Z_c , is defined to be

$$Z_c = \frac{\rho_o c_o^2}{s} \gamma \quad (45)$$

Utilizing these definitions, the fluid pressure and velocity become

$$U(r, z, s) = [A \cosh \gamma z + B \sinh \gamma z] J_0(\alpha r) - A_2/s \quad (46)$$

$$P(r, z, s) = -Z_c [A \sinh \gamma z + B \cosh \gamma z] J_0(\alpha r) \quad (47)$$

The dependence on the radial coordinate may be eliminated by averaging these expressions across the cross section.

$$\bar{U} = [A \cosh \gamma z + B \sinh \gamma z] \frac{2}{\alpha r_0} J_1(\alpha r_0) - A_2/s \quad (48)$$

$$\bar{P} = -Z_c [A \sinh \gamma z + B \cosh \gamma z] \frac{2}{\alpha r_0} J_1(\alpha r_0) \quad (49)$$

Constants, A and B, can be evaluated at the origin of the line (z=0) by applying the boundary conditions.

$$\bar{U}(0, s) = \bar{U}_1 ; \quad \bar{P}(0, s) = \bar{P}_1 \quad (50)$$

which results in the following expressions:

$$\bar{U} = \bar{U}_1 \cosh \gamma z - \frac{\bar{P}_1}{Z_c} \sinh \gamma z - A_2/s (1 - \cosh \gamma z) \quad (51)$$

$$\bar{P} = \bar{P}_1 \cosh \gamma z - Z_c \bar{U}_1 \sinh \gamma z - \frac{Z_c A_2}{s} \sinh \gamma z \quad (52)$$

The desired four-terminal representation for the mean exit pressure and flow velocity are obtained by evaluating the above expressions at z = L.

$$\bar{U}_2 = \bar{U}_1 \cosh \gamma L - \bar{P}_1/Z_c \sinh \gamma L - V_2 (1 - \cosh \gamma L) \quad (53)$$

$$\bar{P}_2 = \bar{P}_1 \cosh \gamma L - Z_c \bar{U}_1 \sinh \gamma L - V_2 \sinh \gamma L \quad (54)$$

where the acceleration has been replaced by its Laplace equivalent $s V_2$. These equations can be referred to local volumetric flow rate by introducing the line cross-sectional area, A.

V.2 Relative Motion of Bellows and PVC Joints

Bellows

Bellows are commonly used elements in propulsion feed systems, and in their most important application, they serve as a "fix"

for the POGO instability. Bellows vary in their structural complexity from the simple array of axisymmetric convolutes shown in Figure 14a to the configuration in Figure 14b which incorporates a gas trap liner. The following discussion is directed toward the latter configuration which includes the simple bellows as a special or degenerate case.

When the ends of a bellows execute relative motion, the change in volume flow rate between the inlet and exit can be considered to be the sum of two separate effects:

- (1) A flow rate change due to the compliance of the gas trapped under the liner, and
- (2) An apparent local volume production.

It should be noted that the first item exists even in the absence of relative motion.

First, the pressure drop across a bellows in the flow direction is expressed in the Laplace domain by

$$P_2(s) = F(\rho V_L^2, G) P_1(s), \quad (55)$$

where $F(\rho V_L^2, G)$ is a loss factor, dependent on the dynamic pressure and bellows geometry. Now, the change in flow rate due to trapped gas can be written in terms of the bellows inlet pressure.

$$q_2' - q_1' = -C \frac{dp_1}{dt} \quad (56)$$

or in the transform domain

$$Q_2'(s) - Q_1'(s) = -Cs P_1(s) \quad (57)$$

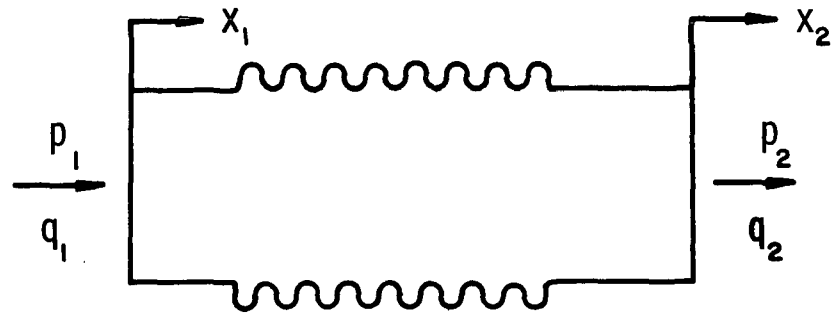
where C is the lumped compliance of the gas and is defined by the ratio of the gas volume to the gas bulk modulus of elasticity.

The apparent volume production can be derived from the continuity equation

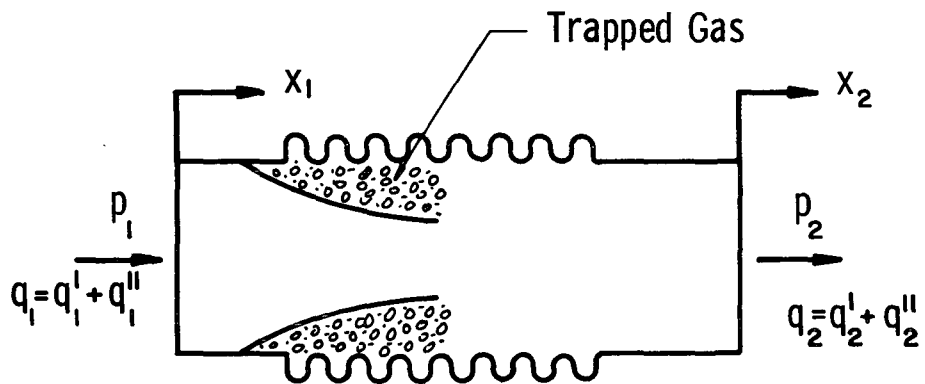
$$q_2'' - q_1'' = dv/dt \quad (58)$$

or in the Laplace domain

$$Q_2''(s) - Q_1''(s) = -s \text{Vol}(s) \quad (59)$$



a. Simple Bellows



()' - quantities associated with compliance of trapped gas

()'' - quantities associated with volume production

b. Bellows With Gas Trap Liner

3442

Figure 14. Nomenclature For Relative Motion Of Bellows

The volumetric production is related to the axial displacement of the bellows ends by

$$\text{Vol}(s) = K_b [X_1(s) - X_2(s)] \quad (60)$$

where K_b is a "volume change" constant, also dependent on the bellows geometry. The resulting flow equation is

$$Q_2''(s) - Q_1''(s) = sK_b [X_1(s) - X_2(s)] \quad (61)$$

or in terms of relative velocities

$$Q_2''(s) - Q_1''(s) = K_b [V_1(s) - V_2(s)]. \quad (62)$$

The combined effect, expressed as the sum of Equations (55) and (62) produces the following result for the change in flow rate:

$$Q_2(s) = Q_1(s) - CsP_1(s) + K_b [V_1(s) - V_2(s)] \quad (63)$$

Equations (55) and (63) describe completely the four terminal pressure-flow relationship for a bellows.

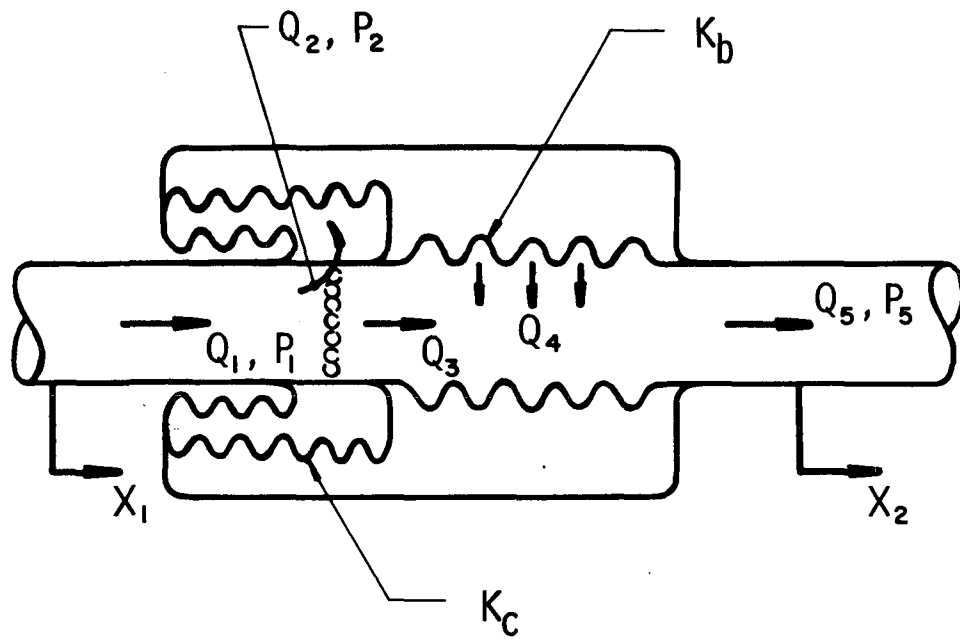
PVC Joints

In many applications, the PVC (pressure-volume compensator) joint is often used in place of an elementary bellows where the local volumetric change effect described above is judged undesirable. A typical PVC joint, shown in Figure 15, generally consists of a bellows to allow line flexibility (either axially, or to allow angulation, or both) and a compensation chamber to "absorb" the excess volume of fluid created in the line when the bellows is displaced axially. In theory, the PVC joint is designed to permit axial length changes without introducing a corresponding fluid volume disturbance in the line. In practice, however, the PVC joint is not a perfect compensation device.

The "volume flow production" of the bellows Q_4 , may be written as

$$Q_4(s) = Q_2(s) - Q_3(s) = K_b [V_1(s) - V_2(s)] \quad (64)$$

where $V_i(s)$, $i = 1$ or 2 , is the transformed velocity associated with coordinate X_i . Similarly, the ideal volume compensation of the PVC may be written as



2756

Figure 15. Illustration Of Typical PVC Joint

$$Q_2(s) = Q_1(s) - Q_3(s) = K_c [V_1(s) - V_2(s)]. \quad (65)$$

Continuity requires that

$$Q_5(s) = Q_1(s) + Q_4(s) - Q_2(s). \quad (66)$$

Combining Equations (64), (65), and (66), the resultant flow becomes

$$Q_5(s) = Q_1(s) + (K_b - K_c) [V_1(s) - V_2(s)]. \quad (67)$$

It is normally intended that $K_b = K_c$ so that perfect compensation is obtained. However, there is a dynamic effect associated with the action of the compensation unit, so a more general form of Equation (65) is

$$Q_2(s) = \frac{K_c}{G(s)} [V_1(s) - V_2(s)] \quad (68)$$

where $G(s)$ might be a simple lag, e.g., $(1 + \tau s)$, caused by a combination of the PVC structure elasticity and fluid compressibility. Equation (67) was selected as the PVC flow rate expression in the feedline computer code. The pressure drop across the joint was assumed to have the same functional form as Equation (55).

V. 3. Forced Changes in Line Length

Propellant feedlines are normally supported by the vehicle structure at discrete points on the line as opposed to a continuous support. A forced change in the length of the line between consecutive supports occurs when vehicle structural inputs to these supports differ in phase and/or magnitude. In an idealized fashion, it can be assumed that the length change is a result of discrete velocity inputs at the extremities of the line, as shown in Figure 16.

The effect that length changes produce on the pressure-flow relationships for the liquid in the line can be analyzed from two different viewpoints. The first approach requires the solution of the fluid dynamic equations of motion subject to an inhomogeneous boundary condition on the spatial variation of axial wall velocity as dictated by the structural inputs, V_1 and V_2 . An alternate approach assumes that the dynamic length change can be modeled as the linear superposition of (1) the axial vibration of a rigid line and (2) a volume production region that reflects the relative motion between the ends of the line as indicated in Figure 17. The results of each

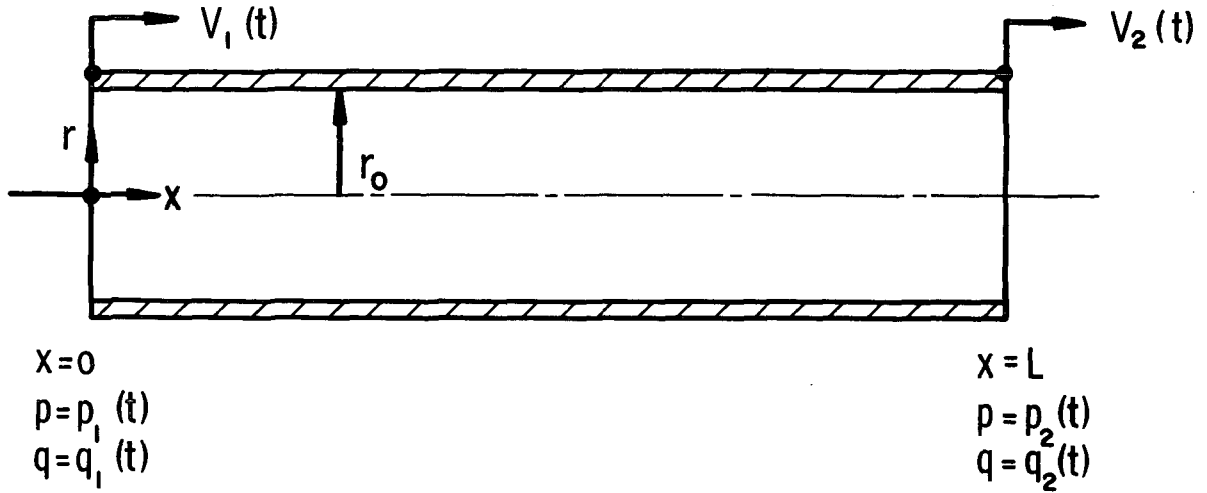


Figure 16. Geometry For Forced Changes In Line Length

analysis technique are summarized below, while specific development details are presented in Appendix D.

The first method of analysis begins with the Laplace transform version of the linearized (1) radial and axial equations of motion for the fluid, (2) continuity equation, and (3) the equation of state. These equations are reduced to one-dimensional form by averaging across the feedline cross section. The solution of the resulting differential equations for the transformed axial velocity is matched to the transformed, inhomogeneous, compatibility condition on wall velocity. This boundary condition is obtained by solving the undamped wave equation for the wall. The resulting transformed pressure-flow equations are:

$$\begin{bmatrix} P_2 \\ Q_2 \end{bmatrix} = \begin{bmatrix} \cosh \gamma L & -Z_c/A \sinh \gamma L \\ -Z_c^{-1} A \sinh \gamma L & \cosh \gamma L \end{bmatrix} \begin{bmatrix} P_1 \\ Q_1 \end{bmatrix} - \frac{\left(\frac{s^2}{c_o^2} - \gamma^2\right) V_1(s)}{\left(\frac{s^2}{c_w^2} - \gamma^2\right)} \begin{bmatrix} \alpha_1 \\ A\alpha_2 \end{bmatrix}$$

$$\alpha_1 = \frac{\rho_o c_o^2}{s} \left[\left(\frac{s}{c_w} \sinh \frac{sL}{c_w} - \gamma \sinh \gamma L \right) + \frac{\left(G - \cosh \frac{sL}{c_w} \right)}{\sinh \frac{sL}{c_w}} \frac{s}{c_w} \times \left(\cosh \frac{sL}{c_w} - \cosh \gamma L \right) \right]$$

$$\alpha_2 = - \left[\left(\cosh \frac{sL}{c_w} - \cosh \gamma L \right) + \frac{\left(G - \cosh \frac{sL}{c_w} \right)}{\sinh \frac{sL}{c_w}} \left(\sinh \frac{sL}{c_w} - \frac{s}{c_w \gamma} \sinh \gamma L \right) \right] \quad (69)$$

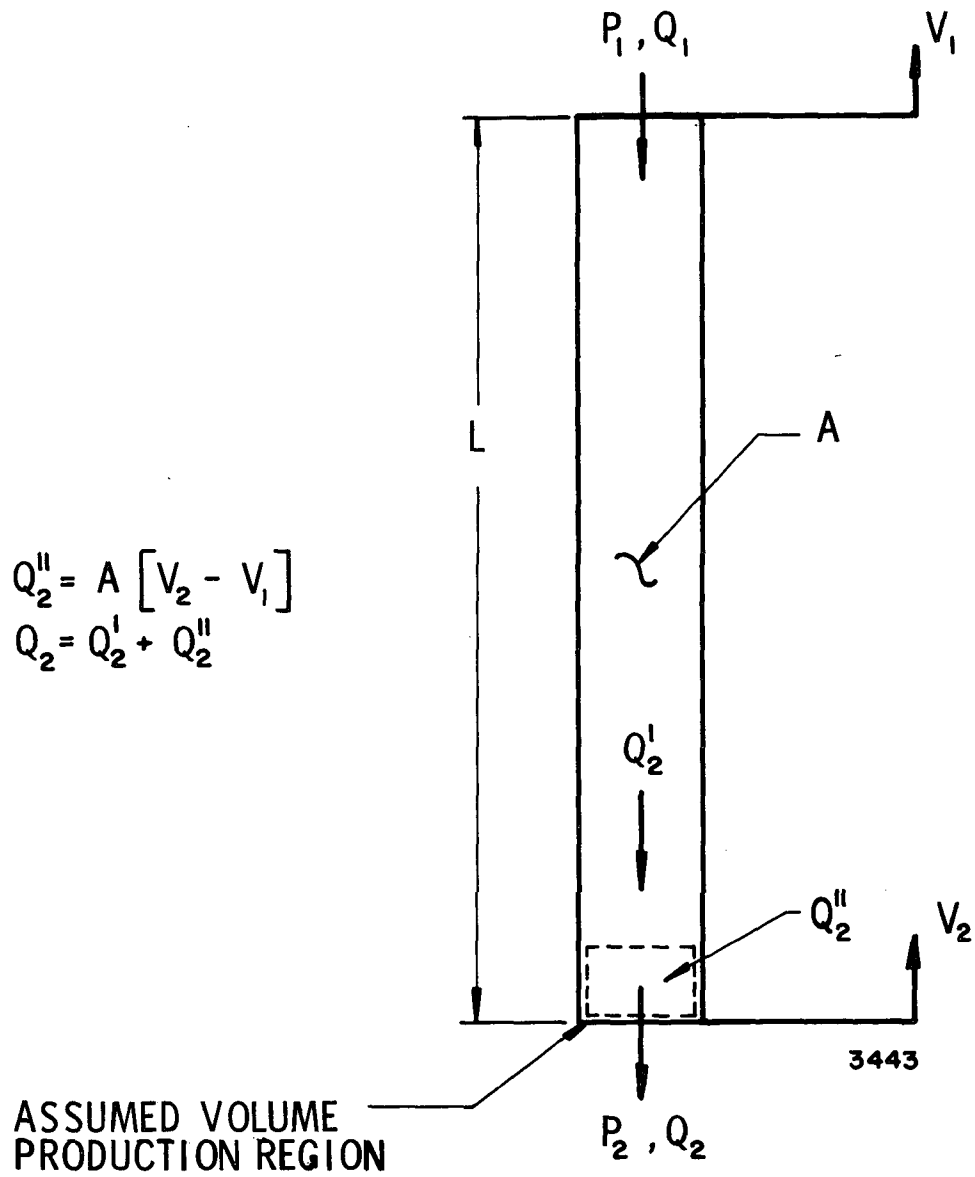


Figure 17. Illustration Of Approximate Modeling Procedure For Forced Changes In Line Length

In these expressions c_w is the longitudinal wave speed in the wall and $G(s)$ is the transfer function relating the structural velocities, V_1 and V_2 . All other terms have been defined in previous sections. It is evident that the effect of forced line length changes is to modify the pressure-flow relationship for a line with no external excitation. It can be shown that when $V_1 = V_2$ the above expressions degenerate to

$$\begin{bmatrix} P_2 \\ Q_2 \end{bmatrix} = \begin{bmatrix} \cosh \gamma L & -Z_c A^{-1} \sinh \gamma L \\ -A Z_c^{-1} \sinh \gamma L & \cosh \gamma L \end{bmatrix} \begin{bmatrix} P_1 \\ Q_1 \end{bmatrix} + V f \begin{bmatrix} Z_c \sinh \gamma L \\ A(1 - \cosh \gamma L) \end{bmatrix} \quad (70)$$

where

$$f = \frac{2 J_1(\xi r_o)}{\xi r_o J_0(\xi r_o)}$$

This latter result was predicted by Gerlach¹⁷ for rigid body, axial vibration of a line.

In the second modeling approach, the pressure-flow equations for the rigid body motion of a line are modified with a volume production element that reflects the relative motion of the ends of the line. For a rigid line oscillating with velocity, V_1 ,

$$\begin{bmatrix} P_2 \\ Q_2' \end{bmatrix} = \begin{bmatrix} \cosh \gamma L & -A^{-1} Z_c \sinh \gamma L \\ -Z_c^{-1} A \sinh \gamma L & \cosh \gamma L \end{bmatrix} \begin{bmatrix} P_1 \\ Q_1 \end{bmatrix} - V_1 \begin{bmatrix} Z_c \sinh \gamma L \\ A(1 - \cosh \gamma L) \end{bmatrix} \quad (71)$$

The rate of volume generation due to relative motion is

$$Q_2'' = A(V_2 - V_1) \quad (72)$$

Total volumetric flow rate is then the sum of Q_2' and Q_2'' . Combining Equations (71) and (72) yields

$$\begin{bmatrix} P_2 \\ Q_2 \end{bmatrix} = \begin{bmatrix} \cosh \gamma L & -A^{-1} Z_c \sinh \gamma L \\ -Z_c^{-1} A \sinh \gamma L & \cosh \gamma L \end{bmatrix} \begin{bmatrix} P_1 \\ Q_1 \end{bmatrix} - V_1 \begin{bmatrix} Z_c \sinh \gamma L \\ A(2 - \cosh \gamma L - G(s)) \end{bmatrix} \quad (73)$$

As before, $G(s)$ describes the relationship between the externally imposed velocities, V_1 and V_2 .

Equations (69) and (73) cannot be compared directly since, in the first case, the excitation is coupled to the fluid by a boundary

condition and, in the latter case, the coupling takes the form of a body force applied to the fluid.

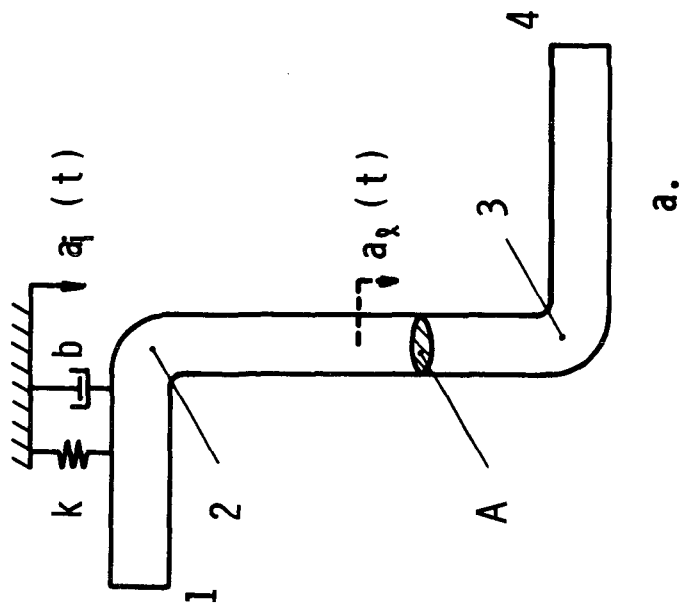
We believe that the result obtained by treating the problem as an inhomogeneous boundary valued problem is the most accurate, and it is this expression, Equation (69), that has been incorporated into the computer code.

V. 4. Mounting Stiffness

Propellant feedlines are anchored to the primary vehicle structure by mounting brackets that exhibit varying degrees of elasticity and damping. These brackets act as filters which modify the structural excitation that is transmitted to the feedline. There are two techniques that can be utilized in modeling the effect of mounting stiffness: (1) discrete parameter-acceleration, and (2) impedance. Both of these methods are summarized in this section; detailed developments are contained in Appendix E. The transfer equations for the discrete parameter-acceleration technique have been programmed as Subroutine Eight in the computer program while the impedance approach is programmed in Subroutine Ten.

Discrete Parameter-Acceleration Technique

Consider the idealized configuration shown in Figure 18. The entire line, which has two bends, is assumed to be infinitely rigid and elastically restrained. A single linear spring in parallel with a viscous damper represents the combined effect of all the discrete mounting stiffnesses whose line of action coincides with that of the equivalent mounting stiffness. In Section V. 1, an expression was derived for the pressure and flow rate in a vertical line that is excited by a velocity, V_ℓ , applied directly to the line. That expression forms the starting point for the analysis of the present configuration. The analytic steps, which will now be summarized qualitatively, are presented quantitatively in Appendix E. Initially, the velocity, $V_\ell(s)$, is replaced by its Laplace equivalent, $a_\ell(s)/s$. The problem is to express the resultant line acceleration, $a_\ell(s)$, in terms of the applied structural acceleration, $a_1(s)$, the viscoelastic support parameters and the fluid mass contained in the horizontal limbs of the feedline. By neglecting the elbow at the exit to the fuel tank, this aspect of the problem is easily overcome by viewing the entire system as a damped, harmonic oscillator whose mass is equivalent to the combined liquid mass in the horizontal limbs. The support is excited by $a_1(s)$, and the inertial effects in the vertical line segment are taken into account by applying the dynamic fluid pressure



3434

b.

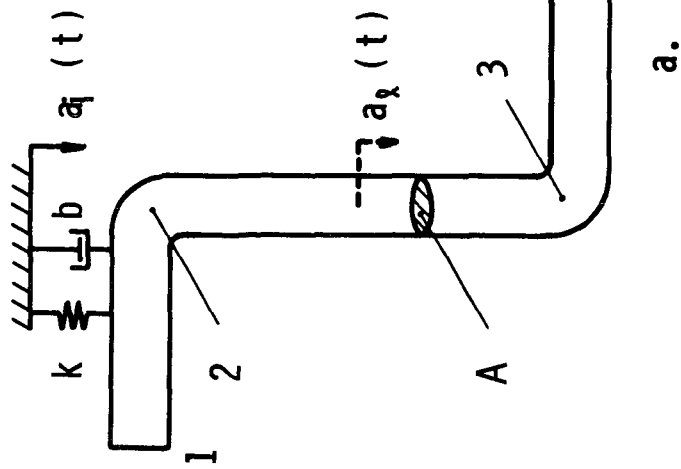


Figure 18. Model For A Line With Mounting Stiffness

forces on the projected areas of the elbows to the system mass, i. e., at Stations 2 and 3. Solution in the Laplace domain yields

$$a_{\ell}(s) = a_1(s) \left[\frac{sb+k}{Ms^2+sb+k} \right] + A(P_3 - P_2) \left[\frac{s^2}{Ms^2+sb+k} \right] \quad (74)$$

where M is the fluid mass of the oscillator. Equation (74) is then substituted into the accelerated line equations, and after simplification, the following result is obtained:

$$\begin{bmatrix} P_3 \\ Q_3 \end{bmatrix} = \begin{bmatrix} \frac{L_{11}+\beta'}{1+\beta'} & \frac{L_{12}}{1+\beta'} \\ \frac{L_{21}+\beta''(1-L_{11})}{1+\beta'} & \frac{L_{22}-\beta''L_{12}}{1+\beta'} \end{bmatrix} \begin{bmatrix} P_2 \\ Q_2 \end{bmatrix} - \frac{a_1(s)}{1+\beta'} \begin{bmatrix} \alpha' \\ \alpha'' \end{bmatrix} \quad (75)$$

The L_{ij} terms are the elements of the original matrix for the accelerated line. The remaining terms, i. e., α' , α'' , β' , and β'' , contain the system mass, support spring constant and damping coefficient. As the support becomes progressively stiffer, Equation (75) degenerates into the expression for a simple accelerated line (Section V. 1).

Impedance Technique

The impedance technique will now be applied to the same line configuration that was used in the previous case with the exception that the mounting stiffness which consisted of a grounded acceleration, a_1 , and a viscoelastic support, is replaced by a driving point impedance, Z_s . As before, the starting point for the analysis is the four-terminal representation of line that is subject to velocity excitation, V_{ℓ} (see Section V. 1). It is required that the line velocity be expressed in terms of the imposed forces and ultimately in terms of the driving point impedance. The equation of motion for the three-segment line in the Laplace domain is

$$F = A(P_3 - P_2) - MsV_{\ell} \quad (76)$$

The quantity, F , represents the lumped external force applied to the line through the impedance element, and it essentially replaces a combined effect of the spring-dashpot combination in the previous development. Using the definition of driving point impedance, F/V_{ℓ} , in conjunction with the above equation of motion, the line velocity can be expressed by

$$V_l = \frac{A(P_3 - P_2)}{Z_s + Ms} \quad (77)$$

where Z_s is the structural impedance. All other quantities have the same definition as before. The resulting transfer matrix for line response is obtained by substituting this expression for the line velocity into the accelerated line equations in Section V.1. The result is

$$\begin{bmatrix} P_3 \\ Q_3 \end{bmatrix} = \begin{bmatrix} \frac{L_{11} + \alpha}{1 + \alpha} & \frac{L_{12}}{1 + \alpha} \\ L_{21} + \frac{\beta(1 - L_{11})}{1 + \alpha} & L_{22} - \frac{\beta L_{12}}{1 + \alpha} \end{bmatrix} \begin{bmatrix} P_2 \\ Q_2 \end{bmatrix} \quad (78)$$

where

$$\alpha = \frac{AZ_{c_2} \sinh \Gamma_2}{Z_s + Ms}$$

$$\beta = \frac{A^2(1 - \cosh \Gamma_2)}{Z_s + Ms}$$

L_{ij} = elements of original accelerated line matrix.

In the case of a rigid support, the structural impedance approaches infinity, and the transfer equation degenerates into the familiar four-terminal representation of a simple, stationary line. It is interesting to note that even though the line is being excited externally, the form of the response equations do not include the trailing excitation terms as is the case with the other forms of excitation that are considered in this report.

VI. GENERALIZED FEEDLINE COMPUTER CODE

A versatile computer code has been generated to calculate the frequency response of propellant feedlines. Program philosophy and logic are discussed in this section, and the mechanics of setting-up and execution including specific example problems are presented in Appendix H.

The construction of a computer code to generate the frequency response of a propellant feedline is a relatively straightforward task when the sequence of feedline components (lines, bellows, PVC joints, etc.) is fixed by a specific design configuration. However, for preliminary design analyses, it is advantageous to determine the effect that a reordering of line components would produce on the overall feedline response. For example, various sequences of components could materially affect the structural-hydraulic coupling that is known to influence the instabilities that were delineated in Section I. It can readily be visualized that reprogramming the feedline response equations for numerous changes in the component sequence is an extremely expensive, time-consuming task. To alleviate this situation, a master computer code was written in FORTRAN IV for the CDC 6400 to provide the systems engineer with a design tool for obtaining the frequency response of a feedline in which the type, number and sequence of basic line components between the propellant tank and the turbopump inlet can be specified in a completely arbitrary fashion. The dominant criterion employed in generating this code was that the "user" be required to perform a minimal amount of manual conditioning of a given problem prior to machine execution.

Formulation of the code is based on the fact that the four-terminal pressure-flow relationship across any line component can be represented in matrix form when the perturbation equations are transformed into the Laplace domain. That is, with no loss in generality,

$$\begin{bmatrix} P_{i+1} \\ Q_{i+1} \end{bmatrix} = \underline{D}_i \begin{bmatrix} P_i \\ Q_i \end{bmatrix} \pm K \underline{C}_i; \quad i = 1, 2, \dots, n \quad (79)$$

where n represents the number of components in the line. In this expression, the transformed output pressure and flow for a given component are related to the corresponding input quantities through a 2×2 square matrix, \underline{D}_i , plus a column matrix, \underline{C}_i , that is present only if that particular component is being excited by an

external forcing function, K . The parameter, K , may be the Laplace transform of an externally imposed acceleration or velocity, or the volume perturbation due to a side branch pulser. In general, it is desired to determine the perturbation pressure at some point in the line in response to any one of the class of forcing functions that K represents. With regard to propellant feedline analyses, the important pressure point is located at the entrance to the turbopump because dynamic variations in the inducer inlet suction head are instrumental in the growth of structural-fluid dynamic instabilities. Having established the desired output variable, the functional form of the transfer function for the overall line is obtained by applying Equation (79) to each line component followed by sequential matrix substitution to arrive at the following generalized transfer equation:

$$\underline{P} = \underline{D} \underline{Q} \pm K \underline{B} \quad (80)$$

Through experience we have found that matrix \underline{D} can be stated a priori for any feedline composed of n ordered components.

$$\underline{D} = \underline{D}_n \underline{D}_{n-1} \underline{D}_{n-2} \dots \underline{D}_1 \quad (81)$$

Matrix \underline{B} , however, does not possess such a well-defined property. In general,

$$\underline{B} = \underline{B}_1 + \underline{B}_2 + \dots + \underline{B}_m \quad (82)$$

The value of "m" is strongly dependent on the line configuration as is the matrix structure of each \underline{B}_j . The distinguishing feature of each \underline{B}_j is that it consists of a column matrix of one of the \underline{C}_1 's pre-multiplied by one or more \underline{D}_i 's. Matrix \underline{P} in Equation (80) contains the desired pressure response to the perturbation, K , and matrix \underline{Q} contains the pressure-flow perturbations at the exit to the fuel tank. By assuming that the impedance at the tank exit, Z_t , is known and that the turbopump-injector-engine combination can be lumped into an equivalent impedance, Z_t , Equation (80) can be expanded into its constituent equations to obtain the explicit form of the transfer function

$$\frac{P_n}{K} = \pm \frac{[(d_{21} Z_1 + d_{22}) b_{11} - (d_{11} Z_1 + d_{12}) b_{21}]}{(d_{21} Z_1 + d_{22}) - (d_{11} Z_1 + d_{12}) / Z_t} \quad (83)$$

where the b_{ij} and d_{ij} are the elements of matrix \underline{B} and \underline{D} , respectively.

To illustrate the concepts that have been presented, consider the feedline shown in Figure 19. It is desired to determine the transfer function relating the pressure at the turbopump inlet, P_6 , to the line excitation velocity, V_ℓ . Adjacent to each line component is a matrix expression of the type presented in Equation (79). Performing the previously indicated matrix substitution yields

$$\begin{bmatrix} P_6 \\ P_6/Z_t \end{bmatrix} = \underline{D}_5 \underline{D}_4 \underline{D}_3 \underline{D}_2 \underline{D}_1 \begin{bmatrix} Z_1 Q_1 \\ Q_1 \end{bmatrix} + V_\ell (\underline{D}_5 \underline{C}_4 - \underline{D}_5 \underline{D}_4 \underline{C}_3 - \underline{D}_5 \underline{D}_4 \underline{D}_3 \underline{C}_2) \quad (84)$$

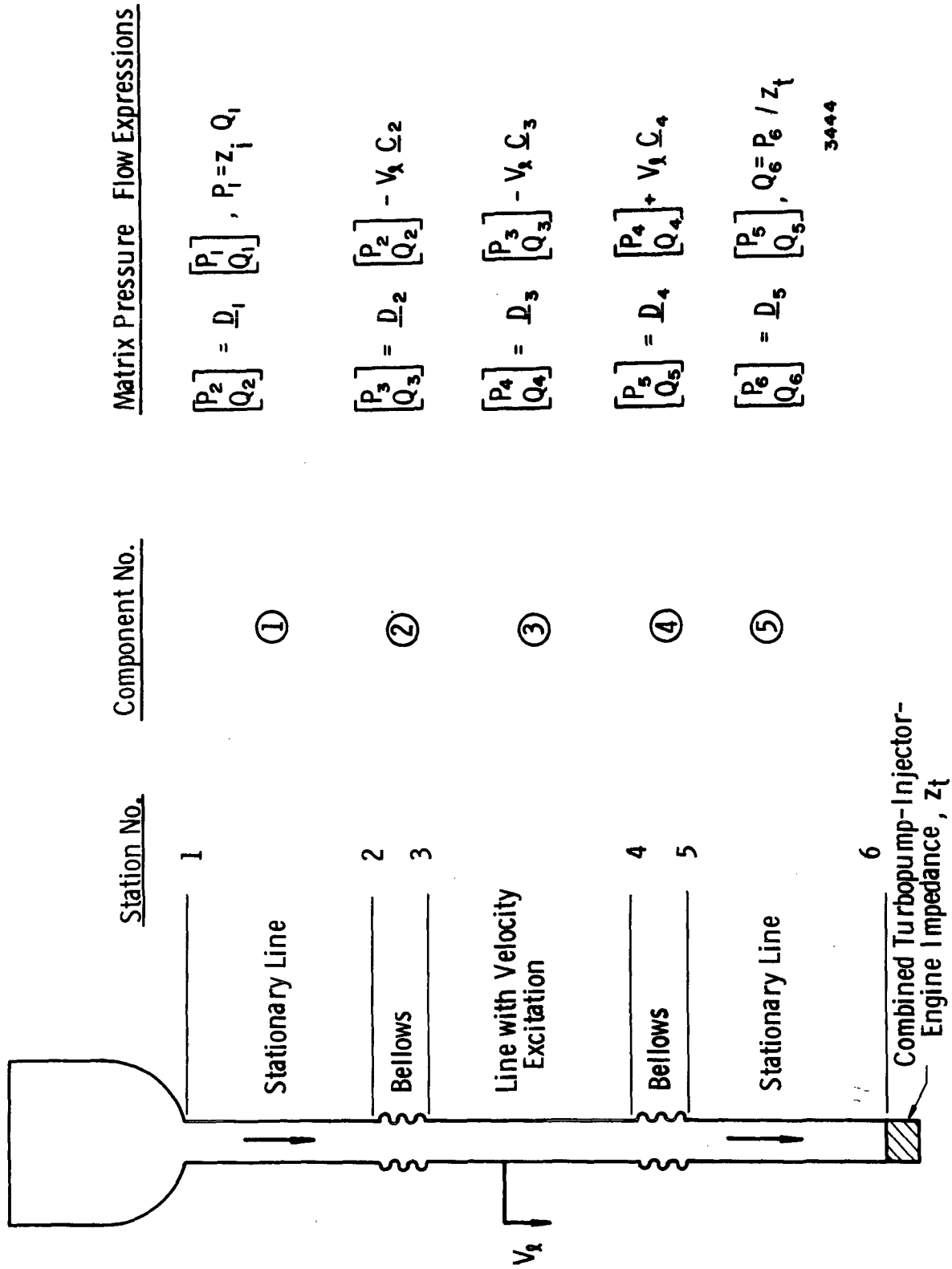
The subscripts on pressure and flow rate pertain to specific points in the line while the subscripts on matrices \underline{D}_1 and \underline{C}_1 refer to the component location in the line. Equation (84) completely defines the generalized matrices in Equation (80). An expression similar to Equation (83) follows directly from Equation (84).

The foregoing discussion forms the basis for constructing a computer code to determine the frequency response of a feedline containing an arbitrary number and sequence of components. The computer code contains a controller program and a separate subroutine for each component in which the elements of each \underline{D}_1 and \underline{C}_1 are calculated. The program has the capability of synthesizing a feedline with as many as fifteen different types of components. However, the program listing that is presented in Appendix H contains eleven component subroutines; the four vacancies are available for the addition of components during future programs. In addition, the source deck contains two subroutines for constructing matrices \underline{B} and \underline{D} and one subroutine for calculating the Bessel functions J_1 and J_0 and their ratio for complex arguments.

Another subroutine calculates the speed of sound in a liquid that may or may not contain a homogeneous distribution of bubbles. In either case, the radial elasticity effects of the line may be taken into account through the Korteweg equation.

Since substitution of $i\omega$ for the Laplace variable "s" implies calculations in the complex plane, liberal use has been made of the complex variable operations afforded by FORTRAN IV. Complex quantities have been subscripted with as many as three indices to facilitate bookkeeping within the program.

In summary, the user merely defines the feedline structure as was done in Figure 19 and indexes the components sequentially beginning with the component that is attached directly to the propellant



Matrix Pressure Flow Expressions

$$\begin{bmatrix} P_2 \\ Q_2 \end{bmatrix} = \underline{D}_1 \begin{bmatrix} P_1 \\ Q_1 \end{bmatrix}, P_1 = Z_i Q_1$$

$$\begin{bmatrix} P_3 \\ Q_3 \end{bmatrix} = \underline{D}_2 \begin{bmatrix} P_2 \\ Q_2 \end{bmatrix} - V_e C_2$$

$$\begin{bmatrix} P_4 \\ Q_4 \end{bmatrix} = \underline{D}_3 \begin{bmatrix} P_3 \\ Q_3 \end{bmatrix} - V_e C_3$$

$$\begin{bmatrix} P_5 \\ Q_5 \end{bmatrix} = \underline{D}_4 \begin{bmatrix} P_4 \\ Q_4 \end{bmatrix} + V_e C_4$$

$$\begin{bmatrix} P_6 \\ Q_6 \end{bmatrix} = \underline{D}_5 \begin{bmatrix} P_5 \\ Q_5 \end{bmatrix}, Q_6 = P_6 / Z_t$$

3444

Figure 19. Matrix Representation Of A Feedline In The Laplace Domain

tank. An expression of the type presented in Equation (80) is then assigned to each component. From this point, a minimal amount of matrix manipulation is then required to arrive at an expression similar to Equation (84), but which reflects the particular configuration under consideration. The flow of subsequent calculations in the program is governed by the following inputs:

- (1) A coded set of integers describing the type of elements in the order in which they appear in the line,
- (2) The number of \underline{B}_1 's that are to be summed to arrive at matrix \underline{B} and
- (3) The number and type of matrices that are contained in each \underline{B}_1 .

Using the codes in Item (1), additional data, relevant to each component type, are read in and associated with a specific component location in the line. Categorically, this data can include component lengths, line radii, friction factors, bubble radii, spring constants, damping constants, liquid-vapor mass ratios, etc. The complete input package also includes information that pertains to the line in general, e. g., input and terminal impedances, thermodynamic and fluid dynamic properties of the propellant, mean flow velocity, the elastic and geometric properties of the conduit wall, and the frequency band over which the response is to be determined.

VII. CONCLUSIONS AND RECOMMENDATIONS

VII.1. Conclusions

The objective of this study has been to develop an analytical model and corresponding computer program to allow for the study of disturbances of liquid propellants in typical engine feedline systems. This model has been completed and includes (a) the effect of steady turbulent mean flow, (b) the influence of distributed compliances, such as dissolved ullage gases and flexible walls, (c) the effects of local compliances, such as cavitation regions and complex side branches, and (d) various factors causing structural-hydraulic coupling, such as bends, mounting stiffness, forced changes in line length and bellows or PVC joints. The computer program has been set up such that the amplitude and phase of the terminal pressure/ input excitation is calculated over any desired frequency range for an arbitrary assembly of various feedline components. A user's manual has been prepared and is attached as Appendix H of this Interim Report.

Investigation has shown that the predominant effect of turbulence is to increase the spatial attenuation at low frequencies; at high frequencies, the laminar and turbulent frequencies coincide. The effect of turbulence also has a tendency to reduce the phase velocity at low frequencies; however, this effect can be neglected for all feedlines where the parameter $r_0^2 \omega / \nu > 10^4$, which includes virtually all cases of interest. An additional factor, Γ_0 , has been added to the laminar propagation operator to account for the turbulent attenuation contribution.

For the homogeneous distribution of very small bubbles entrained in the liquid propellant, the net effect over the frequency range of interest is to lower the phase velocity of the pure liquid. A constant-quality model has been assumed for both single-component and two-component, two-phase flows.

It has been concluded that the effect of the wall compliance can be correctly modeled by the classic Korteweg correction to the phase velocity; the attenuation for the elastic wall is virtually indistinguishable from the attenuation of a rigid wall. We have also concluded that for typical feedline problems, the axial wall stiffness effect will not permit real wave propagation of the higher order modes since the amount of energy which is fed into the higher order modes at the line termination will not permit sustained coupling of the fluid and the wall for these modes.

No other specific conclusions as to the accuracy or applicability of the feedline model can be made until the completion of the experimental study currently in progress at Southwest Research Institute.

VII. 2 Recommendations

Recommendations for future work include:

- (1) The development of a subroutine to compute the speed of sound in two phase, single-component fluids, using the equilibrium model described in Section III. 1 of this report. This would involve programming a vast amount of thermodynamic data for each liquid propellant under consideration.
- (2) Improvement of the model used to compute the bubble dynamics of a large local cavitation bubble. The effective bubble spring rate (or bubble compliance) is also dependent upon the vaporization and condensation rates as the bubble undergoes successive perturbations in pressure.
- (3) The continuation of the experimental program currently in progress. This testing phase of the program will be used to evaluate the applicability of the analytical model and computer program described in this report.

REFERENCES

1. Ryan, R. S., Kiefling, L. A., Jarvinen, W. A., and Buchanan, H. J., "Simulation of Saturn V S-II Stage Propellant Feedline Dynamics," Journal of Spacecraft, Vol. 7, No. 12, December, 1970, pp. 1407-1412.
2. Rubin, S., "Prevention of Coupled Structure-Propulsion Instability (POGO) on the Space Shuttle," Space Transportation System Technology Symposium, NASA TM X-52876, Vol. II, July 1970, pp. 249-262.
3. "Investigation of 17-Hz Closed-Loop Instability on S-II Stage of Saturn V," Rocketdyne/NAR, NASA Contract NAS8-19, August 1969.
4. Sack, I. E. and Nottage, H. B., "System Oscillations Associated with Cavitating Inducers," Journal of Basic Engineering, Vol. 87, Series D., No. 4, December 1965, pp. 917-924.
5. Gerlach, C. R., "The Dynamics of Viscous Fluid Transmission Lines with Particular Emphasis on Higher Mode Propagation," Ph. D. Thesis, Oklahoma State University, July 1966.
6. Gerlach, C. R., "Dynamic Models for Hydraulic Conduits," Proc. 1969 Joint Automatic Control Conference, pp. 416-424, AIChE, N. Y., 1969.
7. Brown, F. T., Margolis, D. L., and Shah, R. P., "Small-Amplitude Frequency Behavior of Fluid Lines with Turbulent Flow," Journal of Basic Engineering, Trans, ASME, Vol. 91, No. 4, pp. 678-693, December 1969.
8. Gouse, S. W., and Brown, G. A., "A Survey of the Velocity of Sound in Two-Phase Mixtures," ASME Paper No. 64-WA/F3-35, presented at ASME Winter Annual Meeting, New York, 1964.
9. Hsieh, Din-Yu, and Plesset, M. S., "On the Propagation of Sound in a Liquid Containing Gas Bubbles," The Physics of Fluids, Vol. 4, No. 3, August 1961.
10. Plesset, M. S., and Hsieh, Din-Yu, "Theory of Gas Bubble Dynamics in Oscillating Pressure Fields," The Physics of Fluids, Vol. 3, No. 6, 1960.

11. Silberman, E., "Sound Velocity and Attenuation in Bubbly Mixtures Measured in Standing Wave Tubes," The Journal of the Acoustical Society of America, Vol. 29, No. 8, August 1957.
12. Spitzer, L., Jr., "Acoustic Properties of Gas Bubbles in a Liquid," O. S. R. D. Report No. 6.1 -sr 20-918, 1943.
13. Koger, H. C., and Houghton, G., "Damping and Pulsation of Large Nitrogen Bubbles in Water," Journal of the Acoustical Society of America, Vol. 43, No. 8, 572, 1968.
14. Chapman, R. B., and Plesset, M. S., "Thermal Effects in the Free Oscillation of Gas Bubbles," ASME Paper No. 70-WA/FE-11, presented at the ASME Winter Annual Meeting, New York, 1970.
15. Lin, T. C., and Morgan, G. W., "Wave Propagation Through Fluid Contained in a Cylindrical Elastic Shell," Journal of the Acoustical Society of America, Vol. 28, pp. 1165-1176, November 1956.
16. Devin, Charles, Jr., "Survey of Thermal, Radiation, and Viscous Damping of Pulsating Air Bubbles in Water," Journal of the Acoustical Society of America, Vol. 31, No. 72, December 1959.
17. Gerlach, C. R., et al., "Study of Fluid Transients in Closed Conduits, Annual Report No. 1," Oklahoma State University, NASA Contract NAS8-11302, July 1965.
18. Oldenberger, R., and Goodson, R. F., "Simplification of Hydraulic Line Dynamics by Use of Infinite Products," Journal of Basic Engineering, Trans. ASME, Vol. 86, No. 4, pp. 1-10, 1964.
19. D'Souza, A. F., and Oldenberger, R., "Dynamic Response of Fluid Lines," Journal of Basic Engineering, September 1964.

APPENDIX A

RATIONAL APPROXIMATE MODEL FOR
DISTRIBUTED PARAMETER SYSTEMS

The four-terminal representation of a transmission line that has been utilized throughout this report is an exact model for the zeroeth mode transfer function equations. The value of this representation for frequency response analyses has been proven. In many problems, however, the time domain solution is required, and the Laplace transform representation constitutes a convenient technique for obtaining the space-dependent solution independently of the time-dependency. In the final analysis, the Laplace inversion integral must be evaluated. When hyperbolic functions are involved in the inversion, as they are in the distributed parameter line model, an infinite series of time-dependent terms is obtained due to the unbounded number of zeros of the hyperbolic functions. In many cases, closure of this series is extremely difficult, and the desired accuracy does not warrant laborious mathematical operations. The obvious conclusion is that there is a definite need for a simple, accurate, approximate technique for obtaining the time domain solution from the frequency domain representation.

The rudiments of such a technique were first proposed by Oldenberger and Goodson¹⁸, and were later refined and put in a practical form by Gerlach^{5,6}. This technique is based upon expanding the hyperbolic functions into an infinite product of second-order polynomials, i. e.,

$$\cosh \Gamma(s) = \prod_{n=0}^{\infty} \left\{ 1 + \frac{2\zeta_{cn}s}{\omega_{cn}} + \frac{s^2}{\omega_{cn}^2} \right\} \quad (\text{A. 1})$$

$$\sinh \Gamma(s) = \Gamma(s) \prod_{n=1}^{\infty} \left\{ 1 + \frac{2\zeta_{sn}s}{\omega_{sn}} + \frac{s^2}{\omega_{sn}^2} \right\} \quad (\text{A. 2})$$

The coefficients, ζ_{cn} , ω_{cn} , ζ_{sn} , ω_{sn} are evaluated by solving for the value of Laplace operator, s_n at the zeroes of the hyperbolic functions. These quantities are conveniently catalogued in Figures A-1 to A-4. To evaluate any one of these coefficients, it is sufficient to calculate the damping number of the line, D_n . The damping number and the desired term number in the expansion completely define the four coefficients. It may be shown that for approximation purposes the term $\Gamma(s)$, in the expansion for the hyperbolic sine, can be represented adequately by sL/c_0 . Characteristic impedance can be approximated by $\rho_0 c_0$.

With these expansions, it is now possible to approximate the hyperbolic functions to any desired degree of accuracy with expressions that can easily be (1) inverted into a time solution using standard transform pairs or (2) integrated in the time domain to

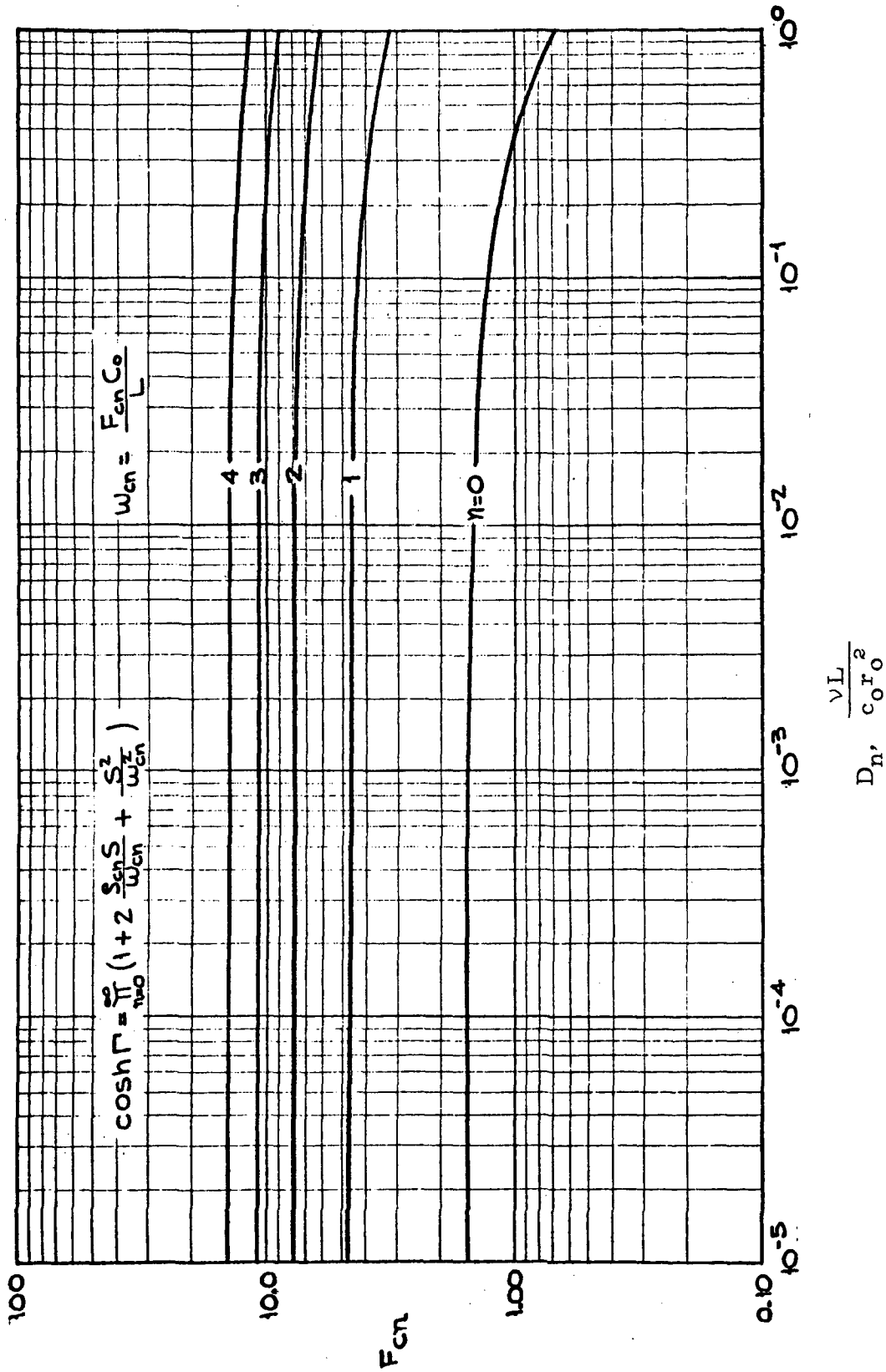


Figure A-1. Variation of the Approximate Model Parameter F_{cn} With Axial Damping Number

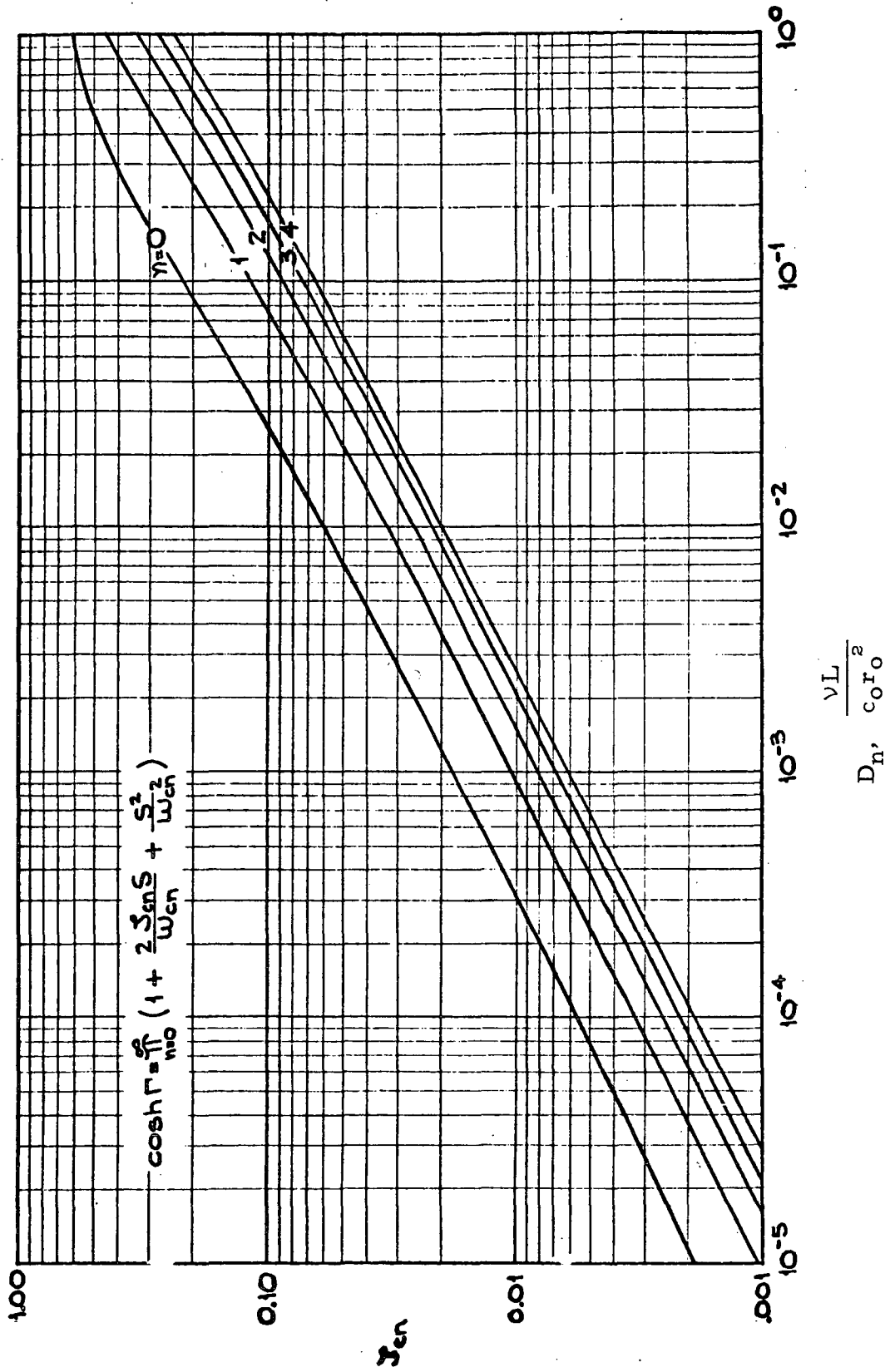


Figure A-2. Variation of the Approximate Model Parameter ζ_{cn} With Axial Damping Number

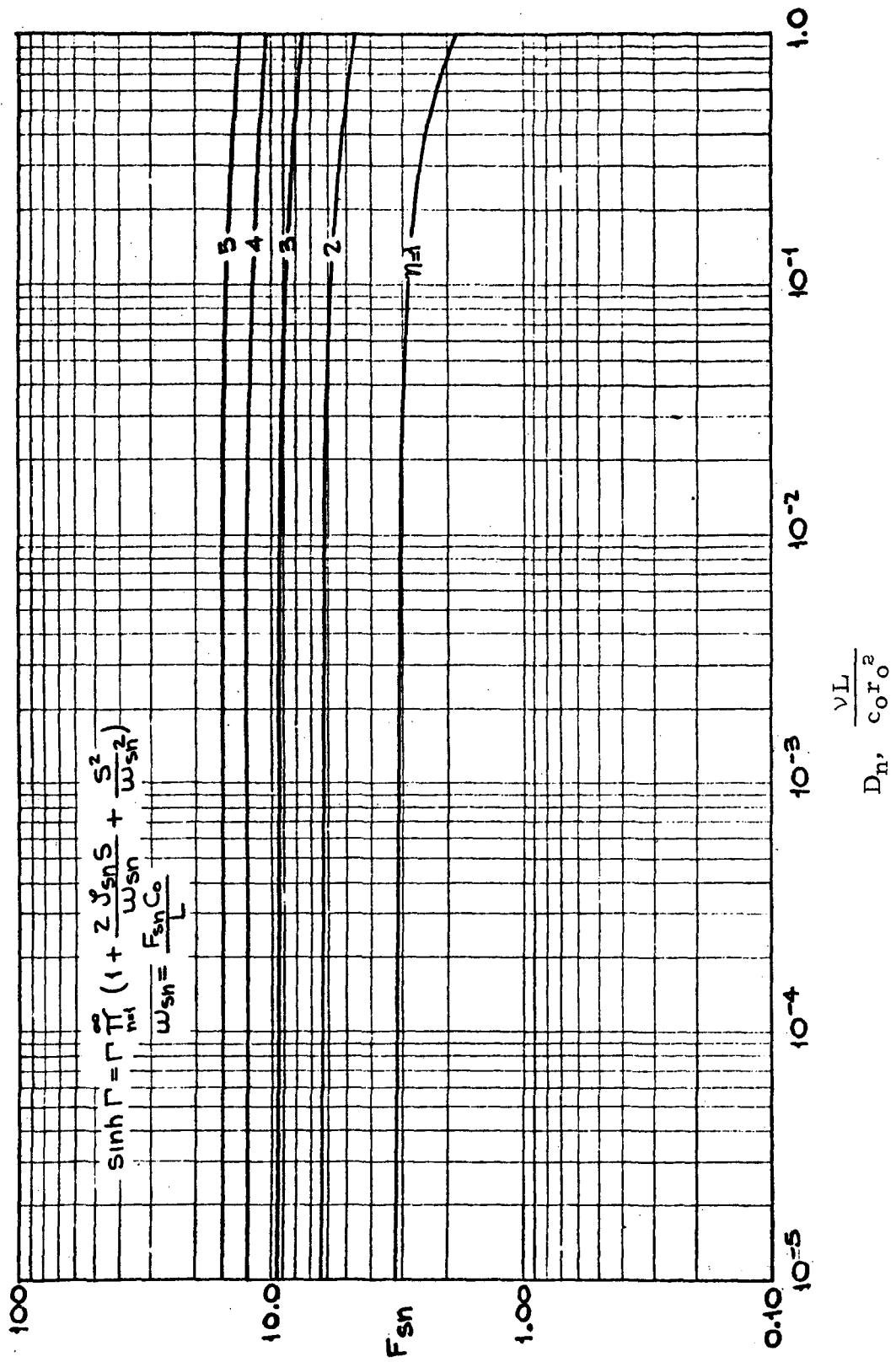
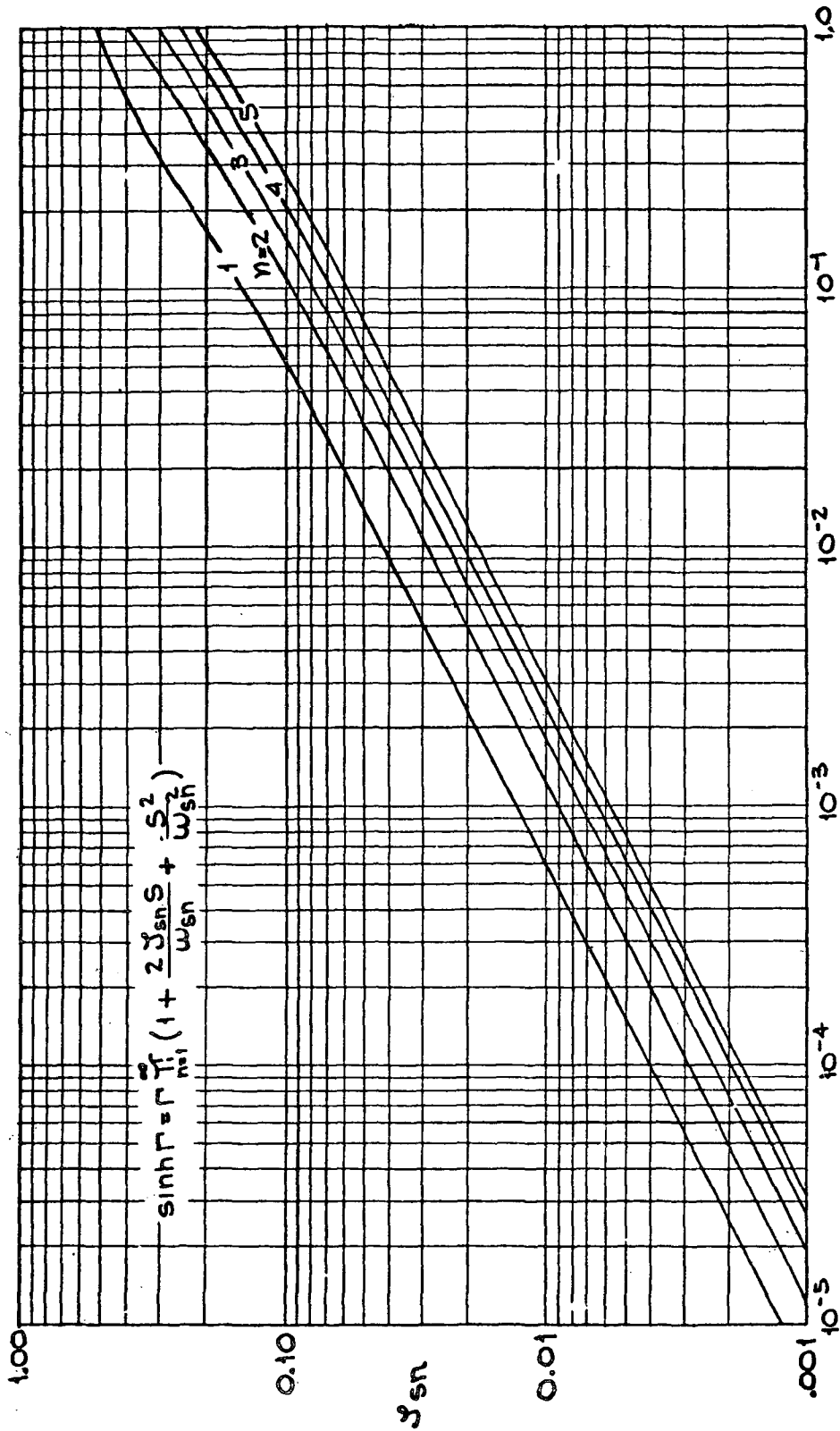


Figure A-3. Variation of the Approximate Model Parameter F_{sn} With Axial Damping Number



$$D_n, \frac{vL}{c_0 r_0^2}$$

Figure A-4. Variation of the Approximate Model Parameter ζ_{sn} With Axial Damping Number

obtain the real time solution. For example, consider a transfer function in which a one-term approximation for the hyperbolic functions produces

$$\frac{P(s)}{\rho_o c_o V_o} = \frac{1}{44} \frac{1}{\left(1 + \frac{.176}{66} s + \frac{s^2}{66^2}\right)} \quad (\text{A. 3})$$

Standard inversion pair yields

$$\frac{p(t)}{\rho_o c_o V_o} = 1.5 e^{-5.8t} \sin(66t) \quad (\text{A. 4})$$

As a second example, consider a transfer function of the type

$$P(s) = -Z_c(s) \tanh \Gamma(s) V(s) \quad (\text{A. 5})$$

A one-term approximation in the model yields

$$\left(1 + \frac{2\zeta_{co} s}{\omega_{co}} + \frac{s^2}{\omega_{co}^2}\right) P(s) = -\rho_o c_o \left(\frac{sL}{c_o}\right) V(s) \quad (\text{A. 6})$$

Interpreting the Laplace operator as a time derivative, the following equation is obtained:

$$\left(1 + \frac{2\zeta_{co}}{\omega_{co}} \frac{d}{dt} + \frac{1}{\omega_{co}^2} \frac{d^2}{dt^2}\right) p(t) = -\rho_o L \frac{dv(t)}{dt} \quad (\text{A. 7})$$

With a second equation relating pressure and flow velocity, a standard numerical integration easily can be obtained on the computer.

The accuracy of this model is summarized below:

- (1) One term of the model well approximates the hyperbolic operators up to the first critical frequency.
- (2) Two terms improve the approximation up to the first critical point and roughly (not well) approximate the hyperbolic operators up beyond the second critical frequency. The use of more terms would improve the results near the second critical frequency.
- (3) A one-term approximation for the hyperbolic function is generally adequate for most engineering problems.

APPENDIX B

SPEED OF SOUND IN A LIQUID CONTAINING
A HOMOGENEOUS DISTRIBUTION OF BUBBLES

Single-Component, Two-Phase Mixture in Equilibrium

The speed of sound in a pure, two-phase substance can be expressed by the standard form

$$a^2 = g_o \left(\frac{\partial p}{\partial \rho} \right)_s \quad (\text{B.1})$$

or, in terms of specific volume rather than density,

$$a^2 = -g_o v^2 \left(\frac{\partial p}{\partial v} \right)_s \quad (\text{B.2})$$

Following the approach of Gouse and Brown⁸, it can be shown that the partial derivative in Equation (B.2) can be expanded such that

$$a^2 = g_o v^2 \left(\frac{\partial s}{\partial v} \right)_p \left(\frac{\partial s}{\partial v} \right)_T \left(\frac{\partial T}{\partial s} \right)_v \quad (\text{B.3})$$

Since constant pressure and temperature lines are coincident in the two-phase region beneath the vapor dome,

$$\left(\frac{\partial s}{\partial v} \right)_p = \left(\frac{\partial s}{\partial v} \right)_T \quad (\text{B.4})$$

or in finite difference form

$$\left(\frac{\partial s}{\partial v} \right)_p = \frac{s_g - s_f}{v_g - v_f} \quad (\text{B.5})$$

The subscripts, f and g, refer to the saturated liquid and vapor state, respectively. Substituting Equations (B.4) and (B.5) into Equation (B.6)

$$a^2 = g_o v^2 \left(\frac{s_g - s_f}{v_g - v_f} \right)^2 \left(\frac{\partial T}{\partial s} \right)_v \quad (\text{B.6})$$

Equation (B.6) can be developed into a form that is suitable for use with a standard temperature-entropy chart. The quality of a two-phase state, x , is defined as

$$x = M_v / (M_\ell + M_v) \quad (\text{B.7})$$

and the specific volume for such a state can be written in terms of quality as

$$v = v_f + x(v_g - v_f) \quad (\text{B.8})$$

Substituting this expression into Equation (B.6), the speed of sound can be written as a function of quality

$$a^2 = g_o \left[\frac{v_f}{v_g - v_f} + x \right]^2 (s_g - s_f)^2 \left(\frac{\partial T}{\partial s} \right)_v \quad (\text{B.9})$$

In finite difference form, the speed of sound in a single-component, two-phase mixture in thermodynamic equilibrium becomes

$$a = \left(\frac{v_f}{v_g - v_f} + x \right) (s_g - s_f) \left[g_o \left(\frac{\Delta T}{\Delta s} \right)_v \right]^{\frac{1}{2}} \quad (\text{B.10})$$

Single-Component or Two-Component, Two-Phase Mixture With Constant Quality

The above section described the acoustic velocity in an equilibrium mixture of a liquid and its vapor phase. In this section, the speed of sound is analyzed for a constant quality mixture of a liquid and a distinctly different gas, but the results also apply to single-component mixtures as long as the vaporization and condensation rates are low enough that no phase change occurs as a result of pressure disturbances (constant quality is assumed at all times). In the development of a constant quality model for the acoustic velocity in a liquid-gas mixture, the following assumptions are made:

- (1) The mixture is homogeneous in phase composition.
- (2) The mass of each phase remains constant.
- (3) The gas behaves as a perfect gas with the appropriate equation of state and constant specific heats.
- (4) The liquid compressibility is ignored.
- (5) The gas and liquid phases are always at the same temperature.

The subsequent derivation is based on total volume as opposed to the specific volume approach that was utilized in the previous section. Assuming an adiabatic process,

$$c^2 = \left(\frac{dp}{d\rho} \right)_s \quad \text{or} \quad \frac{1}{c^2} = \left(\frac{d\rho}{dp} \right)_s \quad (\text{B.11})$$

For a two-component mixture,

$$\rho = \frac{M_l + M_g}{V_l + V_g}$$

$$\frac{1}{c^2} = \frac{d}{dp} \left(\frac{M_l + M_g}{V_l + V_g} \right)$$

$$\frac{1}{c^2} = \left[(V_l + V_g) \frac{d}{dp} (M_l + M_g) - (M_l + M_g) \frac{d}{dp} (V_l + V_g) \right] / (V_l + V_g)^2$$

$$\frac{1}{c^2} = - \left(\frac{M_l + M_g}{V_l + V_g} \right) \frac{1}{V_l + V_g} \frac{d}{dp} (V_l + V_g)$$

$$\frac{1}{c^2} = -\rho \frac{1}{V_l + V_g} \left(\frac{d}{dp} V_l \left(\frac{M_l}{M_l} \right) + \frac{d}{dp} V_g \left(\frac{M_g}{M_g} \right) \right)$$

$$\frac{1}{c^2} = -\rho \frac{M_l}{V_l + V_g} \frac{d}{dp} \left(\frac{1}{\rho_l} \right) - \rho \frac{M_g}{V_l + V_g} \frac{d}{dp} \left(\frac{1}{\rho_g} \right)$$

$$\frac{1}{c^2} = -\rho \left[\frac{M_l}{V_l + V_g} \left(-\frac{1}{\rho_l^2} \right) \left(\frac{d\rho_l}{dp} \right)_g + \frac{M_g}{V_l + V_g} \left(-\frac{1}{\rho_g^2} \right) \left(\frac{d\rho_g}{dp} \right)_g \right] \quad (\text{B.12})$$

$$\frac{1}{c^2} = \rho \left[\frac{M_l}{V_l + V_g} \frac{1}{\rho_l^2} \frac{1}{c_l^2} + \frac{M_g}{V_l + V_g} \frac{1}{\rho_g^2} \frac{1}{c_g^2} \right] \quad (\text{B.13})$$

From the definition for density,

$$V = M/\rho \quad (\text{B.14})$$

$$V_l + V_g = \frac{M_l}{\rho_l} + \frac{M_g}{\rho_g} = \frac{M_l \rho_g + M_g \rho_l}{\rho_l \rho_g} \quad (\text{B.15})$$

The mass ratio, ϕ , is now defined as the mass of vapor/mass of liquid.

$$\phi = M_g/M_l \quad (\text{B.16})$$

Substituting the mass ratio into Equation (B.15),

$$V_l + V_g = \frac{M_l (\rho_g + \phi \rho_l)}{\rho_g \rho_l} \quad (\text{B.17})$$

Thus, the speed of sound in a constant quality mixture becomes

$$\frac{1}{c^2} = \rho \left[\frac{\rho_g}{\rho_g + \phi \rho_l} \frac{1}{\rho_l} \frac{1}{c_l^2} + \frac{\phi \rho_l}{\rho_l + \phi \rho_g} \frac{1}{\rho_g} \frac{1}{c_g^2} \right] \quad (\text{B.18})$$

As mentioned in Section III, the isothermal velocity of sound might be more appropriate for two-component, two-phase mixtures rather than the adiabatic (isentropic) velocity of sound.

Plesset and Hsieh¹⁰ have shown that bubble dynamics are governed by an isothermal process at low excitation frequencies and an adiabatic process at higher frequencies, providing there is a uniform temperature distribution within the gas bubbles. However, this sharp division of thermodynamic behavior is not necessarily the case because the heat conduction rate of the gas is considerably smaller than that in the liquid. The liquid has a large specific heat and thermal conductivity, and behaves as a heat reservoir. Consequently, in the liquid adjacent to the gas-liquid interface, there are no changes in the gas temperature during compression. In the center of the bubble away from a substance having a high specific heat, the gas follows the adiabatic equation of state. Therefore, the overall bubble follows a polytropic process. However, for very small bubbles, the heat diffusion into the liquid is so rapid that temperature changes in the bubble can not take place, and the process is essentially isothermal.

For this reason, the propagation of sound in a liquid with a homogeneous distribution of bubbles (basic assumption No. 1) indicates a speed in agreement with isothermal speed of sound. To compute the isothermal speed of sound in the mixture, the acoustic velocity of the gas in Equation (B.13) should be changed to the isothermal value, or

$$c_g = \sqrt{g_0 \gamma RT} \quad (\text{B.19})$$

where $\gamma = 1.0$ rather than 1.4.

APPENDIX C

COMPLIANCE OF LARGE BUBBLES AND THE
POLYTROPIC EXPONENT

The "complex" compliance of large cavitation bubbles was defined in Section IV. The bubble compliance was shown to be frequency dependent, especially near the bubble resonant frequency. This section describes how the bubble damping and polytropic exponent can be estimated for an arbitrary bubble size and excitation frequency.

In the literature, there is considerable disagreement as to the theoretical expressions that should be used to evaluate the damping constant, δ , which is related to the coefficient of damping, b , by

$$\delta = \frac{b}{\omega m_2} \quad (C.1)$$

The reason for this disagreement is that, while the theory is applicable to all frequencies, experimental verification has been obtained only at the resonant condition. However, it is hypothesized that the theory which is summarized here and has been incorporated into the computer code is valid over a broad range of frequencies.

Total damping, due to the presence of a bubble, is attributed to the losses originating from three processes:

- (1) Thermal damping resulting from the thermal conduction between the gas in the bubble and the surrounding liquid;
- (2) Sound radiation damping caused by energy dispersed by radiating spherical sound waves when the bubble is excited into volume pulsations;
- (3) Viscous damping from viscous forces at the liquid-gas interface.

The total damping constant is given by

$$\delta = \delta_{th} + \delta_{rad} + \delta_{vis} \quad (C.2)$$

or, $b = b_{th} + b_{rad} + b_{vis}$

where

$$b_{th} = \left\{ \frac{\sinh(2\phi_1 R_0) + \sin(2\phi_1 R_0)}{\cosh(2\phi_1 R_0) - \cos(2\phi_1 R_0)} - \frac{1}{\phi_1 R_0} \right\} \times \frac{\eta P_0}{V_0 \omega} \quad (C.3)$$

$$b_{\text{rad}} = \frac{\rho_l \omega^2}{4\pi c_l} \quad (\text{C.4})$$

$$b_{\text{vis}} = \frac{\mu}{\pi R_o^3} \quad (\text{C.5})$$

In these expressions,

μ = liquid viscosity

ρ_l = liquid density

c_l = liquid speed of sound

γ = ratio of specific heats irrespective of the thermodynamic process indicated by the polytropic exponent, η .

Also, the argument

$$\phi_1 R_o = \left(\frac{\omega}{2D_1} \right)^{\frac{1}{2}} R_o \quad (\text{C.6})$$

is a measure of the rate at which heat is conducted over a distance, R_o , from the bubble center to the liquid-gas interface. The thermal diffusivity of the entrained gas is denoted by D_1 .

The correct value of the polytropic exponent, η , depends on the bubble size and excitation frequency. The value of the polytropic exponent has been found to be

$$\eta = \frac{\gamma [1 + \delta_{\text{th}}^2]^{-1}}{\left[1 + \frac{3(\gamma-1)}{2\phi_1 R_o} \left(\frac{\sinh(2\phi_1 R_o) - \sin(2\phi_1 R_o)}{\cosh(2\phi_1 R_o) - \cos(2\phi_1 R_o)} \right) \right]} \quad (\text{C.7})$$

where δ_{th} is equal to the term in brackets in Equation (C.3).

APPENDIX D

FORCED CHANGES IN LINE LENGTH

The POGO phenomenon is a coupled dynamic instability involving the vehicle structure, propulsion system and propellant feed system. As a direct result of this coupling, the structural excitation applied to the feedline may result in a relative motion of the ends of the line, i. e., forced changes in line length. The purpose of this section is to analyze the changes in length from the viewpoint of an inhomogeneous, boundary-valued problem and to derive the form of the transfer matrices that describe the pressure-flow response to this type of excitation.

The physical problem is shown in Figure D-1. Liquid propellant is flowing through a constant area duct of length L , internal radius r_0 , and wall thickness t . The terminal ends of the line are acted upon by structural velocities having arbitrary relative phase and magnitude. The relative motion due to this excitation is assumed to be small in the linearized sense.

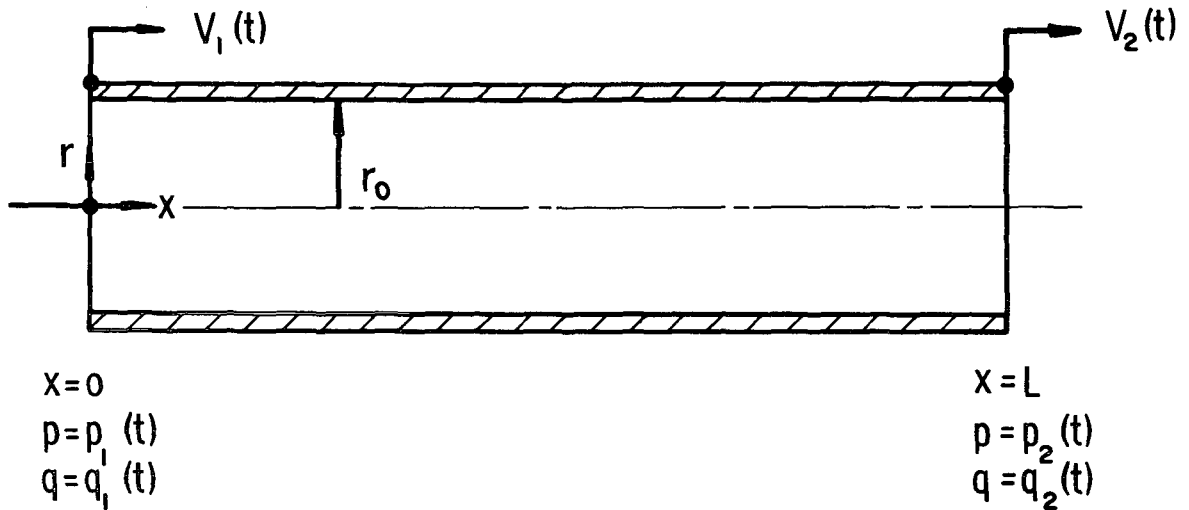


Figure D-1. Geometry For Forced Changes In Line Length

The following assumptions and assertions are made with regard to the fluid flow:

- (1) The flow is viscous, incompressible and axisymmetric;
- (2) Viscosity remains constant;
- (3) The flow is laminar; this assumption is not a severe constraint because the added attenuation due to turbulence can be adequately taken into account through the use of the modified propagation operator described in Section II;

- (4) The pressure and the axial and radial components of flow consist of a steady-state level plus a perturbation value;
- (5) The axial velocity perturbation, u , is much larger than the radial perturbation, v ;
- (6) Velocity gradients in the axial direction contribute a negligible amount to the viscous dissipation forces;
- (7) Spatial derivatives of the density can be neglected since the compressibility of the liquid propellant is extremely low.

D'Souza and Oldenberger¹⁹ have shown that when these assumptions are applied to the Navier-Stoke's equations in cylindrical coordinates, the continuity equation and the equation of state, the following linearized differential equations describe the flow field:

$$\rho_o \frac{\partial u}{\partial t} = -\frac{\partial p}{\partial x} + \mu_o \left[\frac{\partial^2 u}{\partial r^2} + \frac{1}{r} \frac{\partial u}{\partial r} \right] \quad (D.1)$$

$$\frac{1}{\kappa} \frac{\partial p}{\partial t} + \frac{\partial v_r}{\partial r} + \frac{v_r}{r} + \frac{\partial u}{\partial x} = 0 \quad (D.2)$$

These expressions are easily recognizable as the equation of motion in the axial direction and the combined continuity and state equations, where κ is the fluid bulk modulus of elasticity. In addition, absence of an equation of motion in the radial direction implies that the pressure is constant across the cross section, i. e., $p = p(x, t)$.

The relative motion in the line wall is governed by the wave equation

$$\frac{\partial^2 y}{\partial t^2} = c_w^2 \frac{\partial^2 y}{\partial x^2}, \quad c_w^2 = \frac{E_t}{\rho_t} \quad (D.3)$$

where y is the axial displacement of a point in the wall and c_w is the longitudinal wave speed in the wall. Equation (D.3) is subject to the imposed boundary conditions

$$\frac{\partial y(0, t)}{\partial t} = V_1(t) \quad \text{and} \quad \frac{\partial y(L, t)}{\partial t} = V_2(t) \quad (D.4)$$

The no-slip compatibility condition at the wall-fluid interface is

$$\frac{\partial y(\mathbf{x}, t)}{\partial t} = u(\mathbf{x}, r_o, t) \quad (\text{D.5})$$

The solution for the flow field proceeds in the Laplace transform domain noting that the average pressure perturbation at an arbitrary cross section, $\bar{p}(\mathbf{x}, t)$, is equal to the actual perturbation, $p(\mathbf{x}, t)$. The transform of the equation of motion with zero initial conditions yields

$$\frac{\partial^2 U}{\partial r^2} + \frac{1}{r} \frac{\partial U}{\partial r} - \frac{s}{\nu} \left(U + \frac{1}{\rho_o s} \frac{\partial \bar{P}}{\partial \mathbf{x}} \right) = 0 \quad (\text{D.6})$$

where the upper case letters indicate transformed variables. Since \bar{P} is independent of the radial coordinate, Equation (D.6) can be reduced to an expression involving only one dependent variable by the transformation of variables

$$V = U + \frac{1}{\rho_o s} \frac{\partial \bar{P}}{\partial \mathbf{x}} \quad (\text{D.7})$$

Combining Equations (D.7) and (D.6) yields a Bessel type differential equation with one finite solution at $r = 0$.

$$V = f(\mathbf{x}, s) J_o(\xi r) \quad (\text{D.8})$$

where $\xi = \sqrt{-s/\nu}$ and $f(\mathbf{x}, s)$ is an undefined function which must be determined. Therefore, the transformed velocity, U , becomes

$$U = f(\mathbf{x}, s) J_o(\xi r) - \frac{1}{\rho_o s} \frac{\partial \bar{P}}{\partial \mathbf{x}} \quad (\text{D.9})$$

Solution of the wave equation in the wall subject to the prescribed boundary conditions yields

$$Y(\mathbf{x}, s) = B_1 \cosh \frac{s\mathbf{x}}{C_w} + B_2 \sinh \frac{s\mathbf{x}}{C_w} \quad (\text{D.10})$$

where $B_1 = \frac{V_1(s)}{s}$ and $B_2 = \frac{V_2(s) - V_1(s) \cosh sL/C_w}{s \sinh sL/C_w}$.

Combining the transformed compatibility condition, Equations (D.5) and (D.10), produces

$$\frac{1}{\rho_o s} \frac{\partial \bar{P}}{\partial \mathbf{x}} = f(\mathbf{x}, s) J_o(\xi r_o) - s \left[B_1 \cosh \frac{s\mathbf{x}}{C_w} + B_2 \sinh \frac{s\mathbf{x}}{C_w} \right] \quad (\text{D.11})$$

Substituting this result into Equation (D.9) and averaging over the cross section yields

$$\bar{U} = f(x, s) \left[\frac{2J_1(\xi r_o)}{\xi r_o} - J_0(\xi r_o) \right] + s \left[B_1 \cosh \frac{sx}{C_w} + B_2 \sinh \frac{sx}{C_w} \right] \quad (D.12)$$

As before, barred quantities indicate average values. If the continuity equation is transformed and then averaged across the cross section, the result is

$$\bar{P} = -\frac{\kappa}{s} \frac{\partial \bar{U}}{\partial x} \quad (D.13)$$

Note that the dependence on radial velocity vanishes since there is no net radial flow. Differentiating this result with respect to x and incorporating Equations (D.12) and D.11) yields a second-order, inhomogeneous, ordinary differential equation for the arbitrary function $f(x, s)$. After considerable algebraic manipulation, the equation takes the following form:

$$\frac{d^2 f}{dx^2} - \gamma^2 f = -\left(1 - \frac{C_o^2}{C_w^2}\right) \frac{s\gamma^2}{J_0(\xi r_o)} g(x, s) \quad (D.14)$$

where

$$\gamma^2 = \frac{s^2}{C_o^2 \left[1 - \frac{2J_1(\xi r_o)}{\xi r_o J_0(\xi r_o)} \right]}$$

and

$$g(x, s) = B_1 \cosh \frac{sx}{C_w} + B_2 \sinh \frac{sx}{C_w}$$

A particular integral of Equation (D.14) is easily obtained by the method of undetermined coefficients because of the cyclic nature of the inhomogeneous function $g(x, s)$. The general solution of Equation (D.14) is

$$f(x, s) = (A_1 \cosh \gamma x + A_2 \sinh \gamma x) + \left(C_1 \cosh \frac{sx}{C_w} + C_2 \sinh \frac{sx}{C_w} \right) \quad (D.15)$$

where A_1 and A_2 are undetermined functions of the Laplace variable s and C_1 and C_2 are related to B_1 and B_2 by

$$C_i = \frac{-\left(1 - \frac{C_o^2}{C_w^2}\right) s\gamma^2 B_i}{\left(\frac{s^2}{C_w^2} - \gamma^2\right) J_0(\xi r_o)}, \quad i = 1, 2$$

After simplification, the transformed velocity field, Equation (D.12) becomes

$$\bar{U} = (A_1 \cosh \gamma x + A_2 \sinh \gamma x) \left(\frac{2J_1(\xi r_0)}{\xi r_0} - J_0(\xi r_0) \right) + \frac{s \left(\frac{s^2}{C_o^2} - \gamma^2 \right)}{\left(\frac{s^2}{C_w^2} - \gamma^2 \right)} \left(B_1 \cosh \frac{s x}{C_w} + B_2 \sinh \frac{s x}{C_w} \right) \quad (D.16)$$

Noting that $\kappa = \rho_o c_o^2$, the pressure field is obtained from Equation (D.13).

$$\bar{P} = \frac{-\rho_o c_o^2}{s} \left[(A_1 \gamma \sinh \gamma x + A_2 \gamma \cosh \gamma x) \left(\frac{2J_1(\xi r_0)}{\xi r_0} - J_0(\xi r_0) \right) + \frac{s \left(\frac{s^2}{C_o^2} - \gamma^2 \right)}{\left(\frac{s^2}{C_w^2} - \gamma^2 \right)} \left(B_1 \frac{s}{C_w} \sinh \frac{s x}{C_w} + B_2 \frac{s}{C_w} \cosh \frac{s x}{C_w} \right) \right] \quad (D.17)$$

Coefficients A_1 and A_2 can be eliminated by evaluating the pressure and velocity at the extremities of the line, i. e.,

$$\begin{aligned} \bar{P}(0, s) &= \bar{P}_1 & \bar{P}(L, s) &= \bar{P}_2 \\ \bar{U}(0, s) &= \bar{U}_1 & \bar{U}(L, s) &= \bar{U}_2 \end{aligned} \quad (D.18)$$

In the process of making these evaluations, the characteristic impedance, Z_o , can be defined in terms of the propagation operator, γ ,

$$Z_o = \frac{\rho_o c_o^2 \gamma}{s}$$

Applying boundary conditions (D.18) to Equations (D.17) and (D.16) incorporating the expressions for B_1 and B_2 , and imposing the condition that $V_2(s) = G(s) V_1(s)$ yields

$$\begin{bmatrix} \bar{P}_2 \\ \bar{U}_2 \end{bmatrix} = \begin{bmatrix} \cosh \gamma L & -Z_o \sinh \gamma L \\ -Z_o^{-1} \sinh \gamma L & \cosh \gamma L \end{bmatrix} \begin{bmatrix} \bar{P}_1 \\ \bar{U}_1 \end{bmatrix} - \frac{\left(\frac{s^2}{C_o^2} - \gamma^2 \right)}{\left(\frac{s^2}{C_w^2} - \gamma^2 \right)} V_1(s) \begin{bmatrix} \alpha_1 \\ \alpha_2 \end{bmatrix} \quad (D.19)$$

where

$$\alpha_2 = - \left[\left(\cosh \frac{sL}{C_w} - \cosh \gamma L \right) + \frac{\left(G - \cosh \frac{sL}{C_w} \right)}{\sinh \frac{sL}{C_w}} \left(\sinh \frac{sL}{C_w} - \frac{s}{C_w \gamma} \sinh \gamma L \right) \right]$$

$$\alpha_1 = \frac{\rho_o c_o^2}{s} \left[\left(\frac{s}{C_w} \sinh \frac{sL}{C_w} - \gamma \sinh \gamma L \right) + \frac{\left(G - \cosh \frac{sL}{C_w} \right)}{\sinh \frac{sL}{C_w}} \frac{s}{C_w} \left(\cosh \frac{sL}{C_w} - \cosh \gamma L \right) \right]$$

The assumed dependence of $V_2(s)$ on $V_1(s)$ is entirely realistic since the vehicle structural velocities, which are the forcing functions, are generally describable by transfer functions.

Equation (D.19) represents the desired result for forced changes in line length. The column matrix in Equation (D.19) represents a pressure-flow modification to the square matrix that describes pressure and flow in the absence of external excitation. It can be shown, though not conveniently, that when $G(s) = 1$ (rigid body excitation) Equation (D.19) degenerates into the form presented in Section V.

APPENDIX E

MOUNTING STIFFNESS

Discrete Parameter - Acceleration Technique

A typical example of a line with a discrete parameter mounting stiffness is shown in Figure E-1a. The elasticity of the surrounding structure has been simulated by a spring in parallel with a viscous damper. A structural acceleration input, $a_1(t)$, measured with respect to vehicle fixed axes, acts upon the viscoelastic support. Due to the filtering characteristics of the support, the applied acceleration produces a response, $a_l(t)$, of the vertical line segment. It was shown in Section V.1 that the four-terminal representation of a vertically accelerated line is

$$\begin{bmatrix} P_3 \\ Q_3 \end{bmatrix} = \begin{bmatrix} \cosh \gamma L & -Z_c A^{-1} \sinh \gamma L \\ -AZ_c^{-1} \sinh \gamma L & \cosh \gamma L \end{bmatrix} \begin{bmatrix} P_2 \\ Q_2 \end{bmatrix} - \frac{a_l(s)}{s} \begin{bmatrix} Z_c \sinh \gamma L \\ A(1 - \cosh \gamma L) \end{bmatrix} \quad (E.1)$$

Obviously, a_l is identical to a_1 if the support is infinitely rigid and a_l approaches zero if the mount is extremely flexible. In the intermediate range of interest, a_l can be related to a_1 through the equivalent spring-mass-dashpot analog shown in Figure E-1b. During oscillatory motion, the mass of fluid contained in the transverse limbs of the feedline contributes an added mass, $(m_1 + m_3)$, effect. The inertial loading, due to the fluid mass in the vertical segment of the line, is replaced by the equivalent dynamic pressure forces. For a support of negligible mass, the differential equation of motion for mass M about its equilibrium position is

$$M\ddot{x} = -k(x-y) - b(\dot{x}-\dot{y}) + A(p_3-p_2) \quad (E.2)$$

Transforming this result into the Laplace domain and noting that

$$\mathcal{L}\{x\} = X, \quad \mathcal{L}\{y\} = Y$$

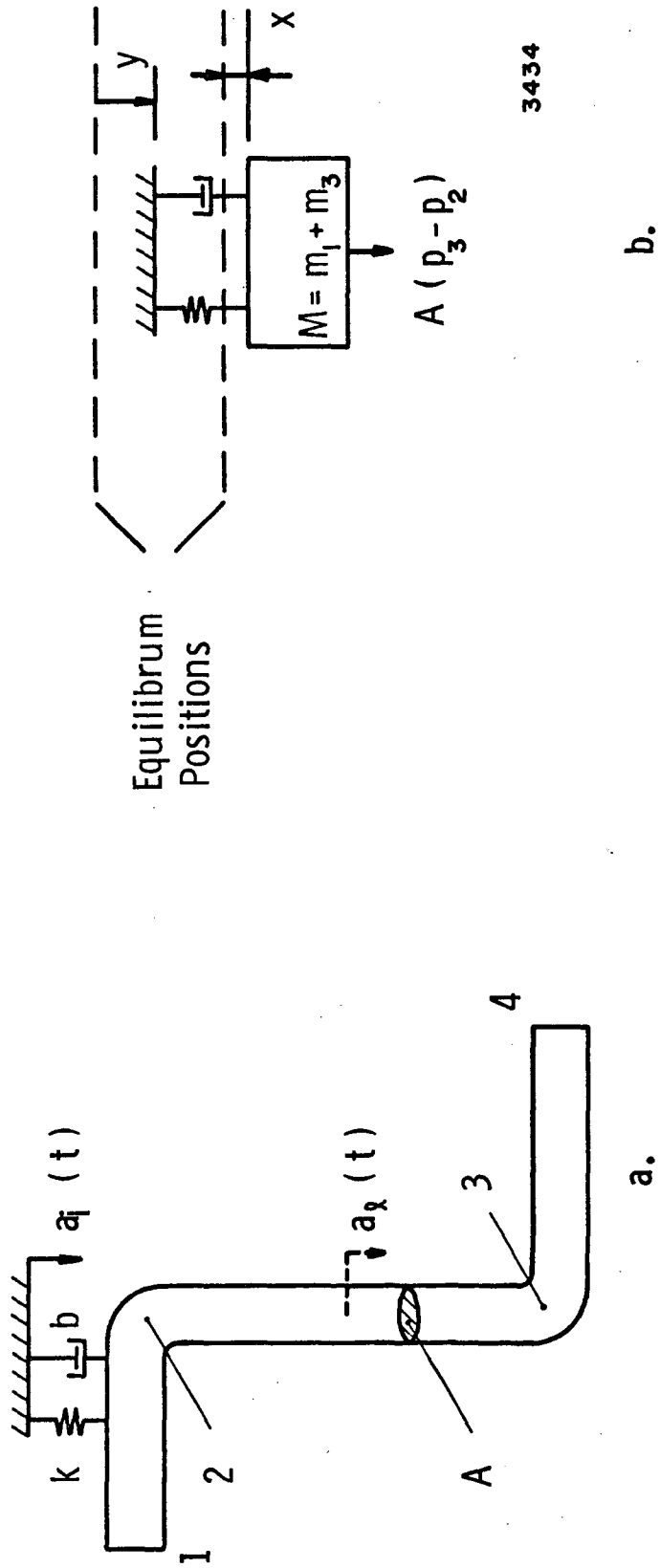
and

$$s^2 X = a_l(s), \quad s^2 Y = a_1(s)$$

the following result is obtained.

$$a_l(s) = a_1(s) \left[\frac{sb+k}{Ms^2+sb+k} \right] + A[P_3(s) - P_2(s)] \left[\frac{s^2}{Ms^2+sb+k} \right] \quad (E.3)$$

The first term in Equation (E.3) reflects the externally imposed acceleration, and the second term reflects a passive inertial loading.



3434

Figure E-1. Model For A Line With Mounting Stiffness

A straightforward combination of Equations (E.3) and (E.1) produces, after some manipulation,

$$\begin{bmatrix} P_3 \\ Q_3 \end{bmatrix} = \begin{bmatrix} \frac{L_{11} + \beta'}{1 + \beta'} & \frac{L_{12}}{1 + \beta'} \\ \frac{L_{21} + \beta''(1 - L_{11})}{1 + \beta'} & \frac{L_{22} - \beta''L_{12}}{1 + \beta'} \end{bmatrix} \begin{bmatrix} P_2 \\ Q_2 \end{bmatrix} - \frac{a_1(s)}{1 + \beta'} \begin{bmatrix} \alpha' \\ \alpha'' \end{bmatrix} \quad (\text{E.4})$$

where the L_{ij} ($i, j = 1, 2$) are the elements of the original square matrix in Equation (E.1) and

$$\alpha' = \frac{sb+k}{s(Ms^2+sb+k)} Z_o \sinh \gamma L$$

$$\beta' = \frac{As}{(Ms^2+sb+k)} Z_o \sinh \gamma L$$

$$\alpha'' = \frac{sb+k}{s(Ms^2+sb+k)} A(1 - \cosh \gamma L)$$

$$\beta'' = \frac{A^2s(1 - \cosh \gamma L)}{Ms^2+sb+k}$$

All other terms have been defined previously. The input acceleration, $a_1(s)$, could be replaced by the equivalent velocity representation, $sV_1(s)$. However, this replacement would require a minor computer code modification since the program currently determines the response to acceleration, $a_1(s)$.

Impedance Technique

Consider a feedline configuration similar to the one in Figure E-1a with the exception that the viscoelastic support is replaced by an equivalent driving point impedance, Z_s . Equation (E.1) applies to the vertical line segment. In this case, however, we choose to replace the coefficient of the third matrix by its equivalent velocity, $V_\ell(s)$. The support exerts a force, F , on the feedline, and the equation of motion for this system that corresponds to Equation (E.2) is

$$M\ddot{x}_\ell = -F + A(p_3 - p_2) \quad (\text{E.5})$$

Applying the Laplace transformation to this expression yields

$$Ms V_\ell(s) = -F(s) + A[P_3(s) - P_2(s)] \quad (\text{E.6})$$

The driving point impedance is, by definition,

$$Z_s(s) = \frac{F(s)}{V_l(s)} \quad (\text{E.7})$$

Eliminating $F(s)$ between Equations (E.6) and (E.7) produces

$$V_l(s) = \frac{A(P_3 - P_2)}{Z_s + M_s} \quad (\text{E.8})$$

Equation (E.8) may be introduced into Equation (E.1), and the following result is obtained after rearrangement:

$$\begin{bmatrix} P_3 \\ Q_3 \end{bmatrix} = \begin{bmatrix} \frac{L_{11} + \alpha}{1 + \alpha} & \frac{L_{12}}{1 + \alpha} \\ L_{21} + \frac{\beta(1 - L_{11})}{1 + \alpha} & L_{22} - \frac{\beta L_{12}}{1 + \alpha} \end{bmatrix} \begin{bmatrix} P_2 \\ Q_2 \end{bmatrix} \quad (\text{E.9})$$

where

$$\alpha = \frac{AZ_{c2} \sinh \Gamma_2}{Z_s + M_s}$$

$$\beta = \frac{A^2(1 - \cosh \Gamma_2)^2}{Z_s + M_s}$$

L_{ij} = elements of original square matrix in Equation (E.1).

The obvious difference between Equations (E.4) and (E.9) is that the latter does not contain the trailing column vector that reflects the enforced excitation. In the latter formulation the effect of the mounting support (structural impedance) is absorbed into the square matrix. Both formulations degenerate into the simple stationary line representation for an infinitely stiff support.

APPENDIX F

PARALLEL LINES

Consider the assemblage of parallel lines shown in Figure F-1. Although this configuration is not used frequently in propellant feed systems, the pressure-flow relationships for this component have been developed and included in the computer code for application in special situations. Assuming that flow losses due to elbow resistance are negligible, a standard four-terminal pressure-flow equation can be written for the i -th line. For this particular problem, however, it is more convenient to express that pressure-flow equation as

$$\begin{aligned} Q_{1i} &= Z_{c_i}^{-1} A_i (P_1 \coth \Gamma_i - P_2 \operatorname{csch} \Gamma_i) \\ Q_{2i} &= Z_{c_i}^{-1} A_i (P_1 \operatorname{csch} \Gamma_i - P_2 \coth \Gamma_i) \end{aligned} \quad (\text{F.1})$$

The terminal pressures, P_1 and P_2 , are common to all line segments. The continuity equation requires that

$$\sum_{i=1}^n Q_{1i} = Q_1 \quad \text{and} \quad \sum_{i=1}^n Q_{2i} = Q_2 \quad (\text{F.2})$$

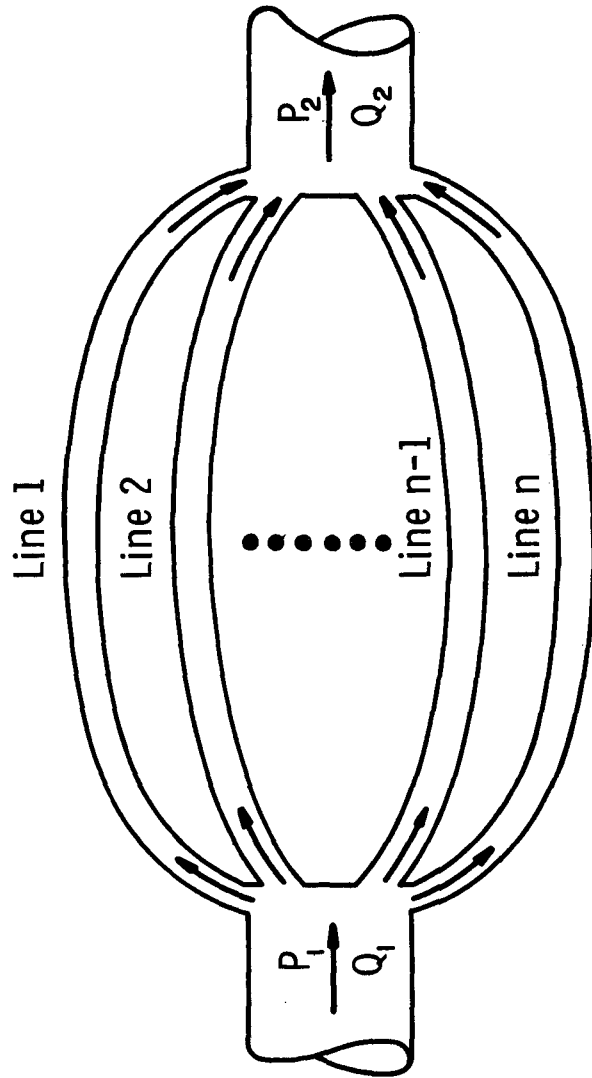
Summing Equations (F.1) and utilizing Equations (F.2) yields

$$\begin{aligned} Q_1 &= P_1 \sum_{i=1}^n Z_{c_i}^{-1} A_i \coth \Gamma_i - P_2 \sum_{i=1}^n Z_{c_i}^{-1} A_i \operatorname{csch} \Gamma_i \\ Q_2 &= P_1 \sum_{i=1}^n Z_{c_i}^{-1} A_i \operatorname{csch} \Gamma_i - P_2 \sum_{i=1}^n Z_{c_i}^{-1} A_i \coth \Gamma_i \end{aligned} \quad (\text{F.3})$$

Equations (F.3) can be easily rearranged into the standard form

$$\begin{bmatrix} P_2 \\ Q_2 \end{bmatrix} = \begin{bmatrix} b_{11} & b_{12} \\ b_{21} & b_{22} \end{bmatrix} \begin{bmatrix} P_1 \\ Q_1 \end{bmatrix} \quad (\text{F.4})$$

where



3435

Figure F-1. Parallel Line Model

$$b_{11} = b_{22} = \frac{\sum_{i=1}^n Z_{c_i}^{-1} A_i \coth \Gamma_i}{\sum_{i=1}^n Z_{c_i}^{-1} A_i \operatorname{csch} \Gamma_i}$$

$$b_{12} = - \frac{1}{\sum_{i=1}^n Z_{c_i}^{-1} A_i \operatorname{csch} \Gamma_i}$$

$$b_{21} = \sum_{i=1}^n Z_{c_i}^{-1} A_i \operatorname{csch} \Gamma_i - \frac{\left(\sum_{i=1}^n Z_{c_i}^{-1} A_i \coth \Gamma_i \right)^2}{\sum_{i=1}^n Z_{c_i}^{-1} A_i \operatorname{csch} \Gamma_i}$$

The line length that appears in the expression for the propagation operator is taken to be the developed length measured along the pipe centerline.

APPENDIX G

COMPLEX SIDE BRANCH

In general, any type of complicated side element may be modeled. These side elements can be visualized as local or lumped "compliances," even though they may not be compliance-like elements. The model used for an arbitrary complex side element, such as a gauge and line connected onto a feedline, may be put in the form of a local compliance, as shown in Figure G-1. This element is assumed to consist of a side branch line having an inertance, I , and resistance, R , and with a capacitance termination, C . The line inertance, I , and the line resistance, R , have been programmed respectively as:

$$I = \rho_o L/A_b \quad (G.1)$$

and

$$R = 128 \frac{\mu L}{\pi d_b^4} \quad (G.2)$$

Here, ρ_o = fluid density, L = side branch length, and A_b is the branch cross sectional area; μ is the fluid viscosity, and d_b is the side branch diameter. To consider the effects of compressibility in the side branch, the inertia and resistance effects are neglected, and

$$q_4 = \frac{V}{\gamma P} \left(\frac{dp}{dt} \right) \quad \text{for gases}$$

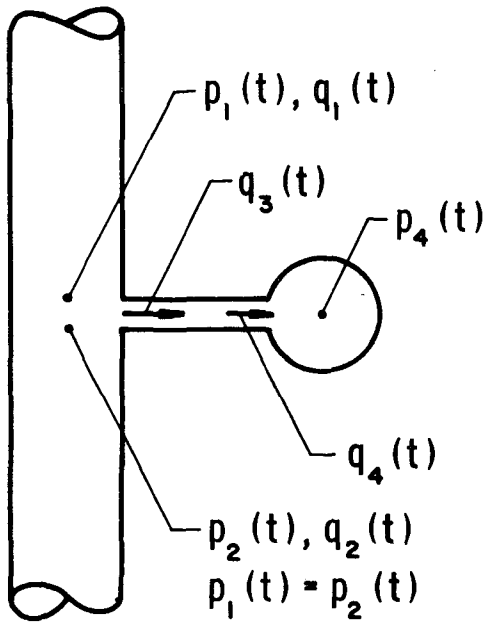
$$q_4 = \frac{V}{\kappa} \left(\frac{dp}{dt} \right) \quad \text{for liquids} \quad (G.3)$$

where q_4 is the flow into the branch, V is the volume of the compressible fluid contained within the side branch, γ is the ratio of specific heats for the fluid (if a gas), and κ is the liquid bulk modulus.

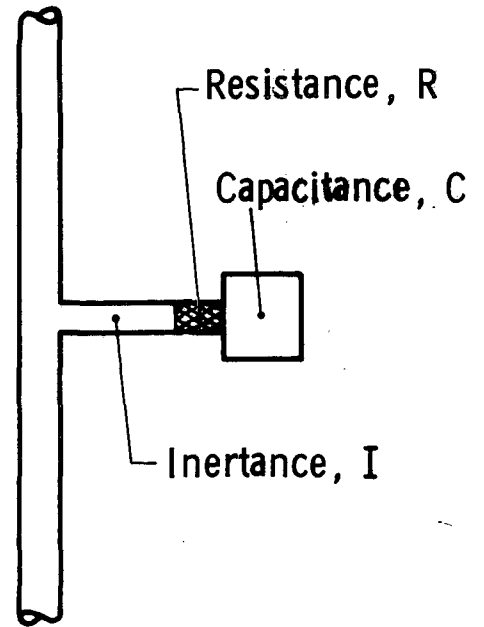
For the case of a gauge connected to a feedline containing a liquid by a branch line partially filled with air, the lumped model is obtained by summing the effects of the branch inertance, resistance, and capacitance.

The resultant expressions in the Laplace domain relating the pressure and flow upstream and downstream of the side branch become

(a) PHYSICAL SITUATION



(b) MODEL



(c) MODEL EQUATIONS IN LA PLACE DOMAIN

CONTINUITY IN LINE

$$Q_1(s) - Q_2(s) = Q_3(s)$$

GAUGE LINE (Assumed simple inertance plus resistance only)

$$Q_3(s) = Q_4(s)$$

$$P_2(s) - P_4(s) = IsQ_3 + RQ_3$$

CAPACITANCE

$$Q_4(s) = CsP_4$$

"COMPLIANCE MODEL"

$$Q_1(s) - Q_2(s) = \left\{ \frac{C}{IC_s^2 + RC_s + I} \right\} s P_1(s)$$

2751

Figure G-1. Example Treatment Of More General "Local Compliance" In Feed Line

$$P_2(s) = P_1(s)$$

$$Q_2(s) = Q_1(s) - \left[\frac{C}{ICs^2 + RCs + 1} \right] sP_1(s) \quad (G.4)$$

The quantity in the brackets can be visualized as a complex "compliance" for this case, and represents a local compliance so far as the feedline is concerned.

APPENDIX H

USER'S MANUAL FOR GENERALIZED
FEEDLINE PROGRAM

H.1 Program Organization

This manual describes the mechanics of the Generalized Feedline Computer Code. It is assumed that the user has had previous experience in FORTRAN IV coding.

The FORTRAN IV source deck is composed of a main or controller program, individual subroutines for each line component and several special purpose subroutines which either perform specific mathematical operations or serve as function evaluators. The subroutine approach was chosen because of its distinct advantages in the areas of program debugging, modification and expansion. Using the Control Data Corporation 6400 system, the source deck is compiled each time the program is submitted to the terminal for execution, thus eliminating tape handling. The function of each routine is presented below in the order in which it will appear in the FORTRAN listing which is included in the next section.

Controller:

The controller program performs the following functions:

- (1) Read-in of all pertinent data for a particular line configuration;
- (2) Execute the calling of subroutines in the proper sequence;
- (3) Evaluate the magnitude of the transfer function at each frequency;
- (4) Increment frequency, the independent variable, within a prescribed range;
- (5) Perform all output operations.

Subroutine ONE: Calculates matrix elements for a straight duct of finite length and constant cross-sectional area having no external excitation.

Subroutine TWO: Calculates matrix elements for a single cavitation bubble including the effects of radiation, thermal and viscous damping.

Subroutine THREE: Calculates the matrix elements of a pressure-volume compensator (PVC) joint including the effects of internal friction.

- Subroutine FOUR: Establishes the continuity requirements for a side branch pulser.
- Subroutine FIVE: Calculates the matrix elements for a straight line which undergoes rigid body motion as a result of an external velocity excitation.
- Subroutine SIX: Calculates the matrix elements for several lines in parallel all of which have a common entrance-exit point.
- Subroutine SEVEN: Calculates the matrix elements for a bellows with gas trap liner. Relative motion between the ends of the bellows is permitted.
- Subroutine EIGHT: Calculates the matrix elements for a line with mounting stiffness having a structural acceleration applied to the viscoelastic support.
- Subroutine NINE: Calculates the matrix elements for a line undergoing forced changes in length.
- Subroutine TEN: Calculates matrix elements for a line with mounting stiffness using the impedance method.
- Subroutine ELEVEN: Calculates the matrix elements for a complex side branch with laminar flow.
- Subroutine TWELVE
to FIFTEEN: Available for future expansion.
- Subroutine SPEED: Calculates the speed of sound in a pure liquid or a liquid with a homogeneous distribution of an ullage gas. A mixture of a liquid and its own vapor may also be considered. However, in the latter case, the results are not precise because the theoretical model does not include the thermodynamic effect of phase change at the bubble surface. Finally, the speed of sound may be corrected for wall elasticity.
- Subroutine DMAT: Calculates the resultant matrix D in Equation (81).
- Subroutine BMAT: Calculates the resultant matrix B in Equation (82).

Subroutine J1ORJ10: Evaluates Bessel functions $J_1(Z)$ and $J_0(Z)$ for complex Z . Series expansion is used for moderate values of the argument; an asymptotic approximation is used for large arguments.

H. 2. Program Listing

This section contains a listing of the program source deck. Program control cards, which are described in Section H. 4, are applicable to CDC 6000 series computer systems.

H. 3. Program Input Package

Due to the generalized nature of this computer program, the length of the input package is variable and is directly related to the number of components in the feedline model. The first card in the package is always an alphanumeric header card on which the user can punch pertinent information such as run number, configuration number, etc., to be printed as the first line of program output. Fifty-five (55) Hollerith fields have been allocated for the information on the header card. The actual data input is a combination of integer or floating point information. Integer data conforms to a (24I3) format, while the floating point data is read in with a (6E12.6) format.

The following data must be supplied in the order and with the units shown:

CARD 1	Header card	
CARD 2	NELM, dimensionless	Designates the number of components in the line.
	JBNUM, dimensionless	Number of matrices that must be summed to arrive at matrix B, Equation (82).
	NGAS, dimensionless	Indicates presence (NGAS = 1) or absence (NGAS = 0) of dissolved gases in propellant.
	NELAST, dimensionless	Includes (NELAST = 1) or excludes (NELAST = 0) line elasticity effects in speed of sound calculation.

```

PROGRAM CONTROL(INPUT,OUTPUT,TAPE 60=INPUT)
C
C   NELM=NUMBER OF DISCRETE ELEMENTS IN THE FEEDLINE,I.E., LINES,
C   BELLOWS, PVC JOINTS,ETC.
C
C   NELM INTEGER CONSTANTS ARE READ IN AND DESCRIBE THE TYPE OF
C   ELEMENTS IN THE ORDER THEY APPEAR IN THE LINE BEGINNING AT THE
C   OUTPUT OF THE FUEL TANK AND TERMINATING WITH THE COMBINED INPUT
C   IMPEDANCE TO THE TURBOPUMP,INJECTOR AND ENGINE. FOR EXAMPLE,
C   ITYPE(J)=M, J=ELEMENT NUMBER, M=ELEMENT TYPE
C   M=1 SIMPLE LINE WITH NO EXTERNAL EXCITATION
C   M=2 CAVITATION BUBBLE
C   M=3 PRESSURE VOLUME COMPENSATOR
C   M=4 SIDE BRANCH PULSER
C   M=5 RIGID BODY MOTION OF A SIMPLE LINE,VELOCITY EXCITATION
C   M=6 NPAR LINES IN PARALLEL WITH A COMMON INPUT-OUTPUT POINT
C   M=7 BELLOWS WITH RELATIVE MOTION BETWEEN THE ENDS
C   M=8 LINE WITH MOUNTING STIFFNESS(OPTION 1)
C   M=9 FORCED CHANGES IN LINE LENGTH
C   M=10 LINE WITH MOUTING STIFFNESS(OPTION 2)
C   M=11 COMPLEX SIDE BRANCH
C   M=12
C   M=13
C   M=14
C   M=15
C
C   JBNUM=NUMBER OF MATRICES THAT MUST BE SUMMED TO CONSTRUCT MATRIX B
C   B=B(1)+B(2)+.....+B(JBNUM)
C
C   JTERM(J) IS THE NUMBER OF SUBMATRICES IN B(J)
C
C   K(J,M) IS AN ARRAY THAT DESCRIBES THE TYPE OF MATRICES THAT ARE TO
C   BE MULTIPLIED TOGETHER TO CONSTRUCT THE COMPONENTS OF MATRIX B.
C   M TAKES ON VALUES FROM 1 THROUGH JTERM(J)
C   FOR EXAMPLE, IF B(2)=D5*D4*C3 THEN K(2,1)=5,K(2,2)=4,K(2,3)=3
C
C   NGAS=0, NO DISSOLVED GASES IN THE PROPELLANT
C   NGAS=1, DISSOLVED GASES IN PROPELLANT WITH GAS-TO-LIQUID MASS
C   FRACTION,PHI
C
C   NELAST=0, SPEED OF SOUND IN PROPELLANT IS BASED ON AN INFINITELY
C   RIGID TRANSMISSION LINE
C
C   NELAST=1, SPEED OF SOUND IN PROPELLANT REFLECTS LINE ELASTICITY
C   (WALL MODULUS EWALL AND WALL THICKNESS HWALL)
C
C   BRCOMP=COMPLIANCE OF SIDE BRANCH ELEMENT
C
C   BRL=LENGTH OF SIDE BRANCH ELEMENT IN FEET
C
C   BDIAM=DIAMETER OF SIDE BRANCH ELEMENT IN INCHES
C
C   BRR=RESISTANCE OF SIDE BRANCH ELEMENT
C
C   * * * * *
C   COMPLEX ETA,ENUM,DENOM,TRANS,B,D,XI,ARG,RJ,GAMMA,ZC,COSHG,SINHG,DD
1,CC,TCOTH,TCSCH,BB,Z1,Z2,X1,X2,X3,X4,QUADRAT,ALPHAP,BETAP,ALPHADP,
2BETADP,GOF5,SLCW,COSHCW,SINHCW,COEFF,ALPHA1,ALPHA2
C   COMPLEX ZSTRUCT,ALPHA,BETA
C   DIMENSION ITYPE(15),JTERM(15),K(15,15),EL(15),RADIUS(15),RBUB(15),
1FPVC(15),AKBPVC(15),AKCPVC(15),PARLEN(15,5),PARRAD(15,5),FREQ(200)
C   DIMENSION B(2,1),D(2,2),SIZE(200),SIZFDB(200),ANGLE(200),FBEL(15),
1COMPLY(15),AKBEL(15),BSIGN(10),DAMPER(15),SPRINGK(15)
C   DIMENSION DD(2,2,15),CC(2,1,15),BB(2,1,15),RADSEC(200),AREA(15)
C   COMMON PI,RADIUS,OMEGA,ENU,ETA,EL,CO,RHOO,THERMK,RBUB,CPCV,PO,VISC
1,FPVC,AKBPVC,AKCPVC,NPAR,PARRAD,PARLEN,BULKMOD,RHOLIQ,NGAS,GASMW
C   COMMON GAMGAS,G,TO,PHI,COMPLY,NELAST,EWALL,HWALL,NELM,JBNUM,JTERM,
1K,DD,CC,D,B,BB,CP,J,AREA,VMEAN,FBEL,AKBEL,BSIGN,DAMPER,SPRINGK
C   COMMON G1,G2,RHOWALL,ZX,ZY
C   COMMON BRCOMP,BRL,BRDIAM

```

```

C      * * * * *
1 READ 1000
  IF(EOF,60)5,10
5 STOP
10 CONTINUE
  READ 1005,NELM,JBNUM,NGAS,NELAST
  READ 1005,(ITYPE(J),J=1,NELM)
  READ 1005,(JTERM(J),J=1,JBNUM)
  DO 15 J=1,JBNUM
  KOUNT=JTERM(J)
15 READ 1005,(K(J,M),M=1,KOUNT)
  READ 1020,(BSIGN(J),J=1,JBNUM)
  READ 1020,HERTZI,DELHZ1,FILIM,DELHZ2,HERTZF
  READ 1020,SIGN,TERMZ,RHOLIQ,THERMK,PD,TD
  READ 1020,EWALL,HWALL,ZINPUT,CPCV,BULKMOD,PHI
  READ 1020,VISC,GASMW,GAMGAS,CP,VMEAN,BRCOMP
C      LOOP FOR READ-IN OF LINE ELEMENT DATA
  PI=3.1415927
  DO 95 J=1,NELM
  INDEX=ITYPE(J)
  GO TO (20,25,30,35,40,45,50,55,60,65,70,75,80,85,90),INDEX
20 READ 1020,EL(J),RADIUS(J)
  AREA(J)=PI*RADIUS(J)**2/144.
  GO TO 95
25 READ 1020,RBUB(J),RADIUS(J)
  GO TO 95
30 READ 1020,FPVC(J),AKBPVC(J),AKCPVC(J)
  GO TO 95
35 GO TO 95
40 READ 1020,EL(J),RADIUS(J)
  AREA(J)=PI*RADIUS(J)**2/144.
  GO TO 95
45 READ 1005,NPAR
  READ 1020,(PARLEN(J,I),PARRAD(J,I),I=1,NPAR)
  GO TO 95
50 READ 1020,FBEL(J),COMPLY(J),AKBEL(J)
  GO TO 95
55 READ 1020,EL(J),RADIUS(J),DAMPER(J),SPRINGK(J)
  AREA(J)=PI*RADIUS(J)**2/144.
  GO TO 95
60 READ 1020,EL(J),RADIUS(J),G1,G2,RHOWALL
  AREA(J)=PI*RADIUS(J)**2/144.
  GO TO 95
65 READ 1020,EL(J),RADIUS(J),ZX,ZY
  AREA(J)=PI*RADIUS(J)**2/144.
  GO TO 95
70 READ 1020,BRL,BRDIAM
  GO TO 95
75 READ 1000
  GO TO 95
80 READ 1000
  GO TO 95
85 READ 1000
  GO TO 95
90 READ 1000
95 CONTINUE
C      * * * * *
  G=32.174049

```

```

ETA=(0.,1.)
IFREQ=1
FREQ(IFREQ)=HERTZI
C  CALCULATION OF MATRIX ELEMENTS
99  OMEGA=2.*PI*FREQ(IFREQ)
    DO 175 J=1,NELM
      INDEX=ITYPE(J)
      GO TO (100,105,110,115,120,125,130,135,140,145,150,155,160,165,170
1),INDEX
100 CALL ONE
    GO TO 175
105 CALL TWO
    GO TO 175
110 CALL THREE
    GO TO 175
115 CALL FOUR
    GO TO 175
120 CALL FIVE
    GO TO 175
125 CALL SIX
    GO TO 175
130 CALL SEVEN
    GO TO 175
135 CALL EIGHT
    GO TO 175
140 CALL NINE
    GO TO 175
145 CALL TEN
    GO TO 175
150 CALL ELEVEN
    GO TO 175
155 CALL TWELVE
    GO TO 175
160 CALL THIRTEEN
    GO TO 175
165 CALL FOURTEEN
    GO TO 175
170 CALL FIVETEN
175 CONTINUE
C  * * * * *
    CALL DMAT
    CALL BMAT
    ENUM=B(1,1)*(D(2,1)*ZINPUT+D(2,2))-B(2,1)*(D(1,1)*ZINPUT+D(1,2))
    DENOM=D(2,1)*ZINPUT+D(2,2)-(D(1,1)*ZINPUT+D(1,2))/TERMZ
    TRANS=SIGN*ENUM/DENOM
    SIZE(IFREQ)=CABS(TRANS)
    SIZEDB(IFREQ)=20.*ALOG10(SIZE(IFREQ))
    ANGLE(IFREQ)=ATAN2(AIMAG(TRANS),REAL(TRANS))*57.29578
180 ANGLE(IFREQ)=ANGLE(IFREQ)-180.
185 RADSEC(IFREQ)=OMEGA
    IF(FREQ(IFREQ).LT.HERTZF) GO TO 190
    GO TO 205
190 IFREQ=IFREQ+1
    IF(FREQ(IFREQ-1)-FILIM)195,195,200
195 FREQ(IFREQ)=FREQ(IFREQ-1)+DELHZ1
    IFINAL=IFREQ
    GO TO 99
200 FREQ(IFREQ)=FREQ(IFREQ-1)+DELHZ2

```

```

    IFINAL=IFREQ
    GO TO 99
205  PRINT 1000
    PRINT 1030
    DO 250 I=1,IFINAL
250  PRINT 1040,RADSEC(I),FREQ(I),SIZE(I),SIZEDB(I),ANGLE(I)
    GO TO 1
C   * * * * *
1000  FORMAT(55H1
1005  FORMAT(24I3)
1020  FORMAT(6E12.6)
1030  FORMAT(14H00MEGA-RAD/SEC,4X,7HFREQ-HZ,8X,5HTRANS,7X,8HTRANS-DB,6X,
    19HANGLE-DEG)
1040  FORMAT(1X,F9.1,F15.1,F13.3,F14.2,F15.1)
1050  FORMAT(1H1,E14.6,6E15.6)
    END

```

```

SUBROUTINE ONE
C THIS SUBROUTINE CALCULATES THE ELEMENTS OF THE TRANSFER MATRIX FOR
C A STRAIGHT LINE OF LENGTH L WITHOUT EXTERNAL EXCITATION
COMPLEX ETA, ENUM, DENOM, TRANS, B, D, XI, ARG, RJ, GAMMA, ZC, COSHG, SINHG, DD
1, CC, TCOTH, TCSCH, BB, Z1, Z2, X1, X2, X3, X4, QUADRAT, ALPHAP, BETAP, ALPHADP,
2BETADP, GOF5, SLCW, COSHCW, SINHCW, COEFF, ALPHA1, ALPHA2
COMPLEX ZSTRUCT, ALPHA, BETA
DIMENSION ITYPE(15), JTERM(15), K(15,15), EL(15), RADIUS(15), RBUB(15),
1FPVC(15), AKBPVC(15), AKCPVC(15), PARLEN(15,5), PARRAD(15,5), FREQ(200)
DIMENSION B(2,1), D(2,2), SIZE(200), SIZEDB(200), ANGLE(200), FBEL(15),
1COMPLY(15), AKBEL(15), BSIGN(10), DAMPER(15), SPRINGK(15)
DIMENSION DD(2,2,15), CC(2,1,15), BB(2,1,15), RADSEC(200), AREA(15)
COMMON PI, RADIUS, OMEGA, ENU, ETA, EL, CO, RHOO, THERMK, RBUB, CPCV, PO, VISC
1, FPVC, AKBPVC, AKCPVC, NPAR, PARRAD, PARLEN, BULKMOD, RHOLIQ, NGAS, GASMW
COMMON GAMGAS, G, TO, PHI, COMPLY, NELAST, EWALL, HWALL, NELM, JBNUM, JTERM,
1K, DD, CC, D, B, BB, CP, J, AREA, VMEAN, FBEL, AKBEL, BSIGN, DAMPER, SPRINGK
COMMON G1, G2, RHOWALL, ZX, ZY
CALL SPEED
REYNOLD=VMEAN*2.*RADIUS(J)/(ENU*12.)
RT=144.*(2.*ENU*0.0055*REYNOLD**0.85)/(RADIUS(J)**2)
Z1=(OMEGA*EL(J)*ETA)/CO
Z2=CSQRT((1.,0.)+RT/(OMEGA*ETA))
XI=SQRT(OMEGA/ENU)*CSQRT(-ETA)
ARG=XI*RADIUS(J)/12.
CALL J10RJO(ARG,RJ)
GAMMA=ETA*OMEGA*EL(J)/(CO*CSQRT((1.,0.)-2.*RJ/ARG))+REAL(Z1*Z2)
ZC=RHOO*CO/(CSQRT((1.,0.)-2.*RJ/ARG))
COSHG=(CEXP(GAMMA)+CEXP(-GAMMA))/2.
SINHG=(CEXP(GAMMA)-CEXP(-GAMMA))/2.
DD(1,1,J)=COSHG
DD(1,2,J)=-ZC*SINHG/AREA(J)
DD(2,1,J)=-AREA(J)*SINHG/ZC
DD(2,2,J)=COSHG
RETURN
END

```

```

SUBROUTINE TWO
THIS SUBROUTINE CALCULATES THE COMPLIANCE OF AND TRANSFER MATRIX
ACROSS A SINGLE BUBBLE
CPCV=RATIO OF SPECIFIC HEATS FOR THE GAS IN THE BUBBLE
CP=SPECIFIC HEAT AT CONSTANT PRESSURE FOR THE GAS IN THE BUBBLE
COMPLEX ETA,ENUM,DENOM,TRANS,B,D,XI,ARG,RJ,GAMMA,ZC,COSHG,SINHG,DD
1,CC,TCOTH,TCSCH,BB,Z1,Z2,X1,X2,X3,X4,QUADRAT,ALPHAP,BETAP,ALPHADP,
2BETADP,GOF8,SLCW,COSHCW,SINHCW,COEFF,ALPHA1,ALPHA2
COMPLEX ZSTRUCT,ALPHA,BETA
DIMENSION ITYPE(15),JTERM(15),K(15,15),EL(15),RADIUS(15),RBUB(15),
1FPVC(15),AKBPVC(15),AKCPVC(15),PARLEN(15,5),PARRAD(15,5),FREQ(200)
DIMENSION B(2,1),D(2,2),SIZE(200),SIZEDB(200),ANGLE(200),FBEL(15),
1COMPLY(15),AKBEL(15),BSIGN(10),DAMPER(15),SPRINGK(15)
DIMENSION DD(2,2,15),CC(2,1,15),BB(2,1,15),RADSEC(200),AREA(15)
COMMON PI,RADIUS,OMEGA,ENU,ETA,EL,CO,RH00,THERMK,RBUB,CPCV,PO,VISC
1,FPVC,AKBPVC,AKCPVC,NPAR,PARRAD,PARLEN,BULKMOD,RHOLI,NGAS,GASMW
COMMON GAMGAS,G,TO,PHI,COMPLY,NELAST,EWALL,HWALL,NELM,JBNUM,JTERM,
1K,DD,CC,D,B,BB,CP,J,AREA,VMEAN,FBEL,AKBEL,BSIGN,DAMPER,SPRINGK
COMMON G1,G2,RHOWALL,ZX,ZY
GASCON=778.*CP*(1.-1./CPCV)
GASDEN=144.*PO/(GASCON*G*(TO+460.))
D THERM=THERMK/(GASDEN*CP*G)
PRO=SQRT(OMEGA*3600./(2.*D THERM))*RBUB(J)/12.
IF(PRO.GT.35.)20,10
10 T1=(SINH(2.*PRO)+SIN(2.*PRO))/(COSH(2.*PRO)-COS(2.*PRO))
T2=(SINH(2.*PRO)-SIN(2.*PRO))/(COSH(2.*PRO)-COS(2.*PRO))
T3=2.*PRO/(3.*(CPCV-1.))
T4=(T1-1./PRO)/(T3+T2)
POLY=CPCV/((1.+T2/T3)*(1.+T4**2))
GO TO 30
20 POLY=CPCV
30 BUBVOL=4.*PI*RBUB(J)**3/(3.*1728.)
CALL SPEED
SPRING=POLY*PO*144./BUBVOL
AMASS2=RH00/(4.*PI*RBUB(J)/12.)
IF(PRO.GT.35.)50,40
40 BTHERM=T4*SPRING/OMEGA
GO TO 60
50 BTHERM=3.*(CPCV-1.)*SPRING/(2.*PRO*OMEGA)
60 BRAD=AMASS2*RBUB(J)*(OMEGA**2)/(12.*CO)
BVIS=1728.*VISC/(PI*RBUB(J)**3)
BDAMP=BTHERM+BRAD+BVIS
DD(1,1,J)=(1.,0.)
DD(1,2,J)=(0.,0.)
DD(2,1,J)=-ETA*OMEGA/(-AMASS2*OMEGA**2+ETA*BDAMP*OMEGA+SPRING)
DD(2,2,J)=(1.,0.)
RETURN
END

```

```

SUBROUTINE THREE
C THIS SUBROUTINE CALCULATES THE TRANSFER MATRIX FOR A PRESSURE-
C VOLUME COMPENSATOR(PVC JOINT)
COMPLEX ETA,ENUM,DENOM,TRANS,B,D,XI,ARG,RJ,GAMMA,ZC,COSHG,SINHG,DD
1,CC,TCOTH,TCSCH,BB,Z1,Z2,X1,X2,X3,X4,QUADRAT,ALPHAP,BETAP,ALPHADP,
2BETADP,GOFS,SLCW,COSHCW,SINHCW,COEFF,ALPHA1,ALPHA2
COMPLEX ZSTRUCT,ALPHA,BETA
DIMENSION ITYPE(15),JTERM(15),K(15,15),EL(15),RADIUS(15),RBUB(15),
1FPVC(15),AKBPVC(15),AKCPVC(15),PARLEN(15,5),PARRAD(15,5),FREQ(200)
DIMENSION B(2,1),D(2,2),SIZE(200),SIZEDB(200),ANGLE(200),FBEL(15),
1COMPLY(15),AKBEL(15),BSIGN(10),DAMPER(15),SPRINGK(15)
DIMENSION DD(2,2,15),CC(2,1,15),BB(2,1,15),RADSEC(200),AREA(15)
COMMON PI,RADIUS,OMEGA,ENU,ETA,EL,CO,RHOO,THERMK,RBUB,CPCV,PO,VISC
1,FPVC,AKBPVC,AKCPVC,NPAR,PARRAD,PARLEN,BULKMOD,RHOLIQ,NGAS,GASMW
COMMON GAMGAS,G,TO,PHI,COMPLY,NELAST,EWALL,HWALL,NELM,JBNUM,JTERM,
1K,DD,CC,D,B,BB,CP,J,AREA,VMEAN,FBEL,AKBEL,BSIGN,DAMPER,SPRINGK
COMMON G1,G2,RHOWALL,ZX,ZY
FRICT=FPVC(J)
AKB=AKBPVC(J)
AKC=AKCPVC(J)
AKPVC=AKB-AKC
DD(1,1,J)=FRICT
DD(1,2,J)=(0.,0.)
DD(2,1,J)=(0.,0.)
DD(2,2,J)=(1.,0.)
CC(1,1,J)=(0.,0.)
CC(2,1,J)=AKPVC
RETURN
END

```

```

SUBROUTINE FOUR
THIS SUBROUTINE CALCULATES THE ELEMENTS OF THE TRANSFER MATRIX FOR
A SIDE BRANCH PULSER
COMPLEX ETA,ENUM,DENOM,TRANS,B,D,XI,ARG,RJ,GAMMA,ZC,COSHG,SINHG,DD
1,CC,TCOTH,TCSCH,BB,Z1,Z2,X1,X2,X3,X4,QUADRAT,ALPHAP,BETAP,ALPHADP,
2BETADP,GOFS,SLCW,COSHCW,SINHCW,COEFF,ALPHA1,ALPHA2
COMPLEX ZSTRUCT,ALPHA,BETA
DIMENSION ITYPE(15),JTERM(15),K(15,15),EL(15),RADIUS(15),RBUB(15),
1FPVC(15),AKBPVC(15),AKCPVC(15),PARLEN(15,5),PARRAD(15,5),FREQ(200)
DIMENSION B(2,1),D(2,2),SIZE(200),SIZEDB(200),ANGLE(200),FBEL(15),
1COMPLY(15),AKBEL(15),BSIGN(10),DAMPER(15),SPRINGK(15)
DIMENSION DD(2,2,15),CC(2,1,15),BB(2,1,15),RADSEC(200),AREA(15)
COMMON PI,RADIUS,OMEGA,ENU,ETA,EL,CO,RHOD,THERMK,RBUB,CPCV,PO,VISC
1,FPVC,AKBPVC,AKCPVC,NPAR,PARRAD,PARLEN,BULKMOD,RHOLIQ,NGAS,GASMW
COMMON GAMGAS,G,TO,PHI,COMPLY,NELAST,EWALL,HWALL,NELM,JBNUM,JTERM,
1K,DD,CC,D,B,BB,CP,J,AREA,VMEAN,FBEL,AKBEL,BSIGN,DAMPER,SPRINGK
COMMON G1,G2,RHOWALL,ZX,ZY
DD(1,1,J)=(1.,0.)
DD(1,2,J)=(0.,0.)
DD(2,1,J)=(0.,0.)
DD(2,2,J)=(1.,0.)
CC(1,1,J)=(0.,0.)
CC(2,1,J)=(1.,0.)
RETURN
END

```

```

SUBROUTINE FIVE
C THIS SUBROUTINE CALCULATES THE ELEMENTS OF THE TRANSFER MATRICES
C FOR THE LONGITUDINAL RIGID BODY MOTION OF A SIMPLE LINE OF LENGTH
C L. THE MOTION IS A RESULT OF VELOCITY EXCITATION.
COMPLEX ETA, ENU, DENOM, TRANS, B, D, XI, ARG, RJ, GAMMA, ZC, COSHG, SINHG, DD
1, CC, TCOth, TCsch, BB, Z1, Z2, X1, X2, X3, X4, QUADRAT, ALPHAP, BETAP, ALPHADP,
2BETADP, GOFs, SLCW, COSHCW, SINHCW, COEFF, ALPHA1, ALPHA2
COMPLEX ZSTRUCT, ALPHA, BETA
DIMENSION ITYPE(15), JTERM(15), K(15,15), EL(15), RADIUS(15), RBUB(15),
1FPVC(15), AKBPVC(15), AKCPVC(15), PARLEN(15,5), PARRAD(15,5), FREQ(200)
DIMENSION B(2,1), D(2,2), SIZE(200), SIZEDB(200), ANGLE(200), FBEL(15),
1COMPLY(15), AKBEL(15), BSIGN(10), DAMPER(15), SPRINGK(15)
DIMENSION DD(2,2,15), CC(2,1,15), BB(2,1,15), RADSEC(200), AREA(15)
COMMON PI, RADIUS, OMEGA, ENU, ETA, EL, CO, RHOO, THERMK, RBUB, CPCV, PO, VISC
1, FPVC, AKBPVC, AKCPVC, NPAR, PARRAD, PARLEN, BULKMOD, RHOLIQ, NGAS, GASMW
COMMON GAMGAS, G, TO, PHI, COMPLY, NELAST, EWALL, HWALL, NELM, JBNUM, JTERM,
1K, DD, CC, D, B, BB, CP, J, AREA, VMEAN, FBEL, AKBEL, BSIGN, DAMPER, SPRINGK
COMMON G1, G2, RHOWALL, ZX, ZY
CALL SPEED
REYNOLD=VMEAN*2.*RADIUS(J)/(ENU*12.)
RT=144.*(2.*ENU*0.0055*REYNOLD**0.85)/(RADIUS(J)**2)
Z1=(OMEGA*EL(J)*ETA)/CO
Z2=CSQRT((1.,0.)+RT/(OMEGA*ETA))
XI=SQRT(OMEGA/ENU)*CSQRT(-ETA)
ARG=XI*RADIUS(J)/12.
CALL J1ORJ0(ARG, RJ)
GAMMA=ETA*OMEGA*EL(J)/(CO*CSQRT((1.,0.)-2.*RJ/ARG))+REAL(Z1*Z2)
ZC=RHOO*CO/(CSQRT((1.,0.)-2.*RJ/ARG))
COSHG=(CEXP(GAMMA)+CEXP(-GAMMA))/2.
SINHG=(CEXP(GAMMA)-CEXP(-GAMMA))/2.
DD(1,1,J)=COSHG
DD(1,2,J)=-ZC*SINHG/AREA(J)
DD(2,1,J)=-AREA(J)*SINHG/ZC
DD(2,2,J)=COSHG
CC(1,1,J)=ZC*SINHG
CC(2,1,J)=AREA(J)*((1.,0.)-COSHG)
RETURN
END

```

```

SUBROUTINE SIX
THIS SUBROUTINE CALCULATES THE ELEMENTS OF THE TRANSFER MATRIX FOR
AN ARBITRARY NUMBER OF LINES IN PARALLEL ALL OF WHICH EMANATE FROM
AND CONVERGE ON COMMON INPUT-OUTPUT POINTS.
COMPLEX ETA,ENUM,DENOM,TRANS,B,D,XI,ARG,RJ,GAMMA,ZC,COSHG,SINHG,DD
1,CC,TCOTH,TCSCH,BB,Z1,Z2,X1,X2,X3,X4,QUADRAT,ALPHAP,BETAP,ALPHADP,
2BETADP,GOFS,SLCW,COSHCW,SINHCW,COEFF,ALPHA1,ALPHA2
COMPLEX ZSTRUCT,ALPHA,BETA
DIMENSION ITYPE(15),JTERM(15),K(15,15),EL(15),RADIUS(15),RBUB(15),
1FPVC(15),AKBPVC(15),AKCPVC(15),PARLEN(15,5),PARRAD(15,5),FREQ(200)
DIMENSION B(2,1),D(2,2),SIZE(200),SIZEDB(200),ANGLE(200),FBEL(15),
1COMPLY(15),AKBEL(15),BSIGN(10),DAMPER(15),SPRINGK(15)
DIMENSION DD(2,2,15),CC(2,1,15),BB(2,1,15),RADSEC(200),AREA(15)
COMMON PI,RADIUS,OMEGA,ENU,ETA,EL,CO,RHOO,THERMK,RBUB,CPCV,PD,VISC
1,FPVC,AKBPVC,AKCPVC,NPAR,PARRAD,PARLEN,BULKMOD,RHOLIQ,NGAS,GASMW
COMMON GAMGAS,G,TO,PHI,COMPLY,NELAST,EWALL,HWALL,NELM,JBNUM,JTERM,
1K,DD,CC,D,B,BB,CP,J,AREA,VMEAN,FBEL,AKBEL,BSIGN,DAMPER,SPRINGK
COMMON G1,G2,RHOWALL,ZX,ZY
DO 5 I=1,NPAR
CALL SPEED
CO=CO/SQRT(1.+BULKMOD*2.*PARRAD(J,I)/(144.*EWALL*HWALL))
SQFT=PI*PARRAD(J,I)**2/144.
XI=SQRT(OMEGA/ENU)*CSQRT(-ETA)
ARG=XI*PARRAD(J,I)/12.
CALL J1ORJ0(ARG,RJ)
GAMMA=ETA*OMEGA*PARLEN(J,I)/(CO*CSQRT((1.,0.)-2.*RJ/ARG))
ZC=RHOO*CO/(CSQRT((1.,0.)-2.*RJ/ARG))
COSHG=(CEXP(GAMMA)+CEXP(-GAMMA))/2.
SINHG=(CEXP(GAMMA)-CEXP(-GAMMA))/2.
TCOTH=TCOTH+SQFT*COSHG/(SINHG*ZC)
5 TCSCH=TCSCH+SQFT/(ZC*SINHG)
DD(1,1,J)=TCOTH/TCSCH
DD(1,2,J)=-1./TCSCH
DD(2,1,J)=TCSCH-TCOTH**2/TCSCH
DD(2,2,J)=TCOTH/TCSCH
RETURN
END

```

SUBROUTINE SEVEN

C THIS SUBROUTINE CALCULATES THE ELEMENTS OF THE TRANSFER MATRIX FOR
C A BELLOWS WITH A LUMPED COMPLIANCE REPRESENTING TRAPPED GAS UNDER
C THE LINER PLUS A PERIODIC VOLUMETRIC CHANGE DUE TO RELATIVE MOTION
C OF THE ENDS OF THE BELLOWS
COMPLEX ETA,ENUM,DENOM,TRANS,B,D,XI,ARG,RJ,GAMMA,ZC,COSHG,SINHG,DD
1,CC,TCOTH,TCSCH,BB,Z1,Z2,X1,X2,X3,X4,QUADRAT,ALPHAP,BETAP,ALPHADP,
2BETADP,GOFS,SLCW,COSHCW,SINHCW,COEFF,ALPHA1,ALPHA2
COMPLEX ZSTRUCT,ALPHA,BETA
DIMENSION ITYPE(15),JTERM(15),K(15,15),EL(15),RADIUS(15),RBUB(15),
1FPVC(15),AKBPVC(15),AKCPVC(15),PARLEN(15,5),PARRAD(15,5),FREQ(200)
DIMENSION B(2,1),D(2,2),SIZE(200),SIZEDB(200),ANGLE(200),FBEL(15),
1COMPLY(15),AKBEL(15),BSIGN(10),DAMPER(15),SPRINGK(15)
DIMENSION DD(2,2,15),CC(2,1,15),BB(2,1,15),RADSEC(200),AREA(15)
COMMON PI,RADIUS,OMEGA,ENU,ETA,EL,CO,RHOO,THERMK,RBUB,CPCV,PO,VISC
1,FPVC,AKBPVC,AKCPVC,NPAR,PARRAD,PARLEN,BULKMOD,RHOLIQ,NGAS,GASMW
COMMON GAMGAS,G,TO,PHI,COMPLY,NELAST,EWALL,HWALL,NELM,JBNUM,JTERM,
1K,DD,CC,D,B,BB,CP,J,AREA,VMEAN,FBEL,AKBEL,BSIGN,DAMPER,SPRINGK
COMMON G1,G2,RHOWALL,ZX,ZY
FRICT=FBEL(J)
C=COMPLY(J)
AKB=AKBEL(J)
DD(1,1,J)=FRICT
DD(1,2,J)=(0.,0.)
DD(2,1,J)=-C*ETA*OMEGA
DD(2,2,J)=(1.,0.)
CC(1,1,J)=(0.,0.)
CC(2,1,J)=AKB
RETURN
END

```

SUBROUTINE EIGHT
THIS SUBROUTINE CALCULATES THE ELEMENTS OF THE TRANSFER MATRICES
FOR THE AXIAL MOTION OF A VERTICAL LINE WITH MOUNTING STIFFNESS
ON THE TWO ADJACENT HORIZONTAL LINES. THE TWO STIFFNESS TERMS ARE
LUMPED INTO ONE EFFECTIVE SPRING IN PARALLEL WITH ONE EFFECTIVE
VISCOUS DAMPER. THE FORCING FUNCTION IS AN ACCELERATION APPLIED
TO THE SPRING-DAMPER SUPPORT PLUS A PASSIVE INERTIAL LOADING
COMPLEX ETA, ENUM, DENOM, TRANS, B, D, XI, ARG, RJ, GAMMA, ZC, COSHG, SINHG, DD
1, CC, TCOOTH, TCSC, BB, Z1, Z2, X1, X2, X3, X4, QUADRAT, ALPHAP, BETAP, ALPHADP,
2BETADP, GOFS, SLCW, COSHCW, SINHCW, COEFF, ALPHA1, ALPHA2
COMPLEX ZSTRUCT, ALPHA, BETA
DIMENSION ITYPE(15), JTERM(15), K(15,15), EL(15), RADIUS(15), RBUB(15),
1FPVC(15), AKBPVC(15), AKCPVC(15), PARLEN(15,5), PARRAD(15,5), FREQ(200)
DIMENSION B(2,1), D(2,2), SIZE(200), SIZEDB(200), ANGLE(200), FBEL(15),
1COMPLY(15), AKBEL(15), BSIGN(10), DAMPER(15), SPRINGK(15)
DIMENSION DD(2,2,15), CC(2,1,15), BB(2,1,15), RADSEC(200), AREA(15)
COMMON PI, RADIUS, OMEGA, ENU, ETA, EL, CO, RHOO, THERMK, RBUB, CPCV, PO, VISC
1, FPVC, AKBPVC, AKCPVC, NPAR, PARRAD, PARLEN, BULKMOD, RHOLIQ, NGAS, GASMW
COMMON GAMGAS, G, TO, PHI, COMPLY, NELAST, EWALL, HWALL, NELM, JBNUM, JTERM,
1K, DD, CC, D, B, BB, CP, J, AREA, VMEAN, FBEL, AKBEL, BSIGN, DAMPER, SPRINGK
COMMON G1, G2, RHOWALL, ZX, ZY
CALL SPEED
REYNOLD=VMEAN*2.*RADIUS(J)/(ENU*12.)
RT=144.*(2.*ENU*0.0055*REYNOLD**0.85)/(RADIUS(J)**2)
Z1=(OMEGA*EL(J)*ETA)/CO
Z2=CSQRT((1.,0.)+RT/(OMEGA*ETA))
XI=SQRT(OMEGA/ENU)*CSQRT(-ETA)
ARG=XI*RADIUS(J)/12.
CALL J10RJO(ARG,RJ)
GAMMA=ETA*OMEGA*EL(J)/(CO*CSQRT((1.,0.)-2.*RJ/ARG))+REAL(Z1*Z2)
ZC=RHOO*CO/(CSQRT((1.,0.)-2.*RJ/ARG))
COSHG=(CEXP(GAMMA)+CEXP(-GAMMA))/2.
SINHG=(CEXP(GAMMA)-CEXP(-GAMMA))/2.
AMASS=RHOO*(AREA(J-1)*EL(J-1)+AREA(J+1)*EL(J+1))
QUADRAT=-AMASS*OMEGA**2+ETA*OMEGA*DAMPER(J)+SPRINGK(J)
ALPHAP=(ETA*OMEGA*DAMPER(J)+SPRINGK(J))*ZC*SINHG/(QUADRAT*ETA*OMEG
1A)
BETAP=AREA(J)*ETA*OMEGA*ZC*SINHG/QUADRAT
ALPHADP=(ETA*OMEGA*DAMPER(J)+SPRINGK(J))*AREA(J)*((1.,0.)-COSHG)/(
1ETA*OMEGA*QUADRAT)
BETADP=(AREA(J)**2)*ETA*OMEGA*((1.,0.)-COSHG)/QUADRAT
DD(1,1,J)=(COSHG+BETAP)/(1.+BETAP)
DD(1,2,J)=-ZC*SINHG/(AREA(J)*(1.+BETAP))
DD(2,1,J)=-AREA(J)*SINHG/ZC+BETADP*((1.,0.)-COSHG)/(1.+BETAP)
DD(2,2,J)=COSHG+BETADP*ZC*SINHG/(AREA(J)*(1.+BETAP))
CC(1,1,J)=ALPHAP/(1.+BETAP)
CC(2,1,J)=ALPHADP/(1.+BETAP)
RETURN
END

```

```

SUBROUTINE NINE
C THIS SUBROUTINE CALCULATES THE ELEMENTS OF THE TRANSFER MATRIX
C FOR A LINE WITH FORCED CHANGES IN LINE LENGTH
COMPLEX ETA,ENUM,DENOM,TRANS,B,D,XI,ARG,RJ,GAMMA,ZC,COSHG,SINHG,DD
1,CC,TCOTH,TCSCH,BB,Z1,Z2,X1,X2,X3,X4,QUADRAT,ALPHAP,BETAP,ALPHADP,
2BETADP,GOFS,SLCW,COSHCW,SINHCW,COEFF,ALPHA1,ALPHA2
COMPLEX ZSTRUCT,ALPHA,BETA
DIMENSION ITYPE(15),JTERM(15),K(15,15),EL(15),RADIUS(15),RBUB(15),
1FPVC(15),AKBPVC(15),AKCPVC(15),PARLEN(15,5),PARRAD(15,5),FREQ(200)
DIMENSION B(2,1),D(2,2),SIZE(200),SIZEDB(200),ANGLE(200),FBEL(15),
1COMPLY(15),AKBEL(15),BSIGN(10),DAMPER(15),SPRINGK(15)
DIMENSION DD(2,2,15),CC(2,1,15),BB(2,1,15),RADSEC(200),AREA(15)
COMMON PI,RADIUS,OMEGA,ENU,ETA,EL,CO,RHOO,THERMK,RBUB,CPCV,PO,VISC
1,FPVC,AKBPVC,AKCPVC,NPAR,PARRAD,PARLEN,BULKMOD,RHOLIQ,NGAS,GASMW
COMMON GAMGAS,G,TD,PHI,COMPLY,NELAST,EWALL,HWALL,NELM,JBNUM,JTERM,
1K,DD,CC,D,B,BB,CP,J,AREA,VMEAN,FBEL,AKBEL,BSIGN,DAMPER,SPRINGK
COMMON G1,G2,RHOWALL,ZX,ZY
GOFS=G1+G2*ETA
CW=SQRT((EWALL*G)/(RHOWALL*12.))
CALL SPEED
REYNOLD=VMEAN*2.*RADIUS(J)/(ENU*12.)
RT=144.*(2.*ENU*0.0055*REYNOLD**0.85)/(RADIUS(J)**2)
Z1=(OMEGA*EL(J)*ETA)/CO
Z2=CSQRT((1.,0.)+RT/(OMEGA*ETA))
XI=SQRT(OMEGA/ENU)*CSQRT(-ETA)
ARG=XI*RADIUS(J)/12.
CALL J10RJO(ARG,RJ)
GAMMA=ETA*OMEGA*EL(J)/(CO*CSQRT((1.,0.)-2.*RJ/ARG))+REAL(Z1*Z2)
ZC=RHO0*CO/(CSQRT((1.,0.)-2.*RJ/ARG))
COSHG=(CEXP(GAMMA)+CEXP(-GAMMA))/2.
SINHG=(CEXP(GAMMA)-CEXP(-GAMMA))/2.
DD(1,1,J)=COSHG
DD(1,2,J)=-ZC*SINHG/AREA(J)
DD(2,1,J)=-AREA(J)*SINHG/ZC
DD(2,2,J)=COSHG
SLCW=ETA*OMEGA*EL(J)/CW
COSHCW=(CEXP(SLCW)+CEXP(-SLCW))/2.
SINHCW=(CEXP(SLCW)-CEXP(-SLCW))/2.
COEFF=(-OMEGA**2/CO**2-(GAMMA/EL(J))**2)/(-OMEGA**2/CW**2-(GAMMA/E
1L(J))**2)
ALPHA1=(RHOO*CO**2/(ETA*OMEGA))*((ETA*OMEGA*SINHCW/CW-GAMMA*SINHG/
1EL(J))+(GOFS-COSHCW)*(COSHCW-COSHG)*ETA*OMEGA/(CW*SINHCW))
ALPHA2=-((COSHCW-COSHG)+(GOFS-COSHCW)*(SINHCW-ETA*OMEGA*EL(J)*SINH
1G/(CW*GAMMA))/SINHCW)
CC(1,1,J)=COEFF*ALPHA1
CC(2,1,J)=COEFF*ALPHA2*AREA(J)
RETURN
END

```

```

SUBROUTINE TEN
THIS SUBROUTINE CALCULATES THE ELEMENTS OF THE TRANSFER MATRIX
FOR THE AXIAL MOTION OF A VERTICAL LINE WITH MOUNTING STIFFNESS.
THE STIFFNESS IS REPRESENTED BY THE IMPEDANCE PRESENTED TO THE
LINE BY THE VEHICLE STRUCTURE.
THIS SUBROUTINE CAN BE USED ONLY WHEN ANOTHER SOURCE OF EXCITATION
IS PRESENT IN THE FEEDLINE, I.E. PULSER OR VERTICAL LINE VELOCITY
EXCITATION. THE FUNCTIONAL FORM OF THE STRUCTURAL IMPEDANCE IS
THAT OF AN EQUIVALENT SPRING AND DASHPOT IN PARALLEL.
ZX AND ZY ARE THE REAL AND IMAGINARY PARTS OF ZSTRUCT.
COMPLEX ETA,ENUM,DENOM,TRANS,B,D,XI,ARG,RJ,GAMMA,ZC,COSHG,SINHG,DD
1,CC,TCOTH,TCSCH,BB,Z1,Z2,X1,X2,X3,X4,QUADRAT,ALPHAP,BETAP,ALPHADP,
2BETADP,GOFS,SLCW,COSHCW,SINHCW,COEFF,ALPHA1,ALPHA2
COMPLEX ZSTRUCT,ALPHA,BETA
DIMENSION ITYPE(15),JTERM(15),K(15,15),EL(15),RADIUS(15),RBUB(15),
1FPVC(15),AKBPVC(15),AKCPVC(15),PARLEN(15,5),PARRAD(15,5),FREQ(200)
DIMENSION B(2,1),D(2,2),SIZE(200),SIZEDB(200),ANGLE(200),FBEL(15),
1COMPLY(15),AKBEL(15),BSIGN(10),DAMPER(15),SPRINGK(15)
DIMENSION DD(2,2,15),CC(2,1,15),BB(2,1,15),RADSEC(200),AREA(15)
COMMON PI,RADIUS,OMEGA,ENU,ETA,EL,CO,RHOO,THERMK,RBUB,CPCV,PO,VISC
1,FPVC,AKBPVC,AKCPVC,NPAR,PARRAD,PARLEN,BULKMOD,RHOLI,NGAS,GASMW
COMMON GAMGAS,G,TO,PHI,COMPLY,NELAST,EWALL,HWALL,NELM,JBNUM,JTERM,
1K,DD,CC,D,B,BB,CP,J,AREA,VMEAN,FBEL,AKBEL,BSIGN,DAMPER,SPRINGK
COMMON G1,G2,RHOWALL,ZX,ZY
CALL SPEED
REYNOLD=VMEAN*2.*RADIUS(J)/(ENU*12.)
RT=144.*(2.*ENU*0.0055*REYNOLD**0.85)/(RADIUS(J)**2)
Z1=(OMEGA*EL(J)*ETA)/CO
Z2=CSQRT((1.,0.)+RT/(OMEGA*ETA))
XI=SQRT(OMEGA/ENU)*CSQRT(-ETA)
ARG=XI*RADIUS(J)/12.
CALL J1ORJ0(ARG,RJ)
GAMMA=ETA*OMEGA*EL(J)/(CO*CSQRT((1.,0.)-2.*RJ/ARG))+REAL(Z1*Z2)
ZC=RHOO*CO/(CSQRT((1.,0.)-2.*RJ/ARG))
COSHG=(CEXP(GAMMA)+CEXP(-GAMMA))/2.
SINHG=(CEXP(GAMMA)-CEXP(-GAMMA))/2.
AMASS=RHOO*(AREA(J-1)*EL(J-1)+AREA(J+1)*EL(J+1))
ZSTRUCT=ZX-ETA*ZY/OMEGA
ALPHA=AREA(J)*ZC*SINHG/(ZSTRUCT+AMASS*ETA*OMEGA)
BETA=(1.-COSHG)*(AREA(J)**2)/(ZSTRUCT+AMASS*ETA*OMEGA)
DD(1,1,J)=(COSHG+ALPHA)/(1.+ALPHA)
DD(1,2,J)=-ZC*SINHG/(AREA(J)*(1.+ALPHA))
DD(2,1,J)=-AREA(J)*SINHG/ZC+BETA*(1.-COSHG)/(1.+ALPHA)
DD(2,2,J)=COSHG+ZC*SINHG*BETA/(AREA(J)*(1.+ALPHA))
RETURN
END

```

```

SUBROUTINE ELEVEN
C THIS SUBROUTINE CALCULATES THE ELEMENTS OF THE TRANSFER
C MATRIX FOR A COMPLEX SIDE BRANCH. THIS MODEL ASSUMES A
C LAMINAR FLOW IN THE SIDE BRANCH.
COMPLEX ETA,ENUM,DENOM,TRANS,B,D,XI,ARG,RJ,GAMMA,ZC,COSHG,SINHG,DD
1,CC,TCOTH,TCSCH,BB,Z1,Z2,X1,X2,X3,X4,QUADRAT,ALPHAP,BETAP,ALPHADP,
2BETADP,GOFS,SLCW,COSHCW,SINHCW,COEFF,ALPHA1,ALPHA2
COMPLEX ZSTRUCT,ALPHA,BETA
DIMENSION ITYPE(15),JTERM(15),K(15,15),EL(15),RADIUS(15),RBUB(15),
1FPVC(15),AKBPVC(15),AKCPVC(15),PARLEN(15,5),PARRAD(15,5),FREQ(200)
DIMENSION B(2,1),D(2,2),SIZE(200),SIZEDB(200),ANGLE(200),FBEL(15),
1COMPLY(15),AKBEL(15),BSIGN(10),DAMPER(15),SPRINGK(15)
DIMENSION DD(2,2,15),CC(2,1,15),BB(2,1,15),RADSEC(200),AREA(15)
COMMON PI,RADIUS,OMEGA,ENU,ETA,EL,CO,RHOO,THERMK,RBUB,CPCV,PO,VISC
1,FPVC,AKBPVC,AKCPVC,NPAR,PARRAD,PARLEN,BULKMOD,RHOLIQ,NGAS,GASMW
COMMON GAMGAS,G,TO,PHI,COMPLY,NELAST,EWALL,HWALL,NELM,JBNUM,JTERM,
1K,DD,CC,D,B,BB,CP,J,AREA,VMEAN,FBEL,AKBEL,BSIGN,DAMPER,SPRINGK
COMMON G1,G2,RHOWALL,ZX,ZY
COMMON BRCOMP,BRL,BRDIAM
COMPLEX S
S=ETA*OMEGA
10 CALL SPEED
AREAB=(PI/4.)*(BRDIAM/12.)**2
BRI=RHOO*BRL/AREAB
BRR=128.*VISC*BRL/(PI*(BRDIAM/12.)**4.)
DD(1,1,J)=(1.,0.)
DD(1,2,J)=(0.,0.)
DD(2,1,J)=-S*BRCOMP/(BRI*BRCOMP*S**2+BRR*BRCOMP*S +1.)
DD(2,2,J)=(1.,0.)
RETURN
END

```

SUBROUTINE SPEED

C
C
C

THIS SUBROUTINE CALCULATES THE SPEED OF SOUND FOR THE FLUID IN THE
FEEDLINE. THIS FLUID MAY BE A LIQUID OR A HOMOGENEOUS MIXTURE OF
A LIQUID AND AN ULLAGE GAS

COMPLEX ETA,ENUM,DENOM,TRANS,B,D,XI,ARG,RJ,GAMMA,ZC,COSHG,SINHG,DD
1,CC,TCOTH,TCSCH,BB,Z1,Z2,X1,X2,X3,X4,QUADRAT,ALPHAP,BETAP,ALPHADP,
2BETADP,GOFS,SLCW,COSHCW,SINHCW,COEFF,ALPHA1,ALPHA2

COMPLEX ZSTRUCT,ALPHA,BETA

DIMENSION ITYPE(15),JTERM(15),K(15,15),EL(15),RADIUS(15),RBUB(15),
1FPVC(15),AKBPVC(15),AKCPVC(15),PARLEN(15,5),PARRAD(15,5),FREQ(200)
DIMENSION B(2,1),D(2,2),SIZE(200),SIZEDB(200),ANGLE(200),FBEL(15),
1COMPLY(15),AKBEL(15),BSIGN(10),DAMPER(15),SPRINGK(15)

DIMENSION DD(2,2,15),CC(2,1,15),BB(2,1,15),RADSEC(200),AREA(15)

COMMON PI,RADIUS,OMEGA,ENU,ETA,EL,CO,RHOO,THERMK,RBUB,CPCV,PO,VISC

1,FPVC,AKBPVC,AKCPVC,NPAR,PARRAD,PARLEN,BULKMOD,RHOLIQ,NGAS,GASMW

COMMON GAMGAS,G,TO,PHI,COMPLY,NELAST,EWALL,HWALL,NELM,JBNUM,JTERM,

1K,DD,CC,D,B,BB,CP,J,AREA,VMEAN,FBEL,AKBEL,BSIGN,DAMPER,SPRINGK

COMMON G1,G2,RHOWALL,ZX,ZY

CLIQUID=SQRT(BULKMOD/RHOLIQ)

IF(NGAS.EQ.1)10,20

10 RHOGAS=144.*PO*GASMW/(1545.*(TO+460.)*G)

CGAS=SQRT(GAMGAS*G*1545.*(TO+460.)/GASMW)

E1=RHOGAS+PHI*RHOLIQ

E2=RHOGAS/(RHOLIQ*CLIQUID**2*E1)+(PHI*RHOLIQ)/(E1*RHOGAS*CGAS**2)

E3=(1.+PHI)*RHOGAS*RHOLIQ

CO=SQRT(E1/(E2*E3))

RHOO=E3/E1

ENU=VISC/RHOO

GO TO 30

20 CO=CLIQUID

RHOO=RHOLIQ

ENU=VISC/RHOO

30 IF(NELAST.EQ.1)40,50

40 CO=CO/SQRT(1.+BULKMOD*2.*(RADIUS(J)+HWALL)/(144.*EWALL*HWALL))

50 RETURN

END

```

SUBROUTINE DMAT
C THIS SUBROUTINE CALCULATES MATRIX D IN THE EXPRESSION P=DQ+VB
  COMPLEX ETA,ENUM,DENOM,TRANS,B,D,XI,ARG,RJ,GAMMA,ZC,COSHG,SINHG,DD
  1,CC,TCOTH,TCSCH,BB,Z1,Z2,X1,X2,X3,X4,QUADRAT,ALPHAP,BETAP,ALPHADP,
  2BETADP,GOFS,SLCW,COSHCW,SINHCW,COEFF,ALPHA1,ALPHA2
  COMPLEX ZSTRUCT,ALPHA,BETA
  DIMENSION ITYPE(15),JTERM(15),K(15,15),EL(15),RADIUS(15),RBUB(15),
  1FPVC(15),AKBPVC(15),AKCPVC(15),PARLEN(15,5),PARRAD(15,5),FREQ(200)
  DIMENSION B(2,1),D(2,2),SIZE(200),SIZEDB(200),ANGLE(200),FBEL(15),
  1COMPLY(15),AKBEL(15),BSIGN(10),DAMPER(15),SPRINGK(15)
  DIMENSION DD(2,2,15),CC(2,1,15),BB(2,1,15),RADSEC(200),AREA(15)
  COMMON PI,RADIUS,OMEGA,ENU,ETA,EL,CO,RHOO,THERMK,RBUB,CPCV,PO,VISC
  1,FPVC,AKBPVC,AKCPVC,NPAR,PARRAD,PARLEN,BULKMOD,RHOLIQ,NGAS,GASMW
  COMMON GAMGAS,G,TO,PHI,COMPLY,NELAST,EWALL,HWALL,NELM,JBNUM,JTERM,
  1K,DD,CC,D,B,BB,CP,J,AREA,VMEAN,FBEL,AKBEL,BSIGN,DAMPER,SPRINGK
  COMMON G1,G2,RHOWALL,ZX,ZY
  DO 10 M=1,2
  DO 10 N=1,2
10 D(M,N)=DD(M,N,1)
  IF(NELM-1)50,20,30
20 RETURN
30 DO 40 J=2,NELM
  X1=DD(1,1,J)*D(1,1)+DD(1,2,J)*D(2,1)
  X2=DD(1,1,J)*D(1,2)+DD(1,2,J)*D(2,2)
  X3=DD(2,1,J)*D(1,1)+DD(2,2,J)*D(2,1)
  X4=DD(2,1,J)*D(1,2)+DD(2,2,J)*D(2,2)
  D(1,1)=X1
  D(1,2)=X2
  D(2,1)=X3
40 D(2,2)=X4
  RETURN
50 PRINT 60
  CALL EXIT
60 FORMAT(28H0ERROR IN NELM SPECIFICATION)
  END

```

```

SUBROUTINE BMAT
C THIS SUBROUTINE CALCULATES MATRIX B IN THE EXPRESSION P=DQ+VB
  COMPLEX ETA,ENUM,DENOM,TRANS,B,D,XI,ARG,RJ,GAMMA,ZC,COSHG,SINHG,DD
  1,CC,TCOTH,TCSCH,BB,Z1,Z2,X1,X2,X3,X4,QUADRAT,ALPHAP,BETAP,ALPHADP,
  2BETADP,GOFS,SLCW,COSHCW,SINHCW,COEFF,ALPHA1,ALPHA2
  COMPLEX ZSTRUCT,ALPHA,BETA
  DIMENSION ITYPE(15),JTERM(15),K(15,15),EL(15),RADIUS(15),RBUB(15),
  1FPVC(15),AKBPVC(15),AKCPVC(15),PARLEN(15,5),PARRAD(15,5),FREQ(200)
  DIMENSION B(2,1),D(2,2),SIZE(200),SIZEDB(200),ANGLE(200),FBEL(15),
  1COMPLY(15),AKBEL(15),BSIGN(10),DAMPER(15),SPRINGK(15)
  DIMENSION DD(2,2,15),CC(2,1,15),BB(2,1,15),RADSEC(200),AREA(15)
  COMMON PI,RADIUS,OMEGA,ENU,ETA,EL,CO,RHOO,THERMK,RBUB,CPCV,PO,VISC
  1,FPVC,AKBPVC,AKCPVC,NPAR,PARRAD,PARLEN,BULKMOD,RHOLIQ,NGAS,GASMW
  COMMON GAMGAS,G,TO,PHI,COMPLY,NELAST,EWALL,HWALL,NELM,JBNUM,JTERM,
  1K,DD,CC,D,B,BB,CP,J,AREA,VMEAN,FBEL,AKBEL,BSIGN,DAMPER,SPRINGK
  COMMON G1,G2,RHOWALL,ZX,ZY
  DO 100 I=1,JBNUM
  KOUNT=JTERM(I)
  L=K(I,KOUNT)
  DO 100 J=1,KOUNT
  IF(J-1)5,5,15
  5 DO 10 M=1,2
  10 BB(M,1,I)=CC(M,1,L)
  GO TO 100
  15 L=K(I,KOUNT-J+1)
  X1=DD(1,1,L)*BB(1,1,I)+DD(1,2,L)*BB(2,1,I)
  X2=DD(2,1,L)*BB(1,1,I)+DD(2,2,L)*BB(2,1,I)
  BB(1,1,I)=X1
  BB(2,1,I)=X2
  100 CONTINUE
  B(1,1)=BSIGN(1)*BB(1,1,1)
  B(2,1)=BSIGN(1)*BB(2,1,1)
  110 DO 200 M=1,2
  DO 200 I=2,JBNUM
  200 B(M,1)=B(M,1)+BSIGN(I)*BB(M,1,I)
  210 RETURN
  END

```

```

SUBROUTINE J10RJO(Z,RJ)
C   CALCULATION OF J0(Z) AND J1(Z)  Z-COMPLEX
COMPLEX Z,J1,J0,TERMO,TERM1,Z1,Z2,P0,Q0,P1,Q1,PH0,PH1,FZ1,FZ2,RJ
X=REAL(Z)
Y=AIMAG(Z)
R=CABS(Z)
IF(R-18.)100,100,110
100 TERM1=Z/2.
    J1=Z/2.
    J0=(1.,0.)
    TERMO=(1.,0.)
    A=1.
    AM=15.+R
101 TERMO=TERMO*(-(Z/2.)**2)/A**2
    J0=J0+TERMO
    TERM1=TERM1*(-(Z/2.)**2)/((A+1.)*A)
    J1=J1+TERM1
    A=A+1.
    IF(A-AM)101,101,115
110 IF(X)111,112,112
111 Z1=-Z
    GO TO 113
112 Z1=Z
113 PI=3.1415926
    Z2=8.*Z1
    IF(CABS(Z2)-5000.)120,120,121
120 P0=(1.,0.)-4.5/Z2**2+3675./(8.*Z2**4)
    Q0=-1./Z2+37.5/Z2**3-59535./(8.*Z2**5)
    P1=(1.,0.)+7.5/Z2**2-4725./(8.*Z2**4)
    Q1=3./Z2-52.5/Z2**3+72765./(8.*Z2**5)
    GO TO 122
121 P0=(1.,0.)-4.5/Z2**2
    Q0=-1./Z2
    P1=(1.,0.)+7.5/Z2**2
    Q1=3./Z2
122 PH0=Z1-PI/4.
    PH1=Z1-.75*PI
    FZ1=2./(PI*Z1)
    FZ2=CSQRT(FZ1)
    AZ1=AIMAG(Z1)
    IF(ABS(AZ1)-50.)116,116,117
116 J0=FZ2*(P0*CCOS(PH0)-Q0*CSIN(PH0))
    J1=FZ2*(P1*CCOS(PH1)-Q1*CSIN(PH1))
    IF(X)114,115,115
114 J1=-J1
115 RJ=J1/J0
    GO TO 119
117 SIN=Y/ABS(Y)
    RJ=(SIN*(0.,1.)*P1+Q1)/(P0-SIN*(0.,1.)*Q0)
119 RETURN
END

```

CARD 3	ITYPE(J), J = 1, NELM dimensionless	A sequence of dimensionless numbers that describes the type of elements in the line in the order in which they appear beginning with the element attached to the fuel tank outlet. See the first page of program listing for an expanded definition.
CARD 4	JTERM(J), J = 1, JBNUM dimensionless	The number of submatrices in B(J). For example, in Equation (84), JBNUM = 3, JTERM(1) = 2, JTERM(2) = 3 and JTERM(3) = 4.
CARD 5 6 4 + BJNUM	K(J, M), dimensionless	An array that fixes the order of matrix multiplication in B(J). For example, in Equation (84), $B(3) = \underline{D}_5 \underline{D}_4 \underline{D}_3 \underline{C}_2$. Then $K(3,1) = 5$, $K(3,2) = 4$, $K(3,3) = 3$ and $K(3,4) = 2$.
CARD (5 + JBNUM)	BSIGN(J), dimensionless	Floating point array that defines the algebraic sign preceding each B(J). Again in Equation (84), BSIGN(1) = +1.0, BSIGN(2) = 1.0 and BSIGN(3) = -1.0.
CARD (6 + JBNUM)	HERTZI, Hz	The initial frequency where response calculations begin.
	DELHZ1, Hz	Frequency step size for frequencies between HERTZI and FLIM.
	FLIM, Hz	Frequency break-point which defines the boundary between regions of different grid size.
	DELHZ2, Hz	Frequency step size for frequencies beyond FLIM.
	HERTZF, Hz	The final frequency to be evaluated.

CARD (7 + JBNUM)	SIGN, dimensionless	Algebraic sign preceding the parameter K in Equation (80).
	TERMZ, lb-sec/ft ⁵	Terminal impedance of the line which reflects the combined effect of the turbopump-injector-engine combination. In its present form, TERMZ is a scalar resistance.
	RHOLIQ, lb-sec ² /ft ⁴	Liquid propellant density.
	THERMK, Btu/(hr-ft-°R)	Thermal conductivity of the gas inside large bubbles.
	P0, psia	Mean propellant pressure.
	T0, °R	Mean propellant temperature.
CARD (8 + JBNUM)	EWALL, lb/in. ²	Wall modulus of elasticity.
	HWALL, in.	Wall thickness.
	ZINPUT, lb-sec/ft ⁵	Scalar flow impedance at the propellant tank outlet.
	CPCV, dimensionless	The ratio of specific heats for the gas in the cavitation bubble at the propellant temperature.
	BULKMOD, lb/ft ²	Bulk modulus of the propellant.
	PHI, dimensionless	Vapor-liquid mass ratio for the bulk propellant flow.
CARD (9 + JBNUM)	VISC, lb-sec/ft ²	Propellant dynamic viscosity.
	GASMW, dimensionless	Molecular weight of dissolved vapor or ullage gas for use in speed of sound calculation.
	GAMGAS, dimensionless	Ratio of specific heats for the gas whose molecular weight is GASMW.

CP, Btu/lb-°R	Specific heat at constant pressure for the gas in the cavitation bubble.
VMEAN, ft/sec	Mean propellant feed velocity.
BRCOMP, ft ⁵ /lb	Compliance of the complex side branch.

The sequence and number of the remaining input cards cannot be stated a priori since they depend on the component structure of the feedline. However, the input for each line component appears sequentially in the same order as the components in the line beginning with the component attached to the fuel outlet. Listed below are the inputs for each class of component.

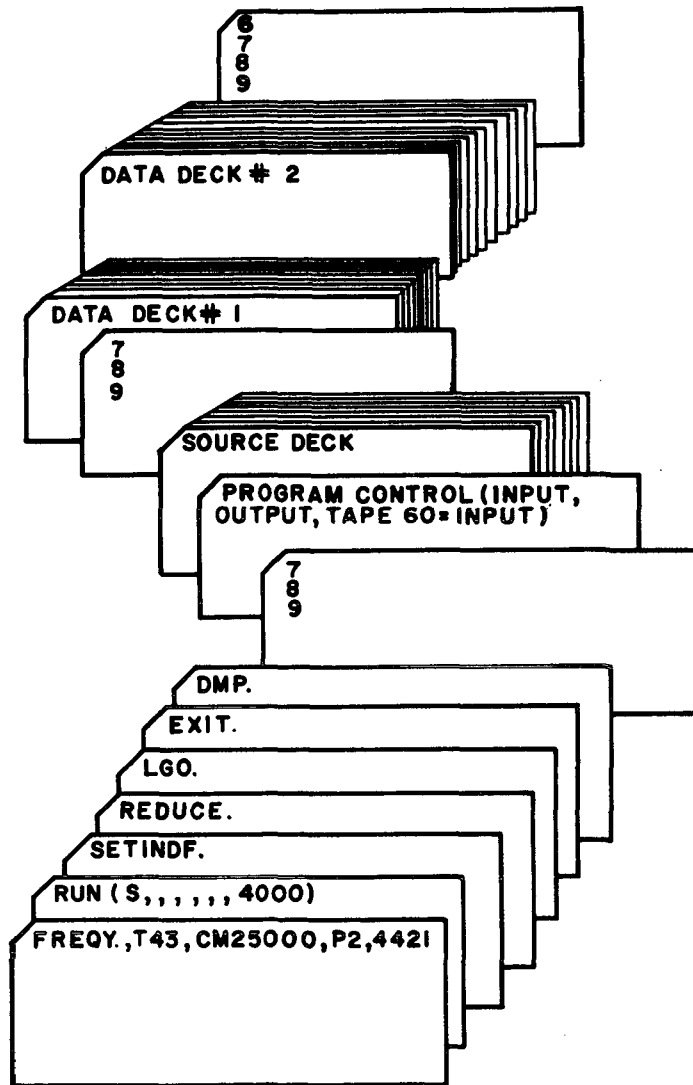
Simple line:	EL, ft	Line length.
	RADIUS, in.	Line radius as measured to the inner surface.
Cavitation bubble:	RBUB, in.	Bubble radius.
	RADIUS, in.	Internal radius of the line surrounding the bubble.
Pressure-volume compensator:	FPVC, dimensionless	Friction factor expressed as the fraction of the inlet pressure remaining at the outlet.
	AKBPVC, ft ²	Volume change constants for compensator.
	AKCPVC, ft ²	
Side branch pulser:		No input required.
Line with velocity excitation:	EL, ft	Same as simple line.
	RADIUS, in.	Same as simple line.
Parallel lines:	NPAR, dimensionless	The number of parallel lines.
	PARLEN, ft	Line length.
	PARRAD, in.	Line radius.
Bellows with relative motion:	FBEL, dimensionless	Bellows friction factor, same definition as FPVC
	COMPLY, ft ⁵ /lb	Compliance of bellows.
	AKBEL, ft ²	Volume change constant. If there is no relative motion, AKBEL = 0.

Line with mounting stiffness (discrete parameter):	EL, ft	Line length.
	RADIUS, in.	Line radius.
	DAMPER, lb-sec/ft	Coefficient of viscous damping.
	SPRINGK, lb/ft	Spring constant.
Forced changes in line length:	EL, ft	Line length.
	RADIUS, in.	Line radius.
	G1, G2	Real and imaginary parts of G(s).
	RHOWALL, lb/in ³	Wall density.
Line with mounting stiffness (impedance technique):	EL, ft	Line length.
	RADIUS, in.	Line radius.
	ZX, ZY	Components of structural impedance.
Complex side branch:	BRL, ft	Branch line length.
	BRDIAM, in.	Branch radius.

H. 4. Deck Structure for a Normal Compilation and Multiple Execution on the CDC 6400 Digital Computer

Deck structure for multiple production runs is shown on the following page.

The anticipated run time, core memory and output lineage information indicated on the first two control cards are for illustration purposes only. Typically, the combined central processor/print processor time for compilation, execution and listing of one run is approximately 25 seconds. In the case of production runs, time-line charges can be improved by inserting a NOLIST card in front of the PROGRAM CONTROL card which will delete the source program listing from the output.



3450

H. 5. Computer Symbol List

In order to facilitate program changes by the user, a correspondence list of the symbols used in the program is given below. The quantities on the left are the FORTRAN alphanumeric symbols in the program; on the right is the corresponding item from the analysis. Dummy variables, which are frequently used to facilitate programming of long equations, have been omitted.

TERMZ	--	Z_t	EL	--	L
RHOLIQ	--	ρ_l	RBUB	--	R_o
		(Mass density of propellant; liquid phase)	PARLEN	--	L_P
THERMK	--	k	PARRAD	--	r_P
PO	--	p_o	FBEL	--	$F(\rho V_z^2, G)_{BEL}$
TO	--	T_o	COMPLY	--	C
EWALL	--	E_t	AKBEL	--	K_B, BEL
HWALL	--	h	FPVC	--	$F(\rho V_z^2, G)_{PVC}$
ZINPUT	--	Z_1	AKBPVC	--	K_B, PVC
CPCV	--	C_p/C_v	ACKPVC	--	K_C, PVC
BULKMOD	--	χ	DAMPER	--	b
PHI	--	ϕ	SPRINGK	--	k
VISC	--	μ	OMEGA	--	ω
GASMW	--	MW	ENU	--	ν
GAMGAS	--	γ	REYNOLD	--	N_R
CP	--	C_P	RT	--	R_t
VMEAN	--	V_o	ETA	--	(+i)
RADIUS	--	r_o	XI	--	ξ

J1ORJ0	--	J_1/J_0	RHOGAS	--	ρ_g
GAMMA	--	Γ	CGAS	--	C_g
ZC	--	Z_o	RHO0	--	ρ_o
COSHG	--	$\cosh \Gamma$	ENU	--	ν
SINHG	--	$\sinh \Gamma$	PRO	--	$\phi_1 R_o$
AREA	--	A	DTHERM	--	D_1
AMASS	--	$m_1 + m_3$	BTHERM	--	b_{th}
ALPHAP	--	α'	BVIS	--	b_{VISC}
BETAP	--	β'	BRAD	--	b_{RAD}
ALPHADP	--	α''	POLY	--	η
BETADP	--	β''	VBUB	--	V_{BUB}
CW	--	C_w	SPRING	--	$\eta P_o / V_{BUB}$
GOFS	--	$G(s)$	ZSTRUCT	--	$Z_s = Z_x - iz_y / \omega$
RHOWALL	--	ρ_t	AREAB	--	A_b
SLCW	--	sL / C_w	BRI	--	I
COSHCW	--	$\cosh (sL / C_w)$	BRCOMP	--	C
SINHCW	--	$\sinh (sL / C_w)$	BRR	--	R
ALPHA1	--	α_1	BRL	--	L_b
ALPHA2	--	α_2	BRDIAM	--	d_b
CLIQUID	--	C_g			

H. 6. Example Problems

This section contains five example problems which will acquaint the user with the mechanics of program setup and execution. The development of each problem follows the same general format: statement of the physical problem, generation of the system matrix equation, presentation of critical input data and a computer listing and graphical representation of the configuration response. In all cases, only a portion of the output is shown since the remaining calculations follow the same format through termination of execution.

Problem No. 1:

The first feedline example, shown in Figure H-1, consists of a rigid length of line, a sidebranch pulser and a cavitation bubble in series with the fuel tank and a scalar terminal impedance, R . The perturbation pressure at Station 1 is assumed to be negligible. This assumption is for illustration purposes only, since the computer program accepts an arbitrary scalar input impedance at Station 1. The physical distance between Stations 2 and 4 is assumed to be small compared to the total line length, L . It is required that the perturbation pressure at Station 4 be determined for oscillatory pulser inputs, Q_d . The first step is to set up the station numbers, component numbers and component matrix equations in the Laplace domain as indicated in the illustration. Note that the subscripts on pressure and flow perturbations correspond to a particular station number, whereas the subscripts on matrices \underline{D}_1 and \underline{C}_1 refer to a specific component number. Beginning with the matrix equation for component number 3, successive substitution of the remaining expressions yields the overall line equation:

$$\begin{bmatrix} P_4 \\ P_4/R \end{bmatrix} = \underline{D}_3 \underline{D}_2 \underline{D}_1 \begin{bmatrix} 0 \\ Q_1 \end{bmatrix} + Q_d(s) (+ \underline{D}_3 \underline{C}_2) \quad (\text{H.1})$$

The fundamental operations involved in the derivation of this system equation are common to the setup of all problems, and the user is required to perform these steps in order to execute the program.

At this point, the user would make the following general observations regarding the program input:

- (1) NELM = 3 The number of components in the line.

INPUT

1 FEEDLINE CHECKOUT RUN NO.4

3 1 0 1
1 4 2
2
3 2

+ .100000+01
+ .100000+01 + .500000+00 + .600000+02 + .500000+00 + .600000+02
+ .100000+01 + .461000+05 + .220000+01 + .460000-02 + .347000+02 - .298000+03
+ .300000+08 + .660000-01 + .000000+00 + .140000+01 + .149000+08 + .000000+00
+ .408000-05 + .000000+00 + .000000+00 + .224000+00 + .500000+02
+ .300000+02 + .400000+01
+ .120000+01 + .400000+01

OUTPUT

FEEDLINE CHECKOUT RUN NO.4

OMEGA-RAD/SEC	FREQ-HZ	TRANS	TRANS-DB
6.3	1.0	1198.086	141.77
9.4	1.5	1810.423	150.03
12.6	2.0	2440.009	156.00
15.7	2.5	3093.494	160.74
18.8	3.0	3778.293	164.74
22.0	3.5	4502.879	168.25
25.1	4.0	5277.145	171.42
28.3	4.5	6112.872	174.36
31.4	5.0	7024.328	177.14
34.6	5.5	8029.074	179.82
37.7	6.0	9149.044	182.43
40.8	6.5	10411.997	185.01
44.0	7.0	11853.479	187.61
47.1	7.5	13519.412	190.24
50.3	8.0	15469.358	192.93
53.4	8.5	17780.115	195.72
56.5	9.0	20548.103	198.61
59.7	9.5	23885.499	201.62
62.8	10.0	27696.005	204.72
66.0	10.5	32596.330	207.84
69.1	11.0	37726.364	210.76
72.3	11.5	42452.590	213.12
75.4	12.0	45336.366	214.44
78.5	12.5	45244.860	214.40
81.7	13.0	42503.523	213.15
84.8	13.5	38465.238	211.15
88.0	14.0	34282.647	208.85
91.1	14.5	30502.971	206.51
94.2	15.0	27270.078	204.27
97.4	15.5	24556.224	202.17
100.5	16.0	22283.124	200.23
103.7	16.5	20369.256	198.44
106.8	17.0	18744.376	196.77
110.0	17.5	17351.841	195.23

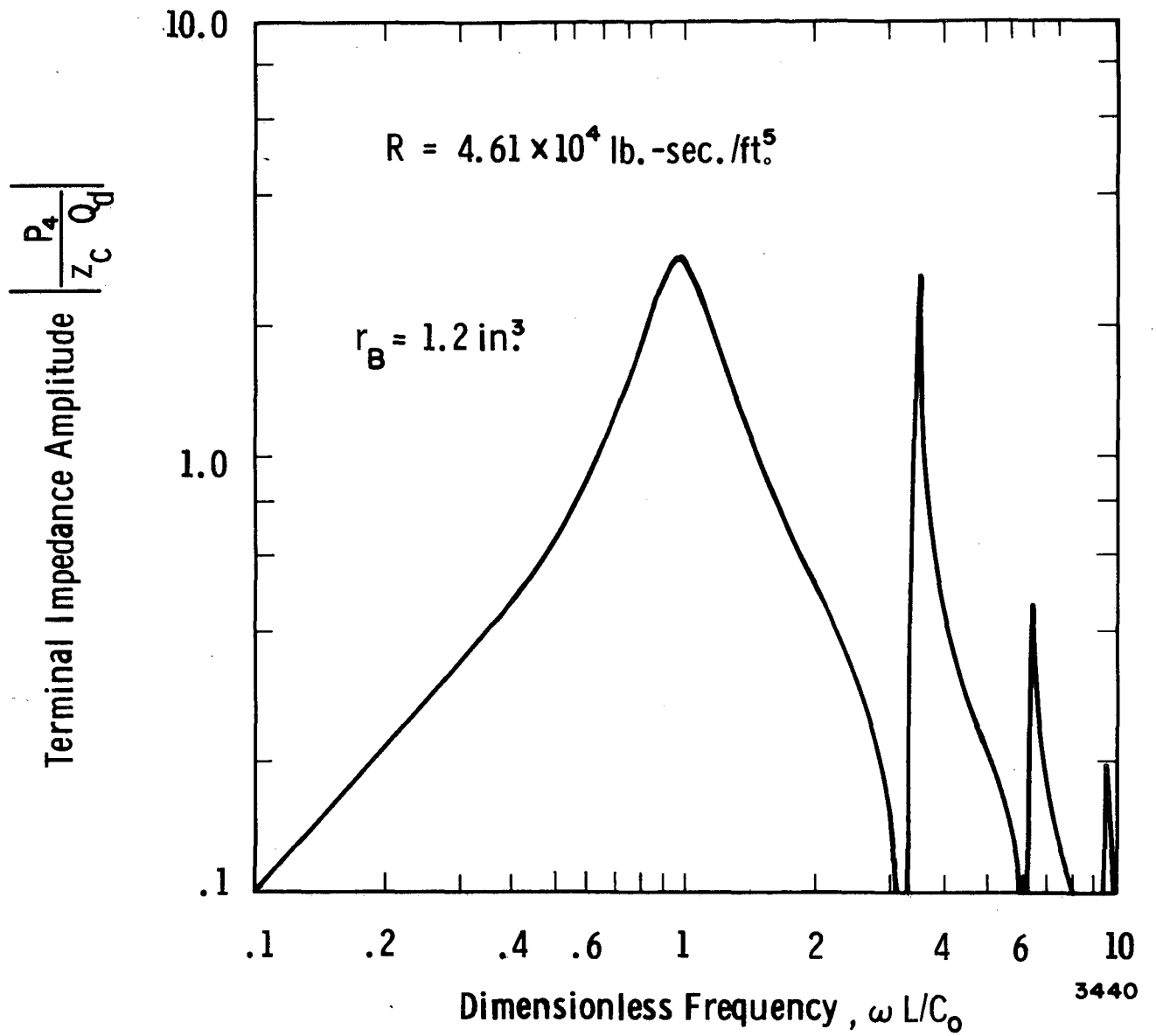


Figure H-2. Frequency Response For The Feedline In Example Problem No. 1

Problem No. 2:

In this example, the feedline configuration consists of a large cavitation bubble situated in the line midway between the fuel tank outlet and the terminal impedance, R. As shown in Figure H-3, the entire line is acted upon by a structural velocity, $V_\ell(s)$. For analysis purposes, it is assumed that bubble acceleration effects are negligible, and that the bubble diameter is small compared to the total line length, $L_1 + L_3$. Proceeding as in Problem No. 1 with the assumption of zero tank exit pressure perturbation, the following system equation is obtained:

$$\begin{bmatrix} P_4 \\ P_4/R \end{bmatrix} = \underline{D}_3 \underline{D}_2 \underline{D}_1 \begin{bmatrix} 0 \\ Q_1 \end{bmatrix} - V_\ell(s) \begin{bmatrix} \underline{D}_3 \underline{D}_2 \underline{C}_1 + \underline{C}_3 \end{bmatrix} \quad (\text{H.2})$$

Note that in this and the preceding example, the number of line components is the same. However, the present configuration results in a more complex functional representation of matrix \underline{B} :

$$\underline{B} = \underline{D}_3 \underline{D}_2 \underline{C}_1 + \underline{C}_3 = \underline{B}_1 + \underline{B}_2 \quad (\text{H.3})$$

The following deductions can be made.

- | | |
|--|--|
| (1) NELM = 3 | The number of elements in the line. |
| (2) JBNUM = 2 | The number of B_1 's that must be summed to form B. |
| (3) JTERM(1) = 3
JTERM(2) = 1 | The number of matrices that comprise \underline{B}_1 and \underline{B}_2 , respectively. |
| (4) K(1,1) = 3
K(1,2) = 2
K(1,3) = 1
K(2,1) = 3 | Two-dimensional integer array designating the ordered subscripts of the matrices that comprise \underline{B}_1 and \underline{B}_2 . |
| (5) ITYPE(1) = 5
ITYPE(2) = 2
ITYPE(3) = 5 | Integers describing the type of component located in the Jth component position. |

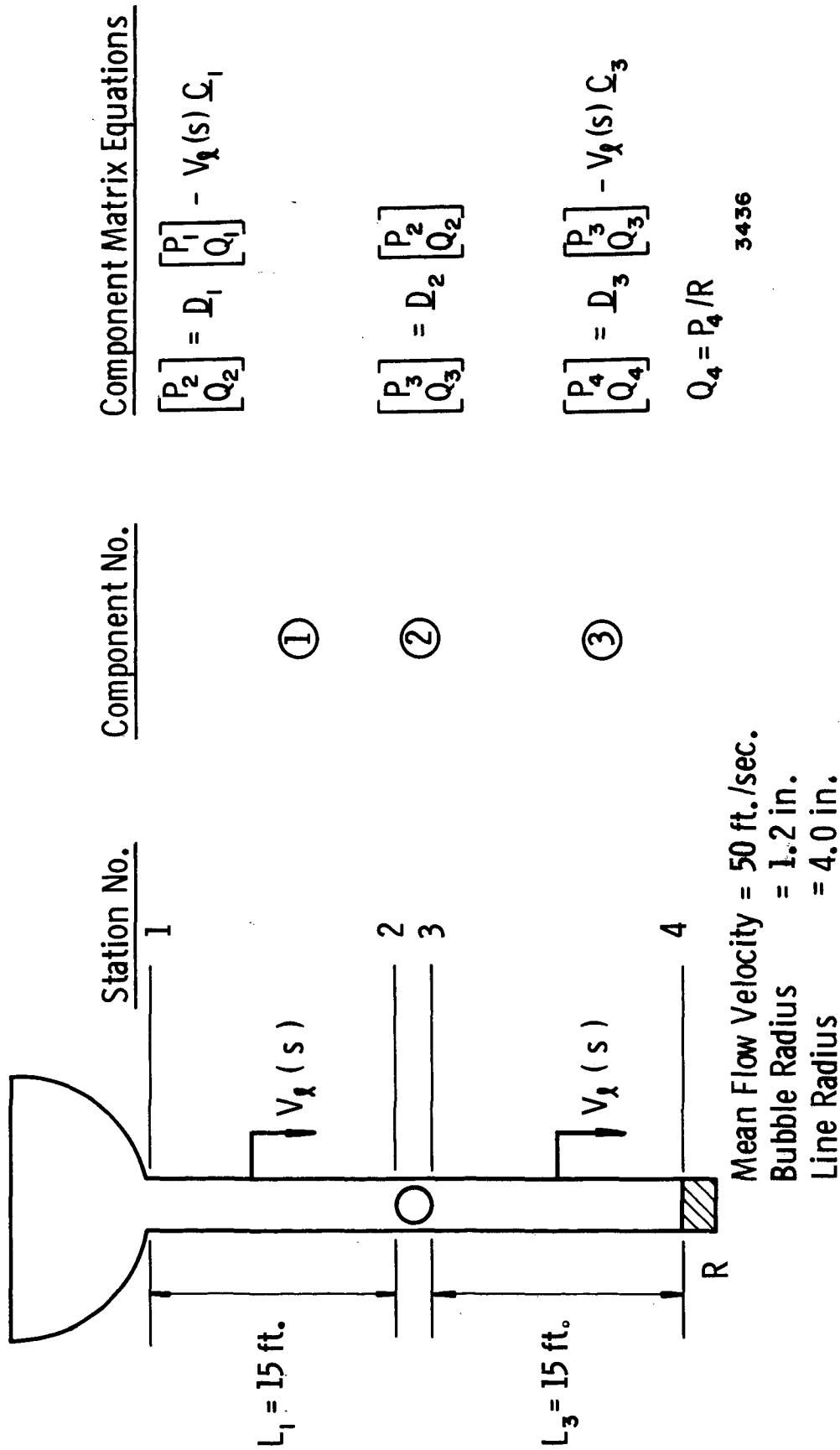


Figure H-3. Line Model For Example Problem No. 2

- (6) $\text{BSIGN}(1) = +1.0$ The algebraic sign preceding the submatrices, \underline{B}_1 .
 $\text{BSIGN}(2) = +1.0$
- (7) $\text{SIGN} = -1.0$ The algebraic sign preceding the excitation, V_ℓ .

The complete input package, followed by the program output is shown on the following page. The transfer function, which is the ratio of P_4 and V_ℓ , may be normalized with respect to the product of the acoustic impedance, Z_c , and the line cross-sectional area, A , as shown in the response plot of Figure H-4. Note that, in this example, both line segments have the same cross-sectional area; however, this is not a prerequisite.

INPUT

IFEEDLINE PROGRAM CHECKOUT RUN NO.5

3 2 0 1
5 2 5
3 1
3 2 1
3
+.100000+01 +.100000+01
+.100000+01 +.500000+00 +.600000+02 +.500000+00 +.600000+02
-.100000+01 +.461000+05 +.220000+01 +.460000-02 +.347000+02 -.298000+03
+.300000+08 +.660000-01 +.000000+00 +.140000+01 +.199000+08 +.000000+00
+.408000-05 +.000000+00 +.000000+00 +.224000+00 +.500000+02
+.150000+02 +.400000+01
+.120000+01 +.400000+01
+.150000+02 +.400000+01

OUTPUT

FEEDLINE PROGRAM CHECKOUT RUN NO.5

OMEGA-RAD/SEC	FREQ-HZ	TRANS	TRANS-DB
6.3	1.0	416.804	120.65
9.4	1.5	627.164	128.82
12.6	2.0	840.211	134.67
15.7	2.5	1056.945	139.26
18.8	3.0	1278.440	143.07
22.0	3.5	1505.862	146.34
25.1	4.0	1740.510	149.24
28.3	4.5	1983.841	151.86
31.4	5.0	2237.523	154.26
34.6	5.5	2503.479	156.51
37.7	6.0	2783.964	158.63
40.8	6.5	3081.641	160.66
44.0	7.0	3399.698	162.63
47.1	7.5	3741.988	164.55
50.3	8.0	4113.216	166.44
53.4	8.5	4519.181	168.32
56.5	9.0	4967.098	170.21
59.7	9.5	5466.009	172.13
62.8	10.0	6027.303	174.08
66.0	10.5	6665.330	176.09
69.1	11.0	7398.010	178.18
72.3	11.5	8247.116	180.35
75.4	12.0	9237.282	182.62
78.5	12.5	10391.344	184.97
81.7	13.0	11716.354	187.37
84.8	13.5	13169.506	189.71
88.0	14.0	14593.687	191.77
91.1	14.5	15652.858	193.17
94.2	15.0	15909.707	193.49
97.4	15.5	15158.146	192.53
100.5	16.0	13655.134	190.44
103.7	16.5	11869.681	187.63
106.8	17.0	10141.404	184.49
110.0	17.5	8612.917	181.22

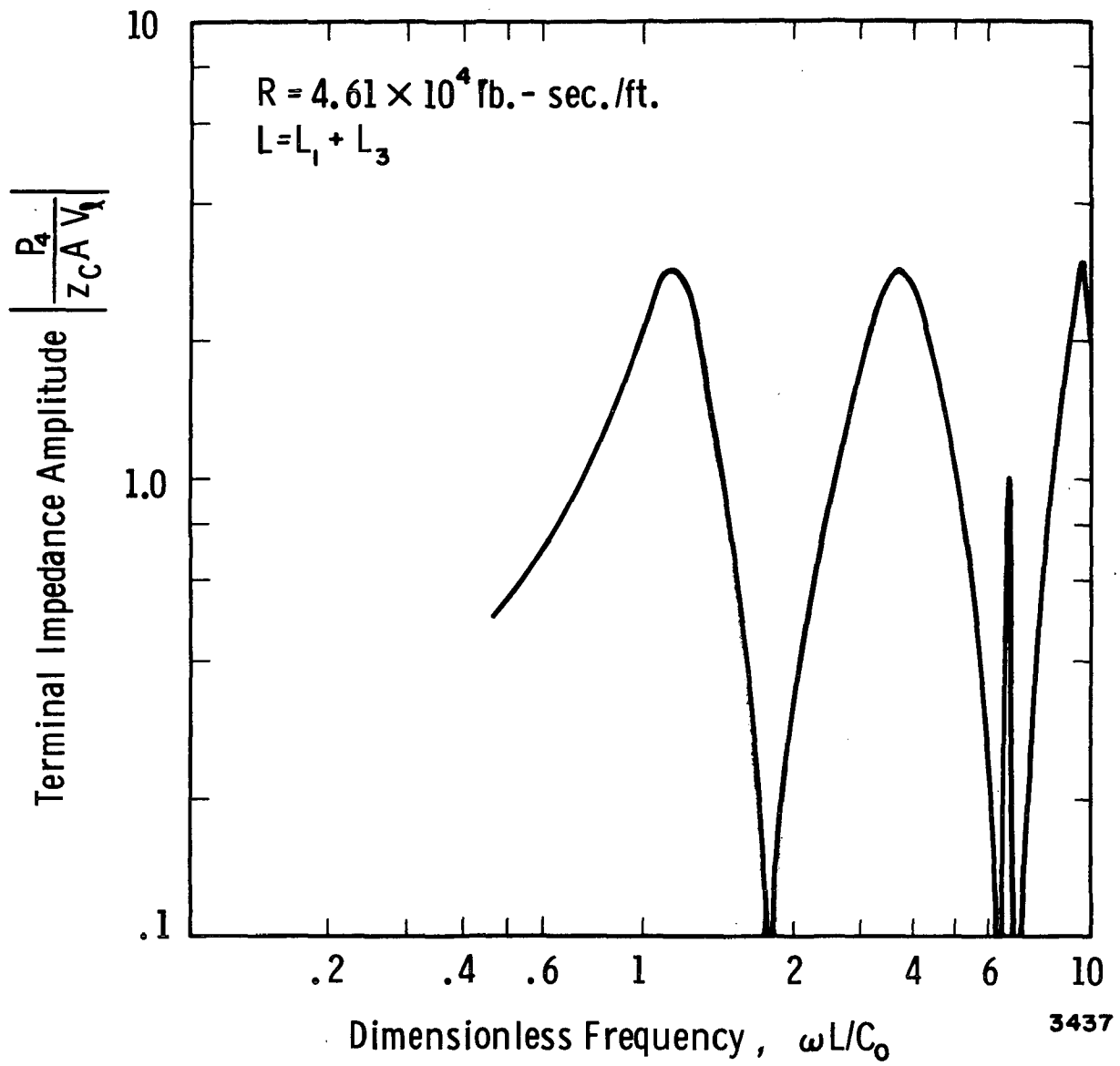


Figure H-4. Frequency Response Of The Feedline In Example Problem No. 2

Problem No. 3:

Setup procedures for the feedline example shown in Figure H-5 parallel quite closely the procedures used in Problem No. 1. The basic difference is in the matrix representation of the center component, which reflects a structural acceleration input to the line through a viscoelastic mounting element. The functional form of the system equation,

$$\begin{bmatrix} P_4 \\ P_4/R \end{bmatrix} = \underline{D}_3 \underline{D}_2 \underline{D}_1 \begin{bmatrix} 0_1 \\ Q_1 \end{bmatrix} - a_1(s) \underline{D}_3 \underline{C}_2 \quad (\text{H.4})$$

is virtually identical to Problem No. 1. Despite this apparent redundancy, this problem affords the opportunity to incorporate a previously unused subroutine, Subroutine EIGHT, into the analysis.

Since most vehicles employ lightly damped structures, a rather large amplification factor, \hat{Q} , was assumed in order to size the spring constant and damping coefficient. By definition,

$$\hat{Q} = \frac{1}{2\zeta} = \sqrt{\frac{km}{b}}.$$

The mass term is taken to be the combined fluid mass contained in the horizontal limbs of the feedline. For the line dimensions shown in Figure H-5 and $\hat{Q} = 100$, k and b were taken to be 88×10^4 lb/ft and 45.2 lb-sec/ft, respectively.

For this problem,

- (1) ITYPE(1) = 1;
ITYPE(2) = 8;
ITYPE(3) = 1;
- (2) SIGN = -1.0

Input values for items (1), (2) and (5) in Problem No. 1 apply also to this example. The response magnitude, normalized with respect to LOX density and a characteristic length, is shown in Figure H-6.

INPUT

1 LINE WITH MOUNTING STIFFNESS SWRI PROJECT 02-2889

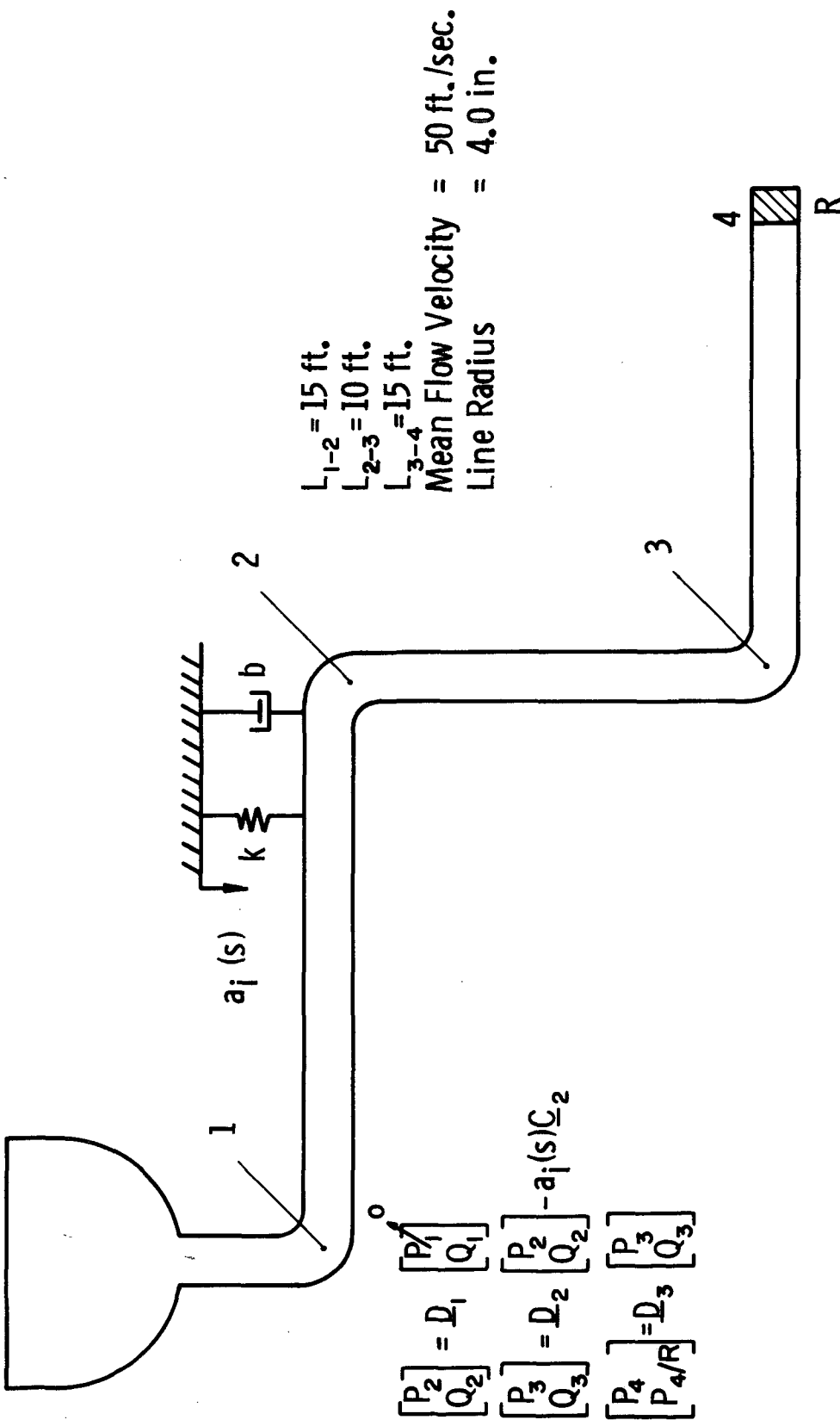
3 1 0 1
1 8 1
2
3 2

+ .100000+01
+ .100000+01 + .500000+00 + .600000+02 + .500000+00 + .600000+02
- .100000+01 + .461000+05 + .220000+01 + .000000+00 + .347000+02 - .298000+03
+ .300000+08 + .660000-01 + .000000+00 + .000000+00 + .199000+08 + .000000+00
+ .408000-05 + .000000+00 + .000000+00 + .000000+00 + .500000+02
+ .150000+02 + .400000+01
+ .100000+02 + .400000+01 + .452000+02 + .880000+06
+ .150000+02 + .400000+01

OUTPUT

LINE WITH MOUNTING STIFFNESS SWRI PROJECT 02-2889

OMEGA-RAD/SEC	FREQ-HZ	TRANS	TRANS-DB
6.3	1.0	22.120	61.93
9.4	1.5	22.226	62.03
12.6	2.0	22.393	62.17
15.7	2.5	22.619	62.38
18.8	3.0	22.907	62.63
22.0	3.5	23.260	62.94
25.1	4.0	23.683	63.30
28.3	4.5	24.181	63.71
31.4	5.0	24.760	64.18
34.6	5.5	25.428	64.72
37.7	6.0	26.196	65.31
40.8	6.5	27.074	65.97
44.0	7.0	28.076	66.70
47.1	7.5	29.218	67.50
50.3	8.0	30.519	68.37
53.4	8.5	32.000	69.31
56.5	9.0	33.686	70.34
59.7	9.5	35.605	71.45
62.8	10.0	37.786	72.64
66.0	10.5	40.260	73.91
69.1	11.0	43.050	75.25
72.3	11.5	46.165	76.64
75.4	12.0	49.585	78.07
78.5	12.5	53.230	79.49
81.7	13.0	56.933	80.84
84.8	13.5	60.406	82.02
88.0	14.0	63.244	82.94
91.1	14.5	64.996	83.49
94.2	15.0	65.328	83.59
97.4	15.5	64.172	83.23
100.5	16.0	61.769	82.47
103.7	16.5	58.545	81.40
106.8	17.0	54.943	80.13
110.0	17.5	51.308	78.76



The line length from Station 1 to the tank exit is assumed to be negligible. Tank exit conditions exist at Station 1.

Figure H-5. Line Model For Example Problem No. 3

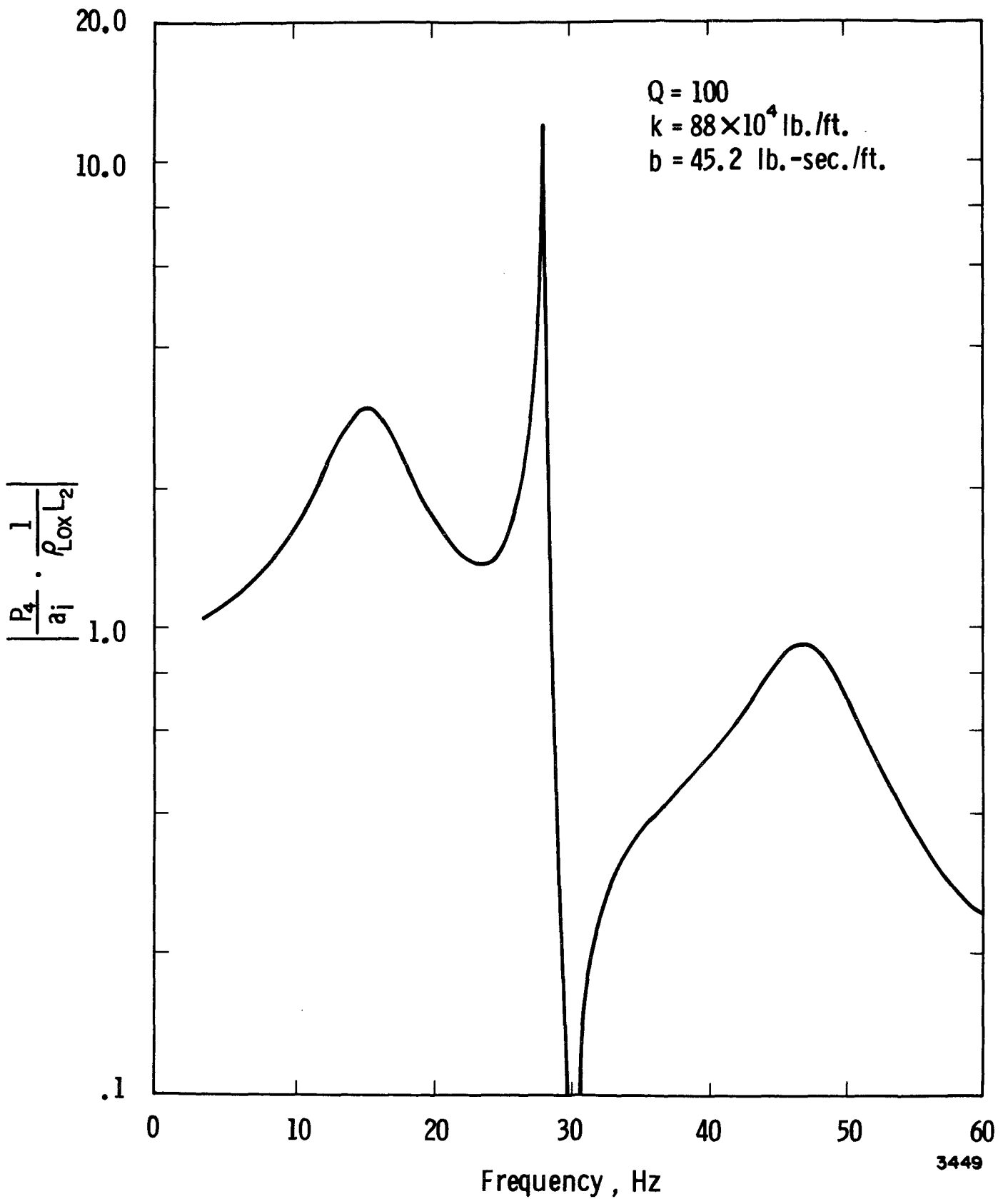


Figure H-6. Frequency Response Of The Feedline In Example Problem No. 3

Problem No. 4:

In this fourth example, shown in Figure H-7, an externally excited segment of line is coupled at its extremities to the remainder of the line through two flexible bellows. This problem was discussed briefly in Section VI.

Initially, the user would set up the physical problem exactly as shown in Figure H-7. Note that the functional form of the bellows equations differs only in the algebraic sign of the excitation term, which reflects the fact that one bellows is compressed while the other is expanded. The response of the turbopump inlet pressure, P_6 , in the presence of the velocity excitation, V_ℓ , is to be determined. The component equations are combined manually to produce the system equation:

$$\begin{bmatrix} P_6 \\ P_6/Z_t \end{bmatrix} = D_5 D_4 D_3 D_2 D_1 \begin{bmatrix} Z_1 Q_1 \\ Q_1 \end{bmatrix} + V_\ell (D_5 C_4 - D_5 D_4 C_3 - D_5 D_4 D_3 C_2) \quad (\text{H.5})$$

Observe that this system equation is more complex than the system equations in the previous examples. The following information is immediately available from the system equation:

(1) NELM = 5

(2) JBNUM = 3; therefore JTERM(1) = 2

JTERM(2) = 3

JTERM(3) = 4

and

K(1,1) = 5

K(1,2) = 4

K(2,1) = 5

K(2,2) = 4

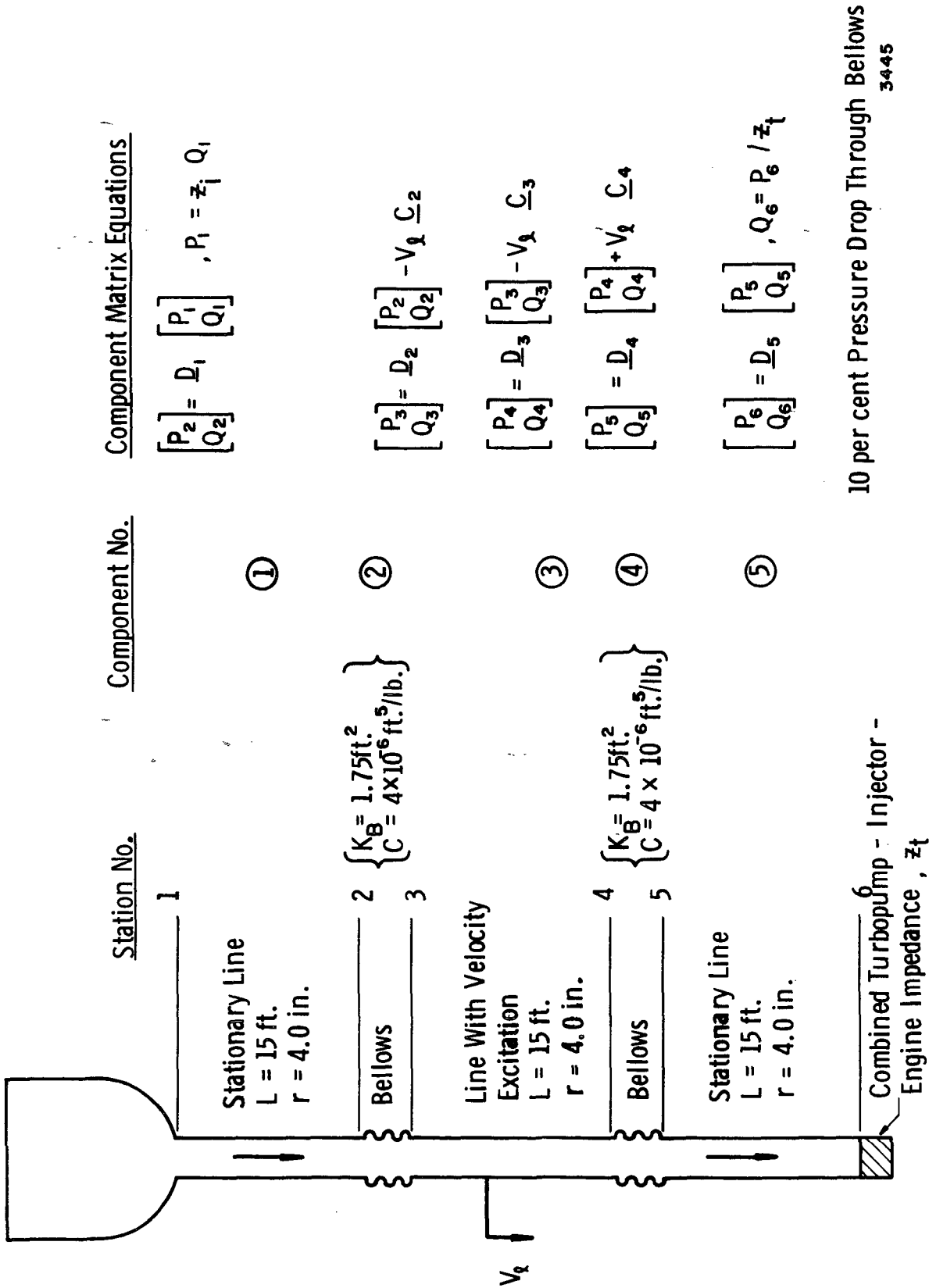
K(2,3) = 3

K(3,1) = 5

K(3,2) = 4

K(3,3) = 3

K(3,4) = 2



Component Matrix Equations

$$\begin{bmatrix} P_2 \\ Q_2 \end{bmatrix} = \underline{D}_1 \begin{bmatrix} P_1 \\ Q_1 \end{bmatrix}, P_1 = z_t Q_1$$

$$\begin{bmatrix} P_3 \\ Q_3 \end{bmatrix} = \underline{D}_2 \begin{bmatrix} P_2 \\ Q_2 \end{bmatrix} - V_t \underline{C}_2$$

$$\begin{bmatrix} P_4 \\ Q_4 \end{bmatrix} = \underline{D}_3 \begin{bmatrix} P_3 \\ Q_3 \end{bmatrix} - V_t \underline{C}_3$$

$$\begin{bmatrix} P_5 \\ Q_5 \end{bmatrix} = \underline{D}_4 \begin{bmatrix} P_4 \\ Q_4 \end{bmatrix} + V_t \underline{C}_4$$

$$\begin{bmatrix} P_6 \\ Q_6 \end{bmatrix} = \underline{D}_5 \begin{bmatrix} P_5 \\ Q_5 \end{bmatrix}, Q_6 = P_6 / z_t$$

10 per cent Pressure Drop Through Bellows
3445

Figure H-7. Line Model For Example Problem No. 4

(3) BSIGN(1) = +1.0

BSIGN(2) = -1.0

BSIGN(3) = -1.0

(4) ITYPE(1) = 1

ITYPE(2) = 7

ITYPE(3) = 5

ITYPE(4) = 7

ITYPE(5) = 1

(5) SIGN = +1.0

For computational purposes, it is assumed that $Z_t = 0$ and $Z_t = R$. In addition, there are no dissolved gases in the propellant (NGAS = 0). Wall elasticity is to be reflected in the speed of sound calculations (NELAST = 1). The entire input package is listed on the following page. At this point, the reader should make the correspondence between each numerical input quantity and the FORTRAN statement governing that input. The response magnitude, shown in the output listing, was normalized manually, and the resultant response is illustrated in Figure H-8.

INPUT

FINAL REPORT EXAMPLE. SWRI PROJECT NO. 02-2889

```
5 3 0 1
1 7 5 7 1
2 3 4
5 4
5 4 3
5 4 3 2
+.100000+01 -.100000+01 -.100000+01
+.100000+01 +.500000+00 +.600000+02 +.500000+00 +.600000+02
+.100000+01 +.461000+05 +.220000+01 +.000000+00 +.347000+02 -.298000+03
+.300000+08 +.660000-01 +.000000+00 +.000000+00 +.199000+08 +.000000+00
+.408000-05 +.000000+00 +.000000+00 +.000000+00 +.500000+02
+.150000+02 +.400000+01
+.900000+00 +.400000-05 +.175000+01
+.150000+02 +.400000+01
+.900000+00 +.400000-05 +.175000+01
+.150000+02 +.400000+01
```

OUTPUT

FINAL REPORT EXAMPLE. SWRI PROJECT NO. 02-2889

OMEGA-RAD/SEC	FREQ-HZ	TRANS	TRANS-DB
6.3	1.0	775.922	133.08
9.4	1.5	1215.373	142.06
12.6	2.0	1730.728	149.13
15.7	2.5	2378.342	155.48
18.8	3.0	3267.702	161.84
22.0	3.5	4652.086	168.90
25.1	4.0	7282.501	177.86
28.3	4.5	14401.926	191.50
31.4	5.0	23174.748	201.02
34.6	5.5	9265.208	182.68
37.7	6.0	4829.452	169.65
40.8	6.5	2810.559	158.82
44.0	7.0	1559.621	147.04
47.1	7.5	614.611	128.42
50.3	8.0	211.526	107.09
53.4	8.5	1022.651	138.60
56.5	9.0	1901.236	151.01
59.7	9.5	2940.050	159.72
62.8	10.0	4278.164	167.23
66.0	10.5	6172.661	174.56
69.1	11.0	9200.728	182.54
72.3	11.5	15035.329	192.36
75.4	12.0	31378.863	207.08
78.5	12.5	141786.521	237.24
81.7	13.0	38505.082	211.17
84.8	13.5	20492.071	198.56
88.0	14.0	14363.492	191.45
91.1	14.5	11283.461	186.62
94.2	15.0	9427.827	183.03
97.4	15.5	8185.881	180.20
100.5	16.0	7295.686	177.90
103.7	16.5	6626.241	175.98
106.8	17.0	6104.734	174.34
110.0	17.5	5687.466	172.92

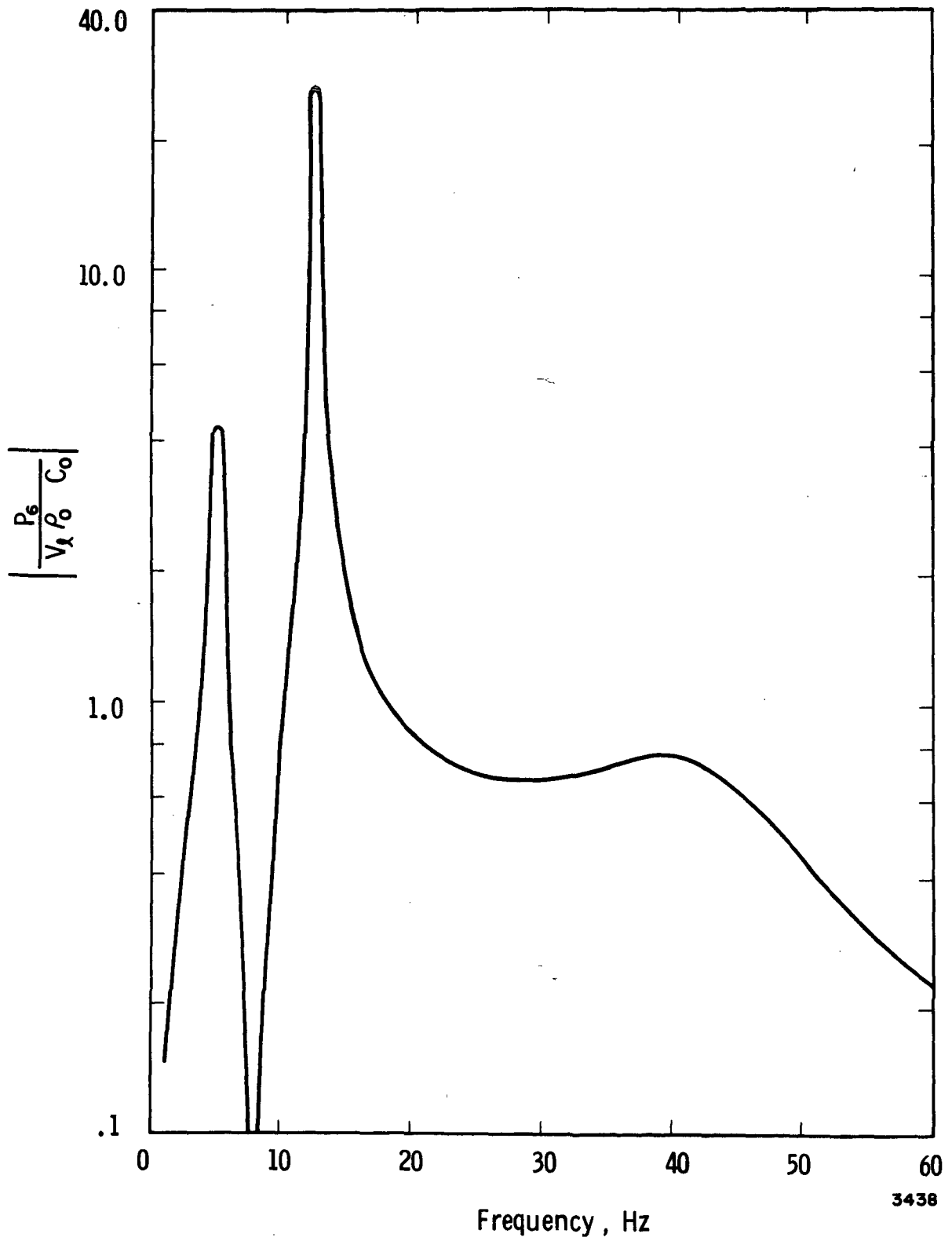


Figure H-8. Frequency Response Of The **Feedline** In Example Problem No. 4

Problem No. 5:

As depicted in Figure H-9, the vertical segment of the propellant feedline is undergoing forced changes in line length. The structural forces applied at Stations 2 and 3 produce measurable velocities which, in general, differ in magnitude and/or phase. Normally, these velocities can be related through a transfer function, $G(s)$. This function has been assigned a simple complex variable form in the computer code: $G = G_1 + iG_2$. The user may wish to alter this form to include a specific type of frequency dependence based on experimental observations of velocity excited lines. Such a program modification can easily be accomplished.

The length changes imposed on the vertical line segment do not influence the pressure-flow relationships of the horizontal segment.

As in the preceding examples, the first step is to describe each component by the appropriate matrix expression. The matrix equations can then be combined to yield the overall line equation which, for this example, is

$$\begin{bmatrix} P_3 \\ P_3/R \end{bmatrix} = \underline{D}_2 \underline{D}_1 \begin{bmatrix} P_1 \\ Q_1 \end{bmatrix} - V_2 \underline{C}_2 \quad (\text{H.6})$$

The effect of the structural velocity at Station 3 is contained in the column matrix, \underline{C}_2 . In computing the response of P_3 to changes in line length, the perturbation pressure at the exit to the fuel tank, P_1 , has been assumed to be negligible.

At this point, the reader should have no difficulty in constructing a data input package for this problem. For example, the input listing may take the form shown below in which the function, G , was taken to be

$$\frac{1}{\sqrt{2}} + i \frac{1}{\sqrt{2}} .$$

The computer input and corresponding output for this package, is shown on the following page. The modulus of the transfer function relating P_3 and V_2 is shown in Figure H-10

INPUT

1 FORCED CHANGE IN LINE LENGTH SWRI PROJECT 02-2889

```

2 1 0 1
1 9
1
2
+.100000+01
+.100000+01 +.500000+00 +.600000+02 +.500000+00 +.600000+02
-.100000+01 +.461000+05 +.220000+01 +.000000+00 +.347000+02 -.298000+03
+.300000+08 +.660000-01 +.000000+00 +.000000+00 +.199000+08 +.000000+00
+.408000-05 +.000000+00 +.000000+00 +.000000+00 +.500000+02
+.100000+02 +.400000+01
+.300000+02 +.400000+01 +.707000+00 +.707000+00 +.280000+00
  
```

OUTPUT

FORCED CHANGE IN LINE LENGTH SWRI PROJECT 02-2889

OMEGA-RAD/SEC	FREQ-HZ	TRANS	TRANS-DB
6.3	1.0	17.366	57.04
9.4	1.5	17.630	57.34
12.6	2.0	17.886	57.68
15.7	2.5	18.148	57.97
18.8	3.0	18.421	58.27
22.0	3.5	18.712	58.58
25.1	4.0	19.024	58.91
28.3	4.5	19.362	59.27
31.4	5.0	19.728	59.64
34.6	5.5	20.127	60.04
37.7	6.0	20.563	60.47
40.8	6.5	21.040	60.93
44.0	7.0	21.564	61.42
47.1	7.5	22.134	61.95
50.3	8.0	22.771	62.51
53.4	8.5	23.467	63.11
56.5	9.0	24.233	63.75
59.7	9.5	25.075	64.44
62.8	10.0	25.997	65.16
66.0	10.5	27.001	65.92
69.1	11.0	28.083	66.70
72.3	11.5	29.224	67.50
75.4	12.0	30.405	68.24
78.5	12.5	31.553	69.03
81.7	13.0	32.576	69.67
84.8	13.5	33.330	70.13
88.0	14.0	33.636	70.31
91.1	14.5	33.312	70.12
94.2	15.0	32.242	69.47
97.4	15.5	30.435	68.31
100.5	16.0	28.045	66.68
103.7	16.5	25.311	64.62
106.8	17.0	22.473	62.25
110.0	17.5	19.714	59.63


 Reproduced from
 best available copy.

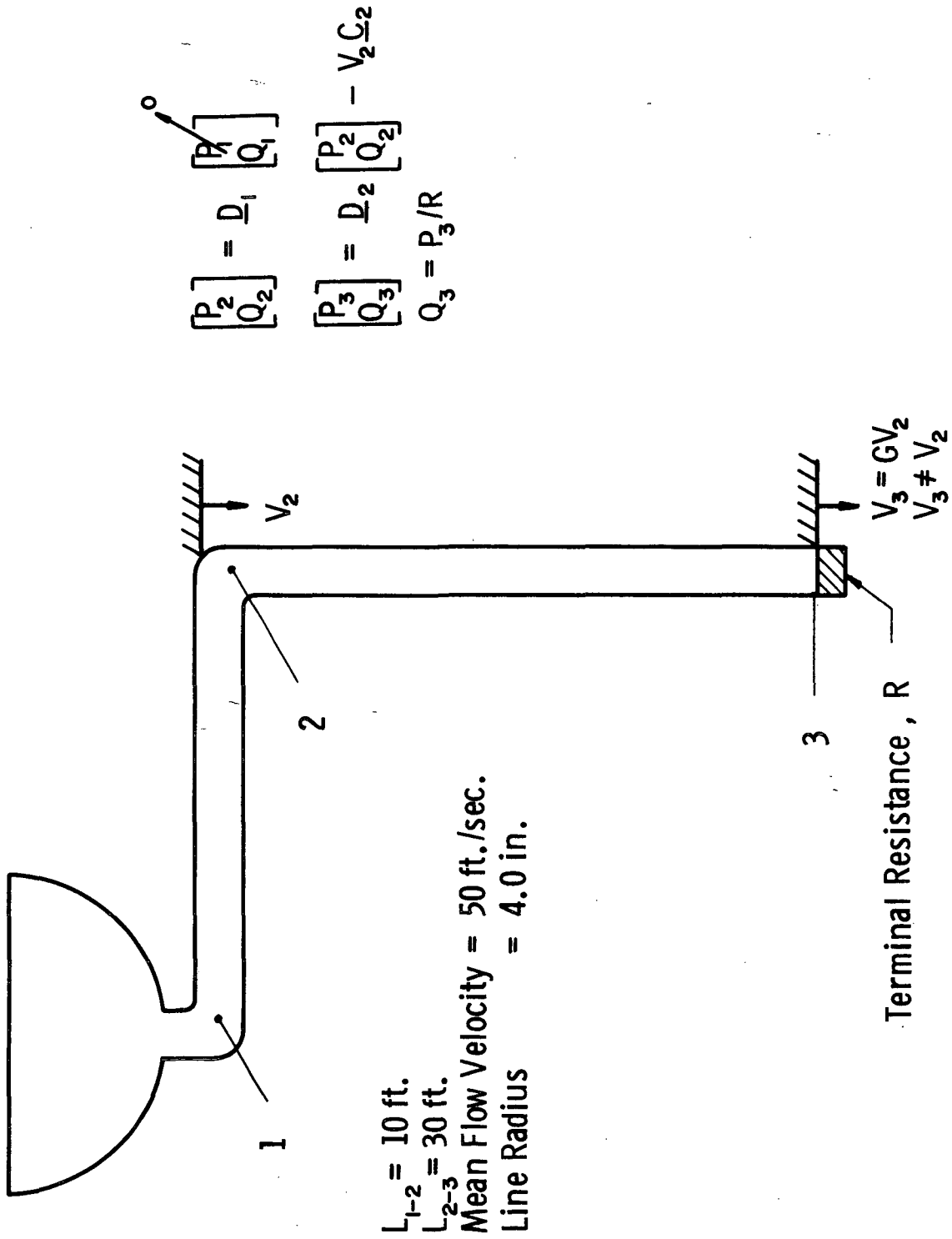


Figure H-9. Line Model For Example Problem No. 5

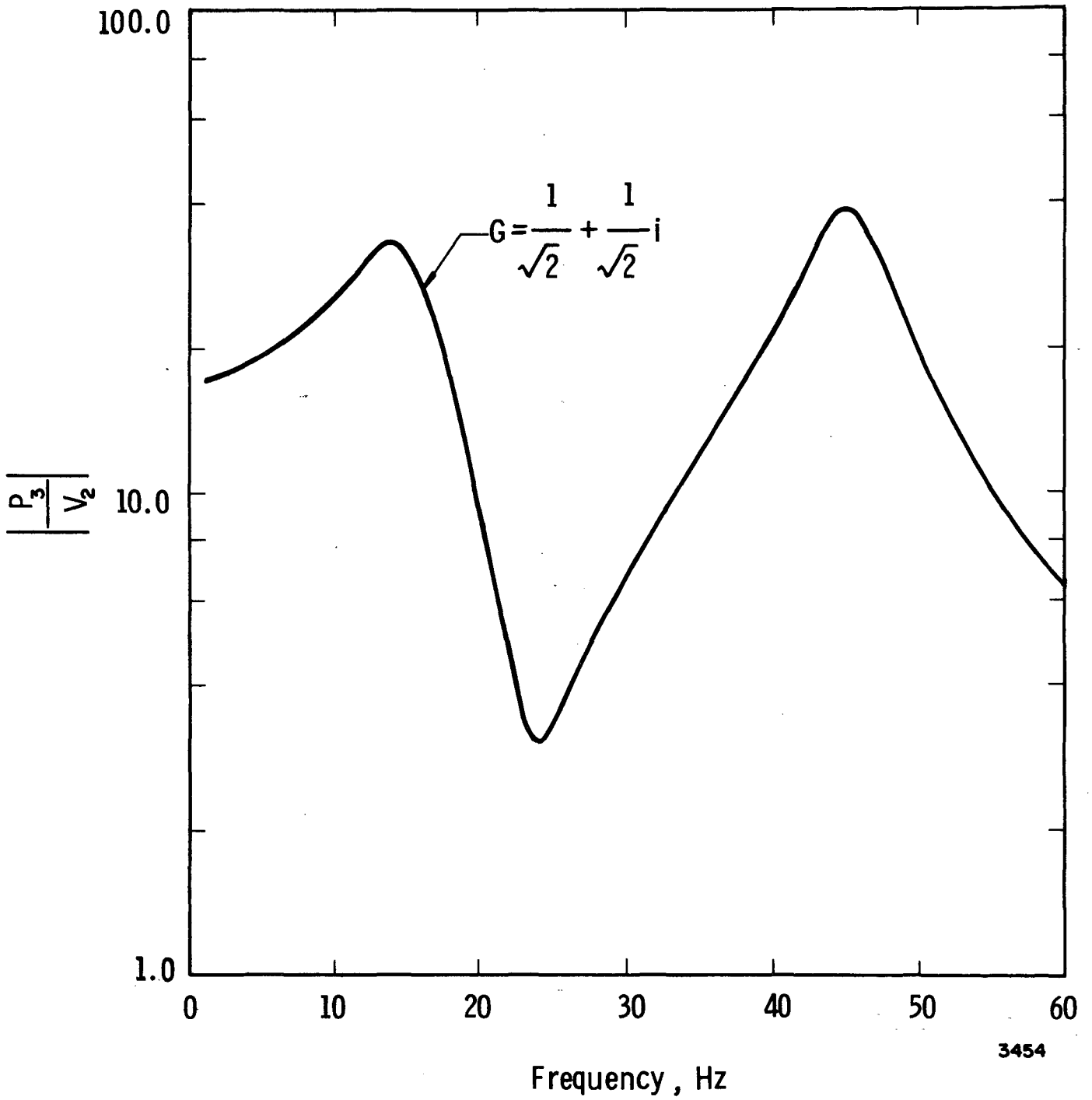


Figure H-10. Frequency Response Of The Feedline In Example Problem No. 5